2016

The Role of Astrocytic Calcineurin Activation and Downstream Signaling in Neurodegenerative Diseases

Melanie M. Pleiss
University of Kentucky, melanie.pleiss@gmail.com
Author ORCID Identifier:
http://orcid.org/0000-0001-5450-937X
Digital Object Identifier: https://doi.org/10.13023/ETD.2016.470

STUDENT AGREEMENT:

I represent that my thesis or dissertation and abstract are my original work. Proper attribution has been given to all outside sources. I understand that I am solely responsible for obtaining any needed copyright permissions. I have obtained needed written permission statement(s) from the owner(s) of each third-party copyrighted matter to be included in my work, allowing electronic distribution (if such use is not permitted by the fair use doctrine) which will be submitted to UKnowledge as Additional File.

I hereby grant to The University of Kentucky and its agents the irrevocable, non-exclusive, and royalty-free license to archive and make accessible my work in whole or in part in all forms of media, now or hereafter known. I agree that the document mentioned above may be made available immediately for worldwide access unless an embargo applies.

I retain all other ownership rights to the copyright of my work. I also retain the right to use in future works (such as articles or books) all or part of my work. I understand that I am free to register the copyright to my work.

REVIEW, APPROVAL AND ACCEPTANCE

The document mentioned above has been reviewed and accepted by the student's advisor, on behalf of the advisory committee, and by the Director of Graduate Studies (DGS), on behalf of the program; we verify that this is the final, approved version of the student's thesis including all changes required by the advisory committee. The undersigned agree to abide by the statements above.

Melanie M. Pleiss, Student

Dr. Christopher M. Norris, Major Professor

Dr. Donna R. Weber, Director of Graduate Studies

THE ROLE OF ASTROCYTIC CALCINEURIN ACTIVATION AND DOWNSTREAM SIGNALING IN NEURODEGENERATIVE DISEASES

DISSERTATION

A dissertation submitted in partial fulfillment of the requirements for the degree of Doctor of Philosophy in the College of Medicine at the University of Kentucky

By

Melanie Marie Pleiss

Lexington, KY

Director: Dr. Christopher Norris

Lexington, KY

2016

ABSTRACT OF DISSERTATION

THE ROLE OF ASTROCYTIC CALCINEURIN ACTIVATION AND DOWNSTREAM SIGNALING IN NEURODEGENERATIVE DISEASES

Calcineurin (CN) is a calcium (Ca^{2+})-sensitive serine/threonine protein phosphatase that plays a significant role in several cell signaling pathways, and has been implicated in many neurodegenerative diseases including Alzheimer's disease (AD) and vascular cognitive impairment and dementia (VCID). Although normally found in neurons, CN also appears at high levels in activated astrocytes under conditions of injury and disease. To elucidate the role of astrocytic calcineurin signaling in neurodegenerative diseases, our lab has used primary rat astrocytes, transgenic and diet-induced mouse models of dementia, and human tissue biospecimens from confirmed AD and VCID cases.

To better understand mechanisms for aberrant activation of CN during injury and disease, we created a custom antibody that selectively identifies a proteolyzed, constitutively active CN fragment. Immunolabeling in human biospecimens was done to determine which cell types express high levels of CN proteolysis and hyperactivation. Our results revealed extensive proteolysis of CN in activated astrocytes near pathologic hallmarks of AD (Aβ plaques) and VCID (microinfarcts). When a similar activated CN fragment was expressed in hippocampal astrocytes of healthy adult rats using adeno-associated virus (AAV) vectors, we observed suppressed function of CA3-CA1 excitatory synapses, suggesting that proteolytic activation of CN in astrocytes is a key mechanism for driving neuronal dysfunction in neurodegenerative diseases.

To explore the interaction between astrocytic CN and a possible downstream signaling target, we studied the hemichannel-forming protein, connexin43 (Cx43). Previous work has shown that serine 368 near the C terminus of Cx43 is dephosphorylated by CN. Here, we found that dephosphorylation of ser368 was increased in human hippocampal specimens from subjects diagnosed with mild cognitive impairment (MCI). Dephospho-Cx43 levels were correlated, within subject, to elevated levels of CN proteolysis and signaling. Moreover, dephosphorylation of Cx43 could be mimicked in rat primary astrocyte cultures using both exogenous Ca^{2+} mobilizers (phorbol ester/ionomycin) and endogenous inflammatory mediators (IL-1β), found previously to activate CN in astrocytes. Finally, we created a custom peptide (^{43}Gap52) that encompasses Ser368 and mimics a portion of the C-terminus of Cx43. ^{43}Gap52 prevented IL-1β-mediated dephosphorylation of Cx43, but did not prevent CN-dependent activation of NFAT transcription factors, suggesting that ^{43}Gap52 selectively disrupts

CN/Cx43 interactions. Using ^{43}Gap52 and the commercial CN inhibitor cyclosporin A (CsA), we found that blockade of CN/Cx43 interactions reduced hemichannel permeability in primary astrocytes following treatment with IL-1β, suggesting that aberrant CN activation in astrocytes may negatively affect neurons via interactions with Cx43-containing hemichannels.

To more clearly understand CN/NFAT signaling in VCID we used a diet-induced model of hyperhomocysteinemia (HHcy) that drives vascular pathology. Using AAV-mediated gene delivery, we injected mice with an astrocyte-targeted inhibitor of CN/NFAT binding (Gfa2-Egfp-VIVIT) or a control virus (Gfa2-Egfp). These mice were further split into two groups, one fed with the HHcy diet and one fed with control diet. Experiments are in progress to assess endpoint measurements including LTP and synaptic strength, RAWM behavior testing, as well as a panel of biochemical measurements.

KEYWORDS: Astrocyte, Calcineurin, Neuroinflammation, Alzheimer's disease, Vascular cognitive impairment and dementia

Melanie Marie Pleiss

November 29, 2016

Date

THE ROLE OF ASTROCYTIC CALCINEURIN ACTIVATION AND DOWNSTREAM SIGNALING IN NEURODEGENERATIVE DISEASES

By

Melanie Marie Pleiss

Christopher M. Norris

Director of Dissertation

Donna R. Weber

Director of Graduate Studies

November 29, 2016

Date

DEDICATION

This work is dedicated to my grandmother, Helen Caplinger, who has been the inspiration and motivation for this work from the beginning.

ACKNOWLEDGEMENTS

First and foremost, I would like to thank Chris Norris for his mentorship and guidance. I truly appreciate all of the effort he put into shaping me into a more diligent and critical thinker. My successes in the lab, my fellowships, my publications, and my dissertation would not have been possible without him. On a less serious note, how about them Cowboys?

I would also like to extend a special thanks to my co-workers present and past: Pradoldej “Bob” Sompol, Irina Artiushin, Jennifer Furman, and Susan Kraner. Not only were they an amazing source of knowledge when I had issues with techniques and protocols, but they also provided great support in the lab from day-to-day. I always enjoyed our discussions, and getting authentic Thai food at NATs with Bob. Irina was a great walking buddy and helped me clear my mind when things got frustrating in the lab. Jenny was my first “teacher” in the lab and became a great friend. Susan was incredibly knowledgeable and always willing to lend a helping hand.

I would like to greatly thank my committee members, Drs Donna Wilcock, Elizabeth Head, and Nada Porter. They were supportive, encouraging, and provided invaluable guidance throughout the completion of my Ph.D. and the writing of this dissertation. Additionally, I would like to thank Dr. Jose Abisambra for so willingly agreeing to be my outside examiner.

I received support and guidance from so many at the Sanders Brown Center on Aging and the Department of Pharmacology and Nutritional Sciences, but I would like to specifically thank Dr. Pete Nelson, Ela Patel, Tiffany Lee, Dr. Colin Rodgers, Linda Simmerman, Dr. Chris Gant, Deann Hopkins, and Kelley Secrest for their specific contributions to my work and/or life during my Ph.D.

My friends have truly helped keep me sane throughout this Ph.D. journey. Caitlin Averill and Aurora Szoka are my once-in-lifetime friends, and I am sincerely grateful for their support, words of love, and open ears when experiments went wrong. Brianna Harfmann has been with me from the beginning to share many coffee breaks, long runs, North Lime donuts, and laughs. Kaia Hampton is my ‘fit friend in science”, and was such a source of inspiration both scientifically and athletically. Scott and Natalie Webster are two of the most wholeheartedly encouraging friends, and sent me a lot of love throughout the Ph.D. process.

I would like to thank my parents, Mark and Cecilia Pleiss, for being a system of endless love and support from preschool through twenty-somethingth grade. I am eternally grateful to my brother, Timothy Pleiss, for his service in the U.S. Navy, and I could not have picked a better partner-in-crime in life if I had the choice. I am also thankful to the rest of my Pleiss and Foley family for their love and support. I greatly thank John Delfino and Ann Long for welcoming me into their family and feeding me many meals during the end of my studies. Last but not least, I would like to thank my love, Evan Delfino, for being my ruggedly-handsome rock amidst the ups-and-downs of this Ph.D. journey. For nearly a year he has asked me, “are you going to graduate today?” and I can finally say without a doubt, “yes”.

TABLE OF CONTENTS

LIST OF TABLES

LIST OF FIGURES

CHAPTER I: NEURODEGENERATIVE DISEASE, NEUROINFLAMMATION, ASTROCYTES, AND CALCINEURIN SIGNALING: A REVIEW

1.1 Neurodegenerative disease

As the world makes advances in both medical technology and healthcare, we see an increase in the aging population. Unfortunately, with the increase in life expectancy we see an increase in the number of people that develop neurodegenerative diseases. Neurodegenerative disease is a broad term that describes a disease characterized by chronic and progressive loss of both structure and function of neurons: *e.g.* amyotrophic lateral sclerosis (ALS) or Parkinson's disease (PD). Although the symptoms vary greatly with each individual disease, individuals with neurodegenerative diseases typically show some type of cognitive and/or motor deficits. It is believed that distinct neurodegenerative diseases are driven by unique pathological features (*e.g.* prions in Creutzfeldt-Jakob disease, amyloid in Alzheimer's disease, microinfarcts in vascular dementia) that lead to the breakdown of neuronal structure and function. Despite differences in pathogenic mechanisms, nearly all neurodegenerative diseases are unified by the appearance of neuroinflammation (Chen et al. 2016), involving feed-forward cycles of cytokine production and neuroglial "activation". For the scope of this dissertation, I will focus on the role of activated astroglia in two of the most common causes of neurodegeneration and dementia: Alzheimer's disease (AD) and cerebrovascular disease.

1.1.1 Alzheimer's disease

AD is a devastating neurodegenerative disorder characterized by progressive cognitive deficits, marked personality changes, and gradual loss of everyday skills and functions. As of 2015, over 5.4 million people in the United States suffer from AD and that number is expected to increase to 16 million by 2050. Moreover, in 2016 the total direct cost of caring for individuals with AD in the United States alone is an estimated

$236 billion. While rates of many other diseases (*i.e.* cardiovascular disease, stroke, and breast cancer) have declined, the prevalence of AD has increased at the alarming rate of 71% between 2000 and 2013. Furthermore, current medications on the market have failed to prevent or cure AD (Alzheimer's Association, 2016 Facts and Figures). It is imperative that we develop treatments that will prevent, or at the very least slow the progression of AD in order to avoid both health and financial crises. Finding effective treatments has proven difficult given that the exact molecular mechanisms responsible for the onset and progression of AD remain poorly understood.

In clinic, AD patients present with some degree of learning and memory impairment (Selkoe, 2001; Mattson, 2004) although symptoms vary from person to person. To make a clinical diagnosis of AD, physicians most often use behavioral or cognitive examinations but can additionally use imaging techniques *i.e.* positron emission tomography (PET) imaging as well as protein biomarkers from cerebrospinal fluid (CSF) (Anoop et al., 2010; Counts et al., 2016). It should be noted that a final and definitive diagnosis of AD cannot be made until brain tissue is examined at autopsy, where macroscopic examination can reveal brain atrophy along with severe neuronal loss, and microscopic examination can reveal the two pathologic hallmarks of AD—beta amyloid (Aβ) plaques and neurofibrillary tangles (NFTs) (Braak and Braak, 1991).

Neurofibrillary tangles are intraneuronal aggregations of hyperphosphorylated tau, a microtubule-stabilizing protein that is abundant in neurons (Avila et al., 2004). Hyperphosphorylation of tau can cause disintegration of microtubules that leads disrupted axonal transport and synaptic dysfunction (Maccioni et al, 2001). Additionally, studies have shown that tau can aberrantly associate with ribosomes in AD, leading to decreased synthesis of synaptic proteins that ultimately contributes to synaptic dysfunction (Meier et al., 2016). Aβ plaques are extracellular aggregations of cleaved amyloid peptides. These peptides are produced by the cleavage of the membrane-

spanning amyloid precursor protein (APP). Normally, APP is cleaved extracellularly by α-secretase which releases a non-toxic, soluble fragment (sAPPα) (Nunan and Small, 2000). However, with AD, APP is cleaved extracellularly by β-secretase (BACE) followed by intra-membrane cleavage by γ-secretase which releases toxic Aβ fragments from the membrane (Haass and Selkoe, 1993; Nunan and Small, 2000). These fragments can remain monomeric or assemble into oligomers, the most toxic form of Aβ, as well as fibrils that form Aβ plaques. All forms are found in AD (Irvine et al., 2008), and while some studies suggest disruption of synaptic function as the main mechanism of Aβ toxicity (Shankar et al., 2008), the exact mechanisms remain poorly understood.

The most widely accepted hypothesis for the mechanisms that lead to memory loss in AD is known as the “amyloid cascade”. In this model, increased production of toxic Aβ oligomers interferes with neuronal synaptic function, resulting in formation of Aβ plaques, neurite atrophy, activation of neuroinflammatory responses (astrocyte and microglial activation), and hyperphosphorylation of tau that eventually culminates in a dementia with hallmark plaque and tangle pathology (Hardy and Higgins, 1992; Lovestone, 2000). However, as treatments that target Aβ clearance or degradation have been largely ineffective at improving cognitive function, it is becoming more accepted that a combinatorial approach to AD that targets mechanisms beyond or in addition to Aβ may prove most effective. The majority of this dissertation will focus on the neuroinflammatory response, namely astrocyte activation, as a possible target for AD therapeutics.

1.1.2 Cerebral small vessel disease

Cerebral small vessel disease (SVD) describes a group of pathologic processes that affects arterioles, capillaries, and venules of the brain. Most commonly, this describes arteriolosclerosis and cerebral amyloid angiopathy (CAA). Damage to the

small vessels can result in white matter lesions (WMLs), lacunar infarcts, and cerebral hemorrhages which can be detected easily by neuroimaging, and thus SVD is often used to describe the above pathologies (Pantoni, 2010). Different studies have suggested that both macroscopic and microscopic infarcts are sufficient on their own to drive vascular cognitive impairment and dementia (VCID) (Smith et al., 2012). The extent of cognitive impairment, however, may depend on number of infarcts as well as brain region affected (Gorelick et al., 2016).

VCID is not only the second leading cause of dementia behind AD, but is also a frequent comorbidity with AD, with up to 40% of patients presenting with a mixed dementia *e.g.* AD and VCID (Dubois and Hebert, 2001; Kammoun et al., 2000; Korczyn et al., 2012). Moreover, some evidence suggests that AD and VCID pathology may act synergistically, requiring less of either pathology to express a state of dementia (Schneider and Bennett, 2010). Risk factors for VCID often overlap with traditional risk factors for stroke or cardiovascular disease and can include hypertension, diabetes, hyperhomocysteinemia, and arterial stiffness (Gorelick et al., 2011).

Due to the heterogeneity of the disease, patients present in clinic with varying symptoms of cognitive impairment. The lack of a precise and uniform pathologic definition for VCID presents somewhat of a challenge as the gold standard for diagnosis involves a neuropathological examination. However, physicians are generally able to make a diagnosis based on a combination of neuropsychological examinations (focused more on executive function than on learning and memory), brain imaging techniques (Peca et al., 2013), and more recently, an assessment of biomarkers in the CSF. Pathologic features of VCID may be any single or combination of brain vascular factors that includes small vessel disease (SVD) including WMLs, infarcts (lacunar, macro-, and micro-), as well as microbleeds (Gorelick et al., 2011).

The mechanisms by which cerebrovascular factors contribute to dementia is still not greatly understood. Pathologies such as microhemorrhages and WMLs may represent direct tissue damage *i.e.* breakage of vessels leading to bleeds or degeneration of white matter resulting in a lesion. For example, several studies have implicated the matrix metalloproteinases 2 and 9 (MMP-2/MMP-9) in the induction of cerebral hemorrhages (Klein and Bischoff, 2011; Candelario-Jalil et al., 2011; Hernandez- Guillamon et al., 2012). Moreover, VCID pathologies can be both focal (*i.e.* single infarct or lesion) as well as diffuse (*i.e.* widespread hypoxia or oxidative stress). These pathologies can have profound and devastating impacts on the integrity of the neurovascular unit *i.e.* the junction of vessel endothelial cells, astrocyte endfeet, and pericytes, as well as on the BBB and white matter. Whether on its own or as a comorbidity with AD, it is critical to find effective therapeutics to slow or treat the multi-varied pathologies of VCID.

1.2 Neuroinflammation

Neuroinflammation is associated with aging, injury, and many neurodegenerative disorders, including AD and VCID (Akiyama et al., 2000; Skaper, 2007). The general hallmarks of neuroinflammation include altered number of neuroglia, change in glial morphology, as well as increased expression of cytokines, chemokines, reactive oxygen species, and other inflammatory mediators (Wisniewski and Wegiel, 1991; Van Eldik and Griffin, 1994; Mrak and Griffin, 2001b, a; Heneka et al., 2015). Acutely, the inflammatory response can isolate and facilitate the repair of sites of injury, pathogen invasion, and protein aggregation. However, it is becoming increasingly clear that a chronic state of neuroinflammation is detrimental to neuronal health and synaptic function (Griffin et al., 1998; Griffin and Mrak, 2002; Mrak and Griffin, 2005b).

The two predominant glial cell types are microglia and astrocytes, both of which are associated with neuroinflammation. Microglia are macrophages that circulate throughout the brain foraging for invading pathogens or foreign molecules which they remove via phagocytosis. Additionally, with neuroinflammation, microglia undergo complex morphological changes where they secrete cytokines, chemokines, complement factors, and reactive oxygen species which aid in recruiting more monocytes and macrophages to the site of injury (Akiyama et al., 2000; Griffin, 2006). Similarly, with neuroinflammation, astrocytes undergo a hypertrophic activation where they increase production of pro-inflammatory factors (Sama et al., 2008; Fuller et al., 2009; Sofroniew, 2009; Fuller et al., 2010; Sofroniew and Vinters, 2010; Colombo and Faring, 2016). With a severe and/or chronic insult such as AD or VCID, the production of pro-inflammatory mediators is nearly continuous, resulting in a positive, feed-forward cycle between astrocytes and microglia that is accompanied by a likely detrimental state of neuroinflammation.

For example, targeting pro-inflammatory molecules *e.g.* TNFα, p38 MAPK, or IL-1β in a mouse model of AD revealed improved functional and reduced pathological outcomes (Munoz et al., 2007; McCoy and Tansey, 2008; Shaftel et al., 2008; Munoz and Ammit, 2010; Kitazawa et al., 2011; Bachstetter et al., 2012), suggesting that neuroinflammation is not only a byproduct of the disease but is also playing a significant role in the progression of AD pathophysiology. Other studies using a diet-induced model of VCID have found an elevated pro-inflammatory cytokine panel *i.e.* IL-1β, IL-6, and TNFα in mice on the diet compared to control mice (Hofmann et al., 2001; Sudduth et al., 2013b), suggesting that neuroinflammation is also a significant contributor to VCID pathology.

In support of these findings, data from epidemiological studies have shown that people who take long-term courses of common anti-inflammatory agents *i.e.* non-

steroidal anti-inflammatory drugs (NSAIDs) have a delayed or decreased risk of developing AD (Andersen et al., 1995; Rich et al., 1995; McGeer et al., 1996; Lee et al., 2010). However, controlled trials have not been able to replicate these findings (Aisen et al., 2003; Reines et al., 2004), possibly due to poor therapeutic targeting or poor drug delivery timing, given that neuroinflammation is a complex process involving several cell types and mediators. Only several pathways have been well-studied to date, so targeting neuroinflammation should not be disregarded in the search for a viable treatment for neurodegenerative diseases.

1.3 Mouse models of neurodegeneration

A multitude of mouse models exist to study AD. The most widely-used models involve a genetic modification of amyloid processing proteins (APP and/or PS1). Models include but are certainly not limited to Tg2576 (Hsaio et al., 1996), APP/PS1 transgenic (Jankowsky et al., 2004), APP/PS1 knock-in (KI) (Flood et al., 2002), 5xFAD (Oakley et al., 2006), and the 3xTg-AD (Oddo et al., 2003). Although these models vary slightly in their mutations within the genes, they all develop parenchymal Aβ plaques and deficits in spatial working memory albeit the timing and extent to which they develop these differs (Elder et al., 2010; Webster et al., 2014). Unlike the others mentioned above, the 3xTg-AD model not only has mutations in amyloid processing genes, but also contains a mutation in the tau gene, making it a more representative model of AD with both amyloid and tau pathology. In addition to the amyloidogenic models of AD, some researchers also use tauopathic models. These can include the P301S (Gotz et al., 2001a) and the rTg (tauP301L) 4510 (Gotz et al., 2001b) mice. Again, although timing of development may differ these mice have profound NFT formation, neuronal loss, as well as cognitive decline (Bryan et al., 2009).

While numerous AD mice are available, some concerns come to mind about their usefulness as a model system. One, while these mice may exhibit striking pathology their cognitive deficits are only lackluster. Moreover, many interventions and therapeutics that are efficacious in mouse models of AD have shown underwhelming results in human clinical trials, bringing into question whether these models are translatable (Bryan et al., 2009). Some research suggests better model systems for studying AD *e.g.* canines (Cummings et al., 1993; Head 2013).

Unlike AD, the heterogeneity of disease pathology that is seen with VCID presents a huge challenge in developing appropriate models. Numerous mouse and/or rat models have been developed to study the different causes of VCID, which has recently been well-reviewed (Gooch and Wilcock, 2016). The bilateral common carotid artery stenosis (BCAS) mouse model is the most widely-used to study subcortical ischemic vascular dementia (Nakaji et al., 2006; Shibata et al., 2007; Yoshizaki et al., 2008; Bink et al., 2013), and less commonly used is the asymmetrical common carotid artery stenosis (ACAS) mouse model (Bink et al., 2013; Hattori et al., 2015). Several genetic variants have been developed to study cerebral autosomal dominant arteriopathy with subcortical infarcts and leukoencephalopathy (CADASIL) (Hainsworth and Markus, 2008; Wallays et al., 2011; Cognat et al., 2014; Ehret et al., 2015), which is the most common genetic cause of VCID. Type 2 diabetes mellitus (T2DM) mice develop vascular pathologies in addition to AD-like neuropathologies (Jiwa et al., 2010; Takeda et al., 2010; Niedowicz et al., 2014). Several transgenic models exist to study cerebral amyloid angiopathy (CAA) (Davis et al., 2004; Herzig et al., 2004; Miao et al., 2005; Kumar-Singh, 2009; Hernandez-Guillamon et al., 2011; Kulic et al., 2012). Additionally, cerebral SVD is most commonly studied in a spontaneously hypertensive (SHR) rat model (Jiwa et al., 2010; Joutel et al., 2010; Yun et al., 2014). Several varying occlusion models have been developed in rats to study cerebral hypoperfusion (Sakai et al., 1996; Roof et al., 2001;

Neto et al., 2005; Pereira et al., 2012). However, none are optimal as they lack metabolic similarity to humans *i.e.* white matter vascular injury and hypertension (Snyder et al. 2015).

Some genetic models exist to study HHcy-induced VCID which are achieved by inducing mutations in enzymes that are critical for converting homocysteine in the transsulfuration pathway, including cystathionine β-synthase (Baumbach et al., 2002) and methylenetetrahydrofolate reductase (Devlin et al., 2004). These models can be helpful for studying the microhemorrhage component of VCID. However, unlike the diet-induced model which will be described in the following section, transgenic models do not easily facilitate the observation of neurodegenerative disease comorbidities. Thus, the diet-induced HHcy mouse appears to be a valuable model for studying VCID and its comorbidities.

1.3.1 Using excess homocysteine to drive VCID in a mouse model

Homocysteine is a sulfur-containing, non-essential amino acid produced in all cells that is a product of normal folate and methionine metabolism. Homocysteine is a transient product that is normally converted to cystathionine via the transsulfuration pathway. With some aging, injury, and even some rare genetic mutations, levels of homocysteine can become elevated in the plasma, which is referred to as hyperhomocysteinemia (HHcy). Buildup of homocysteine in the plasma can occur as a result of mutations in certain enzymes in the transsulfuration pathway *i.e.* cystathionine-β-synthase (CBS) or methylenetetrahydrofolate reductase (MTHFR) as well as from a deficiency of critical co-factors *e.g.* vitamins B_6, B_{12}, and folate and/or an excess of methionine, a precursor for homocysteine (Stipanuk and Ueki, 2011). This dissertation will focus on a diet-induced HHcy model to study VCID.

A Teklad custom research diet (Harlan laboratories) has been developed to induce HHcy, which is deficient in folate, B_6, and B_{12}, and also has excess methionine (7.7 g/kg) versus control diet (3.0 g/kg). Levels of other vitamins and minerals, as well as protein (195 g/kg) are uniform across the HHcy and control diets. Studies suggest that animal placed on the HHcy diet for a minimum of 11 weeks develop a moderate HHcy, defined by plasma homocysteine levels between 30-100 µmol/L (Ernest et al., 2005). This HHcy diet is sufficient to cause cognitive decline (Troen et al., 2008), inflammation (Hoffman et al., 2001), as well as increased microhemorrhages (Sudduth et al., 2013b). Moreover, mice from alternative disease models *e.g.* AD (Sudduth et al., 2014; Weekman et al., 2016) can be placed on the diet, making it an easily-controlled and valuable model for studying not only VCID but also its comorbidities in a mouse model.

1.4 Astrocytes

As one of the most abundant cell types in the brain (Chen and Swanson, 2003), the role and contribution of astrocytes to AD, VCID, and other neurological disorders remains underappreciated. Astrocytes are no longer considered as only “support” cells, as they perform critical functions including but not limited to maintenance of neurons and synapses, regulation of ions, metabolites, and glutamate, as well protection of the blood-brain barrier (Pekny and Nilsson, 2005; Sofroniew and Vinters, 2010; Pekny et al., 2016; Pekny and Pekna, 2016). As mentioned above, astrocytes are also one of the key players in the neuroinflammatory response, where they undergo a hypertrophic morphological change and increase secretion of pro-inflammatory cytokines in a process known as astrocyte activation (Fuller et al., 2009; Sofroniew, 2009; Fuller et al., 2010; Sofroniew and Vinters, 2010). Acutely, astrocyte activation may serve to isolate areas of injury, recruit additional support cells, and prevent any further damage. However, chronic astrocyte activation, as is seen with AD or VCID, may result in a damaging feed-forward

production of pro-inflammatory cytokines, and also in a loss of extracellular glutamate regulation (Sofroniew, 2009; Fuller et al., 2010). Several studies have been performed using mouse models of AD and VCID to target signaling pathways in astrocytes known to result in astrocyte activation. Modulation of astrocyte signaling pathways has been shown to have both beneficial and detrimental effects on neural function, suggesting that activated astrocytes have a complex phenotype and may play a myriad of roles during the progression of neurodegenerative disease. These observations suggest that the refinement of astrocyte-targeting strategies may lead to more effective treatments of neurodegenerative conditions such as AD and VCID. Moreover, work from our lab suggests that astrocytic calcineurin (CN) signaling may be a promising target for ameliorating the synaptic deficits seen in neurodegeneration (Furman et al., 2012; Furman et al., 2016; Pleiss et al., 2016; Pleiss et al., *in preparation*).

1.5 Calcineurin

CN is an exquisitely calcium (Ca^{2+})/calmodulin (CaM)-dependent serine/threonine protein-phosphatase that is expressed in most mammalian cell types, but found in particularly high levels in the CNS (Klee, 1991). In healthy brain tissue, CN is most abundant in neurons where it performs critical functions in the maintenance of synaptic viability and plasticity. In healthy neural tissue, intracellular Ca^{2+} levels are low and tightly regulated; however, under conditions of aging, injury, and disease such as AD and vessel damage, cytosolic Ca^{2+} levels are elevated and regulation is often unchecked (Abdul et al., 2010). Hyperactivation of CN due to aberrant changes in neuronal Ca^{2+} levels, has deleterious effects on synapses and neuronal viability, such as activation of apoptosis cascades (Springer et al., 2000; Norris et al., 2005; Sama et al., 2008). On the other hand, expression of CN in astrocytes is incredibly low in healthy tissue but under neurodegenerative conditions with profound astrocyte activation, there is a striking

increase in CN expression (Hashimoto et al., 1998; Norris et al., 2005; Celsi et al., 2007; Abdul et al., 2009; Pleiss et al., 2016). In mouse models of AD as well as human AD tissue, CN is intensely labeled in astrocytes around amyloid deposits later in the disease stage (Norris et al., 2005; Pleiss et al., 2016). In mouse models of VCID as well as human VCID tissue, CN is strikingly labeled in astrocytes surrounding microinfarcts (Pleiss et al., 2016).

Normally, minor changes in intracellular Ca^{2+} levels result in increased activation of CaM that in turn results in increased activation of CN. Aberrant and unchecked Ca^{2+} dyshomeostasis can lead to activation of calpain (CP), a Ca^{2+}-dependent cysteine protease, which results in a constitutive and irreversible activation of CN (ΔCN) (see Figure 1.1). Proteolyzed calcineurin has been implicated in activation of apoptosis cascades, in part through dephosphorylation of the proapoptotic factor BAD (Wang et al., 1999; Springer et al., 2000) Furthermore, Ca^{2+} dysregulation has been associated with dendritic spine retraction and synaptic dysfunction, likely due to the actions of CN on cytoskeletal proteins and glutamate receptors (Halpain et al., 1998; Shankar et al., 2007; Tackenberg and Brandt, 2009; Wu et al., 2010). In Chapter II, I outline studies that used a novel antibody reagent to show that CN proteolysis occurs extensively in activated astrocytes associated with AD and VCID pathologic features, suggesting that hyperactivation of CN signaling pathways in astrocytes is a critical component of both diseases, possibly through activation of neuroinflammatory cascades. CN interactions with downstream targets, such as NF-κB, have been implicated in production of inflammatory mediators (*e.g.* IL-2) (Crabtree, 2001). As outlined in Chapters III and IV, work from our lab, and others, suggest that the transcription factor NFAT and the hemichannel-forming protein, connexin 43, may be particularly important for coupling CN hyperactivity to astrocyte-dependent neurologic dysfunction.

1.5.1 NFATs

Although they have been extensively studied in peripheral immune cells, little was known about the role of the nuclear factor of activated t-cells (NFATs) in the CNS until recently. NFATs are transcription factors that are normally found in the cytosol in a heavily-phosphorylated state (Crabtree and Olson, 2002). With cellular activation, NFATs translocate to the nucleus following CN-dependent dephosphorylation and exposure of a nuclear localization peptide. Once in the nucleus, NFATs promote the synthesis of pro-inflammatory cytokines, chemokines, and mediators such as IFNγ or TNFα (McCaffrey et al., 1994; Stankunas et al., 1999; Avni et al., 2002; Palanki, 2002; Kitazawa et al., 2004; Demuro et al., 2005; White et al., 2005; Shankar et al., 2008) (see Figure 1.2). NFATs remain in the nucleus in an activated state until they are re-phosphorylated by protein kinases and exported back to the cytosol. Thus, CN/NFAT interactions play a critical role in the peripheral immune/inflammatory response.

In astrocytes, CN and NFAT appear to have many similar functions. Pro-inflammatory factors, excitotoxins (*e.g.* glutamate and ATP), and pathogenic oligomers of Aβ and α-synuclein robustly stimulate CN/NFAT activity in a variety of neural cell types including astrocytes (Sama et al., 2008; Abdul et al., 2009). Once activated, CN/NFAT signaling triggers the production of cytokines that are associated with neurodegeneration *i.e.* IL-6 and TNFα, and has also been shown to downregulate glutamate transporter levels (Van Wagoner et al., 1999; Fernandez et al., 2007; Sama et al., 2008). This can result in a feed-forward cycle of toxic cytokine production and an accumulation of glutamate around synapses, both of which can be detrimental to neurons. Several animal models of injury and disease using commercial calcineurin inhibitors (CNIs) have revealed a reduction of neuroinflammation (Taglialatela et al., 2009; Hong et al., 2010; Rozkalne et al., 2011; Saganova et al., 2012); however, CNIs

have wide volumes of distribution and numerous off-target effects (Marks, 1996; Aliabadi et al., 2007) and thus provide little information about the specific impact of CN signaling in astrocytes. Our work has overcome these difficulties using a small peptide (VIVIT) (Aramburu et al., 1999) directed to astrocytes using adeno-associated virus to specifically inhibit interactions between CN and NFAT. In mouse models of both AD and VCID, inhibition of CN/NFAT interactions ameliorated synaptic function, suggesting that CN/NFAT-mediated activation in astrocytes plays a detrimental role in the commencement and/or progression of neurodegenerative diseases such as AD or VCID (Furman et al. 2012; Pleiss et al. *in preparation*). Using astrocyte-specific AAV-Gfa2-VIVIT to inhibit CN/NFAT in a diet-induced model of VCID will be further explored in Chapter III of this dissertation.

1.5.2 Connexin43

Connexins are membrane-spanning proteins that form hexameric pores used for the transport of small molecules and ions. When unopposed, these hexamers form hemichannels (HCs) that allow for the indiscriminate flow of potassium ions, water, and glutamate between the cytosol and extracellular milieu. A hexamer in direct contact with another hexamer on an adjacent cell, forms a cell-to-cell conduit known as a gap junction (GJ), which allows the shuttling and transfer of small molecules and ions between cells (see Figure 3). In healthy brain tissue, HCs are normally in a closed state while GJs are normally open (Dbouk et al., 2009; Takeuchi and Suzumura, 2014; Moore and O'Brien, 2015; Olsen et al., 2015). However, with neurological insults and diseases this can be reversed, resulting in a leaking of ions/molecules *e.g.* K^+ and glutamate into the extracellular milieu and a loss of communication between cells, both being potentially detrimental to neurons and synapses (Orellana et al., 2009; Koulakoff et al., 2012; Orellana et al., 2012).

Connexin43 (Cx43) is by far the most abundant and ubiquitously expressed connexin across all tissues, and astrocytes are no exception (Solan and Lampe, 2009). The cytosolic C-terminus of Cx43 is thought to be a critical region for regulatory and protein-protein interactions, and is highly regulated by several kinases (Dbouk et al., 2009) *e.g.* protein kinase C (PKC) (Lampe and Lau, 2000) and mitogen-activated protein kinase (MAPK) (Seo et al., 2006). Several studies have shown that changes in phosphorylation state are associated with neurodegenerative conditions such as AD (Lampe and Lau, 2004; Solan and Lampe, 2009; Solan and Lampe, 2014). Work from our lab and others has shown that serine 368 within the Cx43 C-terminus is strongly sensitive to CN activity (Li and Nagy, 2000; Tence et al., 2012; Pleiss et al., *in preparation*). Using an antibody that specifically recognizes Cx43 when dephosphorylated at Ser368, researchers found that levels of dephosphorylated Cx43 were increased in cell cultures under hypoxic conditions. Dephosphorylation of Cx43 was blocked by the addition of commercial CN inhibitors to the culture medium *i.e.* FK506 or cyclosporin A (Li and Nagy, 2000). Together, these results suggest that targeting CN/Cx43 interactions in astrocytes may be a valuable strategy to prevent breakdown of intercellular communication and synaptic function (via HC leakage) during the progression of AD. Chapter IV explores this possibility using human postmortem hippocampal tissues, primary astrocyte cultures, and novel reagents for disrupting CN/Cx43 interactions.

1.6 Summary

Neurodegenerative diseases *i.e.* AD and VCID are often accompanied by robust and striking neuroinflammation, which may significantly contribute to disease processes. Upon activation, astrocytes express unfavorable inflammatory properties and lose many

protective properties, which appears to be mediated, in part, by the activation of CN. The work in my dissertation investigates the role of CN activation and its interactions with downstream targets in neurodegenerative diseases, specifically focusing on AD and VCID. This was accomplished using rat primary astrocyte cell cultures, mouse models of both AD and VCID, as well as human biospecimens from confirmed cases of AD and VCID. My work also explored the use of several novel compounds to study CN activation and to inhibit CN's interactions with its downstream targets. Results showed that CN activation and signaling cascades may play a significant and central role in initiation and/or development of neurodegenerative disease processes like AD and VCID. Together, results suggest that CN activation/signaling is a valuable molecular target for neurodegenerative diseases like AD and VCID.

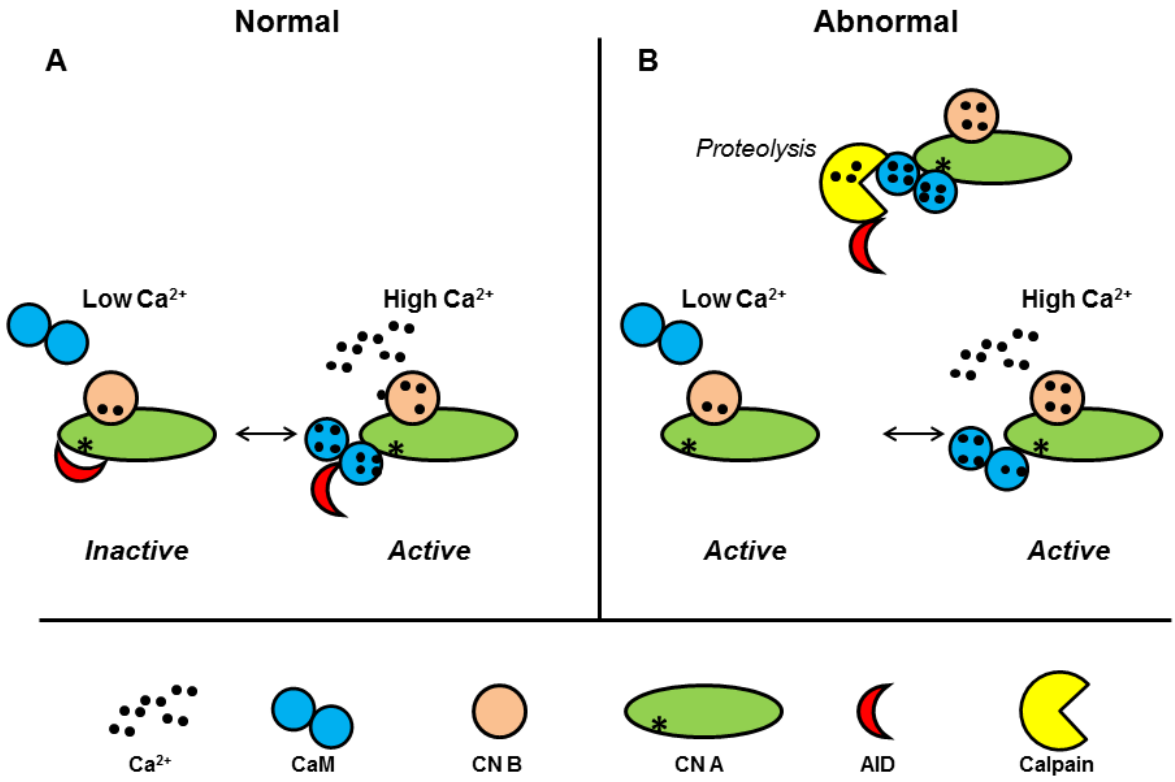

Figure 1.1 Normal versus Aberrant CN Activation. (A) In healthy tissue, CN is extremely sensitive to small changes in intracellar Ca^{2+} levels. Under low intracellular Ca^{2+} levels, an auto-inhibitory domain (AID) covers the catalytic binding site, maintaining CN in an inactive state. Rises in intracellular Ca^{2+} levels cause displacement of the AID, which allows CaM to bind to CN and renders it active. (B) However, with neurodegenerative diseases a profound Ca^{2+} dysregulation occurs resulting in activation of the calcium-dependent cysteine protease, calpain (CP). CP cleaves the AID from CN, exposing the catalytic site and launching it into a state of constitutive and unchecked phosphatase activity independent of intracellular Ca^{2+} levels.

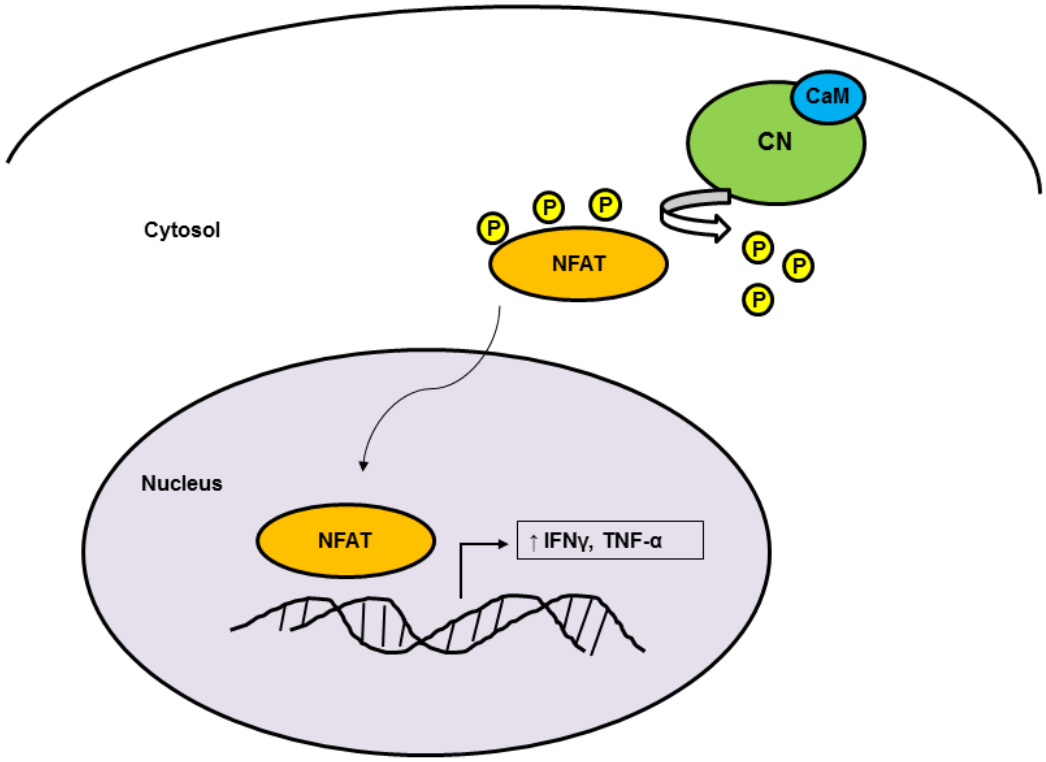

Figure 1.2 NFAT translocation into the nucleus promotes transcription of pro-inflammatory factors. Rises in intracellular Ca^{2+} levels lead to activation of CN via binding of CaM. CN phosphatase activity dephosphorylates the nuclear factor of activated t-cells (NFAT), allowing it to translocate into the nucleus where it promotes the transcription of pro-inflammatory factors *e.g.* TNF-α and IFN-γ.

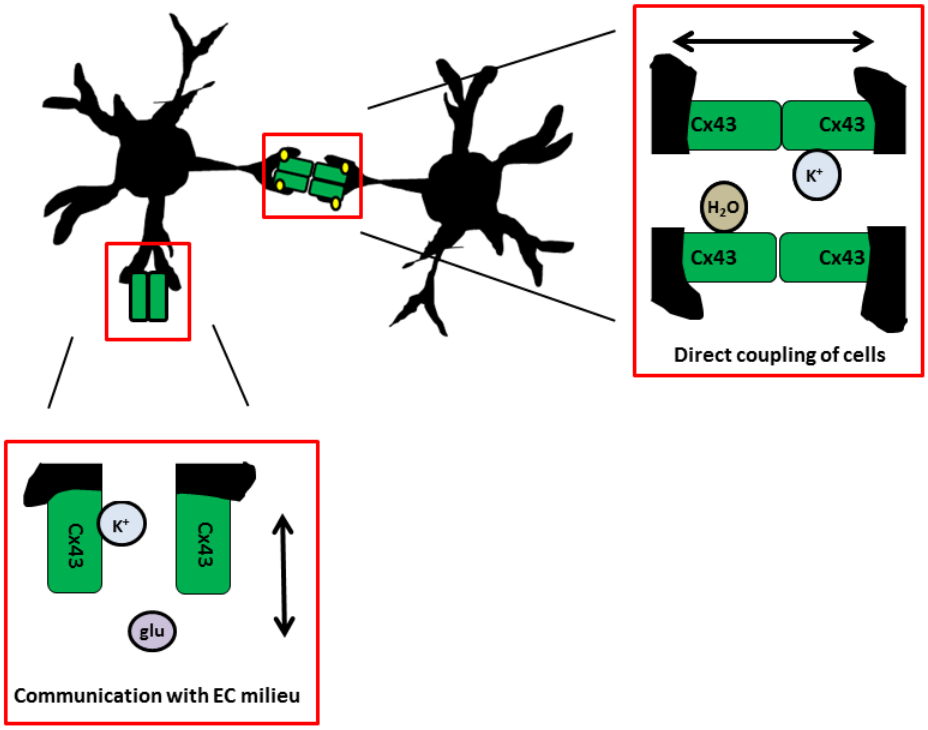

Figure 1.3 Connexin43 hemichannels and gap junctions help form the astrocytic network. Unopposed connexin43 hexamers form hemichannels (HCs) that allow for the passage of small molecules *e.g.* K^+ ions and glutamate between the cell and the extracellular milieu. When connexin43 hexamers are in direct contact with one another, they form gap junctions (GJs) that allow for direct cell-to-cell communication. Both HCs and GJs play a critical role in helping astrocytes maintain the neural metabolic homeostasis.

CHAPTER II: CALCINEURIN PROTEOLYSIS IN ASTROCYTES: IMPLICATIONS FOR IMPAIRED SYNAPTIC FUNCTION

Melanie M. Pleiss[a], Pradoldej Sompol[b], Susan D. Kraner[b], Hafiz Mohmmad Abdul[b], Jennifer L. Furman[a], Rodney P. Guttmann[b], Donna M. Wilcock[b], Peter T. Nelson[b], Christopher M. Norris[b]

[a]Department of Pharmacology and Nutritional Sciences, University of Kentucky, Lexington, KY 40536

[b]Sanders Brown Center on Aging, University of Kentucky, Lexington, KY 40536

2.1 Introduction

Mounting evidence suggests that the hyperactivation of the Ca2+/ calmodulin (CaM) - dependent protein phosphatase calcineurin (CN) is a key contributor to the patho-physiologic and clinical symptoms of Alzheimer's disease (AD) and other neurodegenerative disorders (Norris et al., 2005; Reese et al., 2008; Abdul et al., 2009; Wu et al., 2010; Furman et al., 2012; Rojanathammanee et al., 2013; Rojanathammanee et al., 2015; Taglialatela et al., 2015). The detrimental effects of CN dysregulation may arise through unique alterations in neurons and glial cells (Abdul et al., 2010; Reese and Taglialatela, 2011; Furman and Norris, 2014). In astrocytes and microglia, CN controls immune/inflammatory phenotypes through activation of key transcription factors including nuclear factor of activated T cells (NFAT), nuclear factor κB (NFκB), and FOXO, among others (Fernandez et al., 2007; Canellada et al., 2008; Sama et al., 2008; Abdul et al., 2010; Fernandez et al., 2012; Fernandez et al., 2016). Previously, we showed that the selective blockade of astrocytic CN/NFAT signaling with the NFAT-inhibitory peptide, VIVIT, suppresses markers of glial activation, alleviates amyloid pathology, and protects against cognitive deficits in experimental models of AD (Sama et al., 2008; Abdul et al., 2009; Furman et al., 2012) and prevents synapse dysfunction in models of AD and acute brain injury (Furman et al., 2012; Furman et al., 2016). These results suggest that astrocytes are a key locus of hyperactive CN signaling during the progression of AD. However, little is known about the mechanisms that lead to or sustain aberrant astrocytic CN/NFAT signaling.

Hyperactivation of CN in other cell types, including neurons and cardiomyocytes, can arise from the disruption, or proteolytic removal, of a critical autoinhibitory domain (AID) located near the C-terminus of the CN catalytic subunit (CN A) (for review, see

Norris, 2014). Normally, when Ca^{2+} levels are low, the AID strongly limits phosphatase activity until it is displaced from the catalytic site by Ca^{2+}/CaM (Perrino et al, 1995). Proteolytic removal of the AID by the cysteine protease, calpain (CP), can occur after cellular insults and large surges in intracellular Ca^{2+} (Wu et al., 2004). Without the AID, CN A is largely, and irreversibly uncoupled from local Ca^{2+} gradients, resulting in elevated phosphatase activity, whether normal levels of Ca^{2+} are restored or not (Wu et al., 2004). Many commercial antibodies to the C-terminus of CN A recognize full length CN (FL-CN, ~60 kDa), but fail to detect CN proteolytic fragments (i.e. ΔCNs) because the epitope is located in the region that is cleaved away. In contrast, N-terminus antibodies identify both FL-CN and ΔCNs. Use of Western blot techniques and N-terminus CN antibodies has revealed the presence of ΔCNs in whole brain tissue under several neurodegenerative conditions (Huang et al., 2005; Liu et al., 2005; Shioda et al., 2006; Shioda et al., 2007; Wu et al., 2010; Rosenkranz et al., 2012). Previous work from our group on human subjects with mild cognitive impairment revealed elevated hippocampal levels of a ΔCN fragment in the 45-48 kDa range (Abdul et al., 2011). A similar fragment was generated in mixed (neurons and glia) primary hippocampal cultures, coincident with elevated NFAT activity and frank neuronal degeneration, following treatment with oligomeric amyloid-β peptides. The appearance of ΔCN at early stages of neurologic dysfunction suggests that CN proteolysis is more than a biomarker of neurodegeneration, and may be an antecedent for later neurodegenerative events.

Unfortunately, because of the cell-type heterogeneity of whole brain homogenates, it's nearly impossible to discern where (i.e. in what cell type) CN proteolysis is occurring. In immunohistochemical (IHC) applications, N terminus antibodies reveal the presence of CN in multiple cell types, including activated astrocytes (Norris et al., 2005; Abdul et al., 2009). However, it remains unclear whether the labeled CN is of the intact, full-length

variety or of the proteolyzed, highly active variety. To resolve this issue, we generated custom antibodies to CN A based on previously identified CP-cleavage sites (Wu et al., 2004). One of these antibodies selectively detected a 45-48 kDa fragment (∆CN) in Western blot assays. IHC investigations of human brain tissue revealed the presence of ∆CN in numerous astrocytes, especially those associated with Aβ deposits and microinfarcts. Adeno-associated virus (AAV)-mediated delivery of a similar ΔCN fragment to hippocampal astrocytes of healthy adult rats caused a reduction in CA1 synaptic strength. Together, the results are consistent with the hypothesis that CN dysregulation in activated astrocytes is attributable, in part, to limited proteolysis. Moreover, the presence of proteolyzed CN in astrocytes appears to be sufficient for disrupting synaptic function, indicating a possibly critical mechanism for synaptic decline in AD and other neurodegenerative conditions.

2.2 Methods

2.2.1 ∆CN antibody production and purification. Peptides based on known CP dependent cleavage sites (Wu et al., 2004) were generated by PrimmBiotech (West Roxbury, MA) and used to inoculate adult rabbits. Antisera from rabbits inoculated with the peptide, ESVLTLK (amino acid sequence immediately upstream of the 48 kDa CN cleavage site) detected a 45-48 kDa fragment in initial Western blot assays. The antisera were then purified using a negative selection approach. In brief, the ESVLTLK peptide was coupled to HiTrapTM NHS-activated HP columns (GE Healthcare, Little Chalfont, United Kingdom) followed by addition of antisera. Antibodies were then eluted and collected according to manufacturer instructions. Following a second round of column-purification, the eluate was aliquoted and frozen for additional Western blot screening.

2.2.2 Primary cell culture. Primary mixed (astrocytes and neurons) hippocampal cultures were prepared from embryonic day 18 Sprague-Dawley rat pups as described previously (Porter et al., 1997; Norris et al., 2006; Sama et al., 2008). Cells were investigated at between 14 and 21 days in vitro (DIV). To generate CN proteolysis, cultures plated in 35 mm dishes were treated for 24 h with synthetic oligomeric β-amyloid 1-42 (Aβ1-42) peptides (~65 nM) prepared as described in our previous work (Abdul et al., 2009; Abdul et al., 2011). Aβ1-42 was delivered in the presence or absence of the CP inhibitor, calpeptin (10 μM), obtained from EMD Millipore (Gibbstown, NJ). Calpeptin was added to cultures approximately 2 h prior to the addition of Aβ1-42.

2.2.3 Western blot analysis. At 24 h post- Aβ treatment, cells were homogenized in high sucrose buffer and protein concentration determined using the Lowry method. Samples were loaded onto a Bio-Rad gradient gel (4-20%) with protein concentrations held constant across lanes. Proteins were resolved by electrophoresis and transferred to PVDF membranes for Western blot analysis. Membranes were blocked then incubated overnight at 4°C in the following primary antibodies: 1:3000 anti-CN-Aα (Millipore) and 1:1000 anti-ΔCN (custom). Primary antibodies were labelled with appropriate HRP-conjugated secondary antibodies and detected using the ECL Plus Western Blotting system (GE Healthcare). Relative molecular weights of full length CN and ΔCN were quantified using a Bio Rad Chemidoc XRS Gel imager and Quantity One Software (Hercules, CA).

2.2.4 Human biospecimens. Post-mortem brain specimens from the amygdala, hippocampus, and superior and middle temporal gyri (SMTG) were obtained from the University of Kentucky Alzheimer's Disease Center (UK-ADC) Tissue Repository. Amygdala and hippocampal specimens from 6 different AD cases and 2 different age-matched control cases were investigated. SMTG biospecimens were from five individual subjects. All subjects were participants in the UK-ADC Autopsy program. Postmortem autopsy intervals for UK-ADC samples, including the ones used in this study, is approximately 3 hours (e.g. see [Nelson et al., 2007; Abdul et al., 2009; Abdul et al., 2011]). The presence of AD pathology (amyloid plaques and neurofibrillary tangles) and vascular pathology (microinfarcts) in all human cases was confirmed by personnel in the UK-ADC neuropathology core.

2.2.5 Histology. Paraffin-embedded SMTG sections were cut to ~8 µm thickness and baked overnight at 40°C. Sections were deparaffinized in fresh Xylene and rehydrated through a series of graded alcohols to water. Sections were dipped into Harris's hematoxylin for 4 minutes then rinsed in running water. Following a water rinse, sections were dipped twice into acid alcohol, rinsed in running water, dipped twice into 1% ammonia water, and rinsed in water for 10 minutes. Sections were dipped into Eosin solution for 15-20 seconds and then dehydrated through graded alcohols, cleared using Xylene, and mounted.

2.2.6 Immunohistochemistry. Amygdala, hippocampal, and SMTG specimens were fixed in 10% formaldehyde, embedded in paraffin, and cut into ~8 µm thick sections. Slides were baked in a 40°C oven overnight, deparaffinized using SafeClear (Fisher

Scientific), and rehydrated through a series of graded alcohols to water. Slides were boiled for 10 minutes in Borg Decloaker antigen retrieval solution, pH = 6.0 (Biocare Medical) before blocking endogenous peroxidase activity with 3% hydrogen peroxide + 10% methanol. The slides were blocked (0.1 M Tris buffer with 0.1% Triton X-100 and 2% bovine serum albumin) and incubated overnight at 4°C in the following primary antibodies: 1:25 rabbit polyclonal anti-ΔCN; 1:500 mouse monoclonal anti-CN-Aα (C-terminus) (Sigma); 1:50 mouse monoclonal anti-Aβ (Vector Laboratories. Secondary antibodies were added at a 1:200 dilution for 1 hour at room temperature as follows: anti-mouse IgG + horse normal serum or anti-rabbit IgG + goat normal serum. Following secondary antibody, signal was amplified with avidin-biotin complex for 1 hour at room temperature and then detected using either DAB or SG substrates (Vector Laboratories). Following dehydration through a series of graded alcohol and clearing (SafeClear), slides were permanently mounted using VectaMount (Vector Laboratories) and coverslipped.

2.2.7 Immunofluorescence. Amygdala, hippocampal, and SMTG sections were fixed in 4% paraformaldehyde and preserved in sucrose buffer. Slices were cut on a freezing microtome to 50μM thickness. Free-floating sections were blocked (0.1 M Tris buffer with 0.1% Triton X-100 and 2% bovine serum albumin) and incubated overnight at 4°C with primary antibodies including: 1:25 anti-ΔCN; 1:50 anti-GFAP directly conjugated to Alexa 594 (Cell Signaling); 1:100 anti-NeuN (Millipore). After washing, sections were incubated 1:500 in Alexa Fluor 488 or 594 secondary antibodies (Life Technologies). Fluorescent sections were mounted with ProLong Gold Antifade Reagent with DAPI (Molecular Probes) and coverslipped.

2.2.8 Animals. Adult male Sprague Dawley rats were obtained from Harlan Laboratories (Indianapolis, IN). Rats were held in standard laboratory cages under 12-h light/12-h dark cycles in a pathogen free environment in accordance with University of Kentucky guidelines. The animals had access to food and water ad libitum. All animal procedures were conducted in accordance with the National Institutes of Health Guide for the Care and Use of Laboratory Animals and were approved by University of Kentucky Institutional Animal Care and Use Committees.

2.2.9 Intrahippocampal delivery of adeno-associated virus (AAV). cDNA encoding the first 398 amino acids of the CN Aα isoform (ΔCN), which lacks the Ca2+/CaM binding domain and the AID (Kincaid et al., 1990), was subcloned into the polylinker site of a hybrid pCI vector containing IRES2-DsRed-Express (Clontech, Mountain View, CA). IRES-DsRed2 (control construct) or ΔCN-IRES-DsRed2 were then inserted into pAAV2-Gfa104-EGFP (University of Pennsylvania Vector core) in place of EGFP. High titer (1012 IFU/mL) AAV vectors (AAV-Gfa104-DsRed and AAV-Gfa104-ΔCN) were then generated in the University of Kentucky Vector core using an AAV5 helper plasmid and HEK293 cells. The Gfa104 promoter has been characterized previously, and has been shown to drive transgene expression selectively in astrocytes of intact animals (Ortinski et al., 2010; Cui et al., 2014), similar to that seen with the Gfa2 promoter (*e.g.* see Furman et al., 2016).

Rats were placed in a stereotaxic frame (David Kopf Instruments Tujunga, CA) and anesthetized with isoflurane (2.5%) throughout the surgery process. For each rat, AAV-Gfa104-DsRed and AAV-Gfa104-ΔCN were loaded into separate microinjectors and delivered into alternate hemispheres, such that one hippocampus was treated with Gfa104-DsRed and the other hippocampus was treated with Gfa104-ΔCN. Each

hemisphere was injected with 4 µL of AAV (1012 IFU/mL) at 0.2 µL/min. Injection coordinates were -3.8mm anteroposterior and +1.8mm mediolateral relative to bregma, and -1.8mm dorsoventral relative to dura. DsRed visualization in formaldehyde-fixed tissue sections was achieved using a rabbit polyclonal antibody to red fluorescent protein (Abcam) and Alexa Fluor secondary antibodies as described above for human sections.

2.2.10 Hippocampal slice electrophysiology. At 4 months after AAV injection, rats were euthanized under CO_2 anesthesia and decapitated. Brains were rapidly removed and placed in ice-cold, oxygenated (95% O2, 5% CO2) artificial cerebrospinal fluid (ACSF) containing (in mM) 124 NaCl, 2 KCl, 1.25 KH2PO4, 2 MgSO4, 0.5 CaCl2, 26 NaHCO3, and 10 dextrose (pH 7.4). Brains were hemisected and glued to a specimen mounting block and submerged in oxygenated, ice-cold ACSF. Brains were then sectioned coronally into ~400 µm slices using a Vibratome® 1000 (Leica Biosystems, Buffalo Grove, IL) and transferred to a custom interface holding chamber (Mathis et al., 2011) and incubated with warmed (32° C) oxygenated ACSF containing 2 mM CaCl2 until electrophysiological recordings (usually 1.5-5 h).

Slices were transferred to a Kerr Tissue Recording system (Kerr Scientific Instruments, Christchurch, New Zealand) and submerged in warmed (~32° C) oxygenated ACSF containing 2mM CaCl2 and 2mM MgSO4. Schaffer collaterals were activated with a bipolar stainless steel electrode located in *stratum radiatum*. Stimulus intensity was controlled by a constant current stimulus isolation unit (World Precision Instruments, Sarasota, FL), and stimulus timing was controlled by LabChart 8 software (ADInstruments Inc., Colorado Springs, CO). Field potentials were recorded in CA1 *stratum radiatum* using a Ag/AgCl wire located ~1-2 mm from the stimulating electrode.

Field potentials were amplified 100X and digitized at 10kHz using the Kerr Tissue Recording System amplifier and a 4/35 PowerLab analog-to-digital converter (ADInstruments). To assess basal synaptic strength, 100 μs stimulus pulses were given at 12 intensity levels (range 25–500 μA) at a rate of 0.1 Hz. Five field potentials at each level were averaged, and measurements of fiber volley (FV) amplitude (in mV) and excitatory postsynaptic potential (EPSP) slope (mV/ms) were performed offline using LabChart 8 software. Synaptic strength curves were constructed by plotting EPSP slope values against FV amplitudes for each stimulus level. Curves were fit with a three parameter sigmoidal equation using SigmaPlot 12 software (Systat Software Inc. San Jose, CA) (Norris et al., 2016). Curve parameters included maximal EPSP amplitude (Max), curve slope, and the FV amplitude associated with the half-maximal EPSP amplitude (half-Max). Maximal synaptic strength for each slice was also estimated by taking the maximal EPSP slope amplitude during the input/output curve and dividing by the corresponding FV amplitude. To estimate population spike (PS) threshold, the EPSP slope amplitude at which a population spike first appeared in the ascending phase of the field potential was calculated and averaged across five successive trials at the spike threshold stimulation level.

2.2.11 Statistics. For slice electrophysiology studies, one to three slices from each hemisphere (either the Gfa104-DsRed or the Gfa104-ΔCN-treated hemisphere) were analyzed. Synaptic measures were averaged across all slices within each hemisphere and these averaged values were compared across hemispheres using paired T-tests, with significance set at $p < 0.05$.

2.3 Results

2.3.1 Custom antibody shows greater selectivity to a ΔCN fragment. The CN A subunit is a 521 amino acid protein consisting of a catalytic domain and an autoinhibitory domain (AID), as well as binding sites for the CN B regulatory subunit and Ca^{2+}/calmodulin (Ca^{2+}/CaM) (Hashimoto et al., 1990; Kincaid et al., 1990, see Figure 1). Proteolysis of CN A near the carboxy-terminus by calpains results in the disruption or removal of the AID leading to reduced Ca^{2+} sensitivity and constitutive phosphatase activity (Wu et al., 2004). Calpain-mediated generation of 45 and 48 kDa ΔCN fragments are found at elevated levels in human brain tissue during cognitive decline, are triggered by oligomeric Aβ, and are causatively linked to greater CN signaling and neurodegeneration (Wu et al., 2004; Abdul et al., 2011).

CN A antibodies that target epitopes between amino acid residues 425 and 521 (*i.e.* C terminus antibodies) recognize full length CN (FL-CN), but do not detect ΔCN fragments and may therefore fail to identify important pathological changes in CN regulation. In contrast, N terminus-directed antibodies identify CN proteolysis in Western blot applications, but do not distinguish between FL-CN and ΔCN in immunohistochemical applications, making it difficult to pinpoint where CN proteolysis occurs in a heterogeneous cell population. We therefore set out to make new antibody reagents with greater selectivity to ΔCN, relative to FL-CN. Peptides composed of amino acids found immediately upstream of calpain-dependent cleavage sites (Wu et al., 2004) were used to immunize rabbits (Figure 2.1). Antisera generated by immunization with the ESVLTLK peptide, found immediately upstream from lysine 424, revealed a 45-48 kDa band in preliminary Western blots (not shown) and was therefore subjected to further affinity purification (see Methods) to obtain ΔCN antibodies (Figure 2.1A,B). We then performed Western blots (Figure 2.1C) on whole cell lysates obtained from rat primary mixed

(neurons + glia) hippocampal cultures exposed to oligomeric Aβ peptides (65 nM for 24 h) to stimulate CN proteolysis, as described in our earlier work (Abdul et al., 2011). The same samples were processed in parallel for Western blot using a commercially available N terminus CN antibody for comparison. Both antibodies showed diffuse labeling in the 70-75 kDa range. However, unlike the ΔCN antibody, the N terminus antibody showed a prominent band in the 60 kDa range (where FL-CN is found) in untreated cultures, along with lower molecular weight bands between 25 and 37 kDa (Figure 2.1C, lane 5). Both antibodies revealed bands in the 45-48 kDa range when cultures were treated with oligomeric Aβ (Figure 2.1C, lanes 2 and 6), the appearance of which was blocked by co-application of the calpain inhibitor, calpeptin (Figure 2.1C, lanes 3 and 7), but not by the caspase inhibitor Z-YVAD (Figure 2.1C, lanes 4 and 8). Together, these data demonstrate that, relative to the N-terminus antibody, the ΔCN antibody shows far greater selectivity to calpain-dependent CN proteolytic products in the 45-48 kDa range.

2.3.2 Astrocytes in AD brain tissue are labeled intensely with the ΔCN antibody.

Western blot analyses have shown elevated levels of ΔCN in brain homogenates from human subjects with mild-cognitive impairment (Abdul et al., 2011) or AD (Wu et al., 2010), relative to age-matched non-demented human subjects. Though CN is primarily found in neurons, it can also appear at high levels in activated astrocytes during injury and disease, especially around Aβ deposits (Norris et al., 2005; Celsi et al., 2007; Abdul et al, 2009). To determine if ΔCN is found in activated astrocytes, we immunohistochemically (IHC) labeled human postmortem brain sections (encompassing the amygdala and overlying entorhinal cortex) from subjects with confirmed AD (see Methods). These brain regions show high levels of CN expression in healthy adult

animals (Goto et al., 1986; Kuno et al., 1992), and exhibit extensive amyloid and neurofibrillary tangle pathology during AD (Kromer Vogt et al., 1990). Concurrent with AD-related pathological changes, these brain regions also show widespread GFAP labeling indicative of gliosis, or astrocyte activation (Murphy et al., 1992 and see Figure 2.2A).

In IHC applications, the ΔCN antibody provided excellent labeling intensity with low background (Figure 2.2B-E). With rare exceptions (see arrow in Figure 2.2E), most of the labeled cells exhibited a clear astrocyte morphology, with thick ramified processes, characteristic of astrocyte activation (Figure 2.2B, 2.2C). Unlike the GFAP antibody, which provided labeling across most of the tissue (Figure 2.2A), the ΔCN antibody generally provided only faint labeling, except for numerous discrete regions characterized by astrocyte "clusters" (Figure 2.2B and C). Cells within these clusters showed intense labeling, which appeared throughout the soma and usually throughout several major processes (Figure 2.2C). Many of the most intensely labeled astrocytes were in close juxtaposition to blood vessels (Figure 2.2D, arrow). Co-staining with an antibody to Aβ showed that many ΔCN-positive clusters occurred around extracellular amyloid plaques (Figure 2.2E), suggesting that the proteolysis of CN in astrocytes is strongly coupled to amyloid pathology, consistent with previous reports (Wu et al., 2010; Abdul et al., 2011).

In contrast to the conspicuous labeling patterns shown in human AD tissue, staining with the ΔCN antibody appeared much less prominent in the amygdala of age-matched control subjects (Figure 2.7). We also observed sparse labeling when tissue sections were incubated with the ΔCN antibody alone (*i.e.* without secondary antibody, Figure 2.7) or with the ΔCN antibody plus ESVLTLK blocking peptide (Figure 2.2F and 2.2G). These results demonstrate that antibody labeling was specific.

Finally, to confirm that ΔCN is definitively expressed in astrocytes, AD amygdala sections were co-labeled with a GFAP antibody and confocal microscopy was used to assess co-localization. As illustrated in Figures 2.2H-K, GFAP and ΔCN were co-localized in numerous cells. Note, however, that ΔCN was not present in all GFAP positive cells. For instance, arrowheads in Figures 2.2H-J show two immediately adjacent astrocytes, with one cell expressing ΔCN and the other cell apparently devoid of ΔCN (also see Figure 2.2K). These images, along with the immunohistochemical evidence shown in Figures 2.2B-2.2E highlight the heterogeneous nature of CN proteolysis in astrocyte populations associated with AD pathology.

As mentioned, a relatively small number of ΔCN-positive cells in the amygdala exhibited a clear neuronal morphology (see Figure 2.2E, arrow). As a further attempt to explore neuronal labeling with the ΔCN antibody, we investigated hippocampal sections using both immunohistochemistry and confocal microscopy. The hippocampus is advantageous for immunohistochemical investigations because its neurons are densely packed into discrete layers and are easy to identify, even in unstained tissue. Moreover, studies from our group have reported signs of hyperactive CN signaling in the hippocampus during the progression of AD (Abdul et al., 2009; Abdul et al., 2011).

As shown in Figures 2.3A and B, neurons in the CA1 and dentate granule layers of AD subjects showed abundant expression of the full length form of CN (Goto et al., 1986; Kuno et al., 1992), as revealed using a commercial antibody to the CN carboxyl terminus. The ΔCN antibody also labeled neurons, albeit more sparsely (Figure 2.3C and 2.3D) than the commercial antibody. Similar to amygdala sections, hippocampal tissue from control subjects provided little to no labeling (Figure 2.7). When present, ΔCN expression was generally limited to the somal and proximal apical dendritic regions (for CA1 pyramidal neurons), and tended to be faint, even when other structures in the

same region, including perivascular elements (Figure 2.3C) and astrocytes (inset, Figure 2.3D), were strongly labeled. In many neurons, ΔCN co-localized with the nuclear marker, NeuN, which is consistent with earlier work that found elevated levels of proteolyzed CN in nuclear extracts from AD subjects (Wu et al., 2010). Thus, while activated astrocytes appear to provide the most striking ΔCN labeling patterns associated with AD, these cells are not the only source for CN proteolysis.

2.3.3 Association of ΔCN with microinfarcts. In addition to AD, ΔCN fragments have been observed in a number of other neurodegenerative conditions, particularly those caused by vasculature disruption and/or occlusion (Shioda et al., 2006; Shioda et al., 2007; Rosenkranz et al., 2012). Vascular pathology is highly co-morbid with AD pathology and likely exacerbates cognitive decline with the progression of AD (Kalaria et al., 2012; van Norden et al., 2012; Raz et al., 2016; Corriveau et al., 2016; Nelson et al., 2016; Vemuri and Knopman, 2016; Wilcock et al., 2016). Mounting evidence suggests that microinfarcts are among the most common and insidious contributors to vascular cognitive impairment and dementia (VCID) (Smith et al., 2012; Kapasi and Schneider, 2016). Moreover, microinfarcts are commonly enveloped by activated astrocytes (Wang et al., 2012; van Veluw et al., 2015).

To determine whether the appearance of ΔCN coincides with vascular disruption, we investigated cortical brain sections from subjects with confirmed microinfarct pathology. Figure 2.4A-E shows ΔCN labeling in SMTG sections from a 90 year old human subject with multiple microinfarcts, but little-to-no AD pathology (Braak stage II). At low magnification, several discrete regions show very intense ΔCN labeling (Figure 2.4A). The region marked by the arrowhead in Figure 2.4A is shown at higher magnification in an H&E labeled serial section in Figure 2.4B and confirms the presence of a microinfarct

approximately 400 μm in greatest dimension (approximate center shown with arrow). This microinfarct is surrounded by numerous cells intensely labeled for ΔCN (Figure 2.4C), many of which exhibit clear activated astrocyte histomorphology (Figures 2.4D-E). When the ΔCN antibody was delivered in the presence of the ESVLTLK peptide (Figure 2.4F and 2.4G), cellular labeling was greatly diminished, confirming binding specificity. Interestingly, ΔCN-positive microinfarcts were not labeled with a commercial C-terminus-directed antibody that selectively detects full length CN (Figure 2.4H and I). Note, however, that the C-terminus antibody does label neurons within the same brain section (Figure 2.8). Thus, microinfarcts appear to be more strongly associated with proteolyzed CN than with full-length CN.

Confocal micrographs showed that ΔCN was associated with both activated astrocytes and neurons in the immediate vicinity of microinfarcts (Figure 2.5). ΔCN localization to astrocytes was most prominent around the microinfarct core, with expression diminishing with increasing distance from the injury (Figure 2.5A-2.5D). For neurons, ΔCN was most highly expressed within the microinfarct core, though many ΔCN/NeuN positive cells could also be found outside the core as well (Figure 2.5E-H). Together; these observations demonstrate that CN proteolysis can occur in the immediate vicinity of small vessel pathology in the human brain.

2.3.4 Forced overexpression of ΔCN in astrocytes of intact rats disrupts synaptic function. The consequences of CN proteolysis in neurons have been investigated in many different model systems (Norris, 2014). Conversely, little is known about the functional outcomes of CN proteolysis in astrocytes. Hyperactivation of CN signaling in astrocytes has been linked to the elevated expression of inflammatory mediators, impaired glutamate regulation, Aβ production, and altered astrocytic Ca^{2+} dynamics

(Norris et al., 2005; Fernandez et al., 2007; Canellada et al., 2008; Sama et al., 2008; Jin et al., 2012; Grolla et al., 2013; Norris, 2014). Using adeno-associated virus (AAV) vectors, equipped with astrocyte specific promoters, we have shown that the selective inhibition of astrocytic CN/NFAT signaling provides numerous beneficial effects in a mouse model of AD (Furman et al., 2012), and a rat model of traumatic brain injury (Furman et al., 2016). These results suggest that hyperactivation of CN in astrocytes can mediate and/or exacerbate pathophysiological processes.

One of the primary responsibilities of astrocytes is to regulate synaptic transmission and plasticity (Allen, 2014). Since we previously found that inhibition of astrocytic CN/NFAT signaling protects multiple synaptic properties, we sought to test whether the presence of ΔCN in astrocytes is sufficient to drive synaptic dysfunction. AAV2/5 vectors expressing ΔCN-DsRed2 or DsRed2 alone (control vector) were injected into the hippocampus of adult rats. One hemisphere received ΔCN and the other hemisphere received DsRed2 control vector (Figure 2.6A). The ΔCN used here lacks the CN AID, is nearly identical in size to the ΔCN fragment found in human AD brain (Figures 2.2 and 2.3, and see Furman et al., 2012), and shows increased phosphatase activity when expressed in many different cell types (Wang et al., 1999; De Windt et al., 2000; Friday et al., 2000; Norris et al., 2010), including primary astrocytes (Sama et al., 2008). Both ΔCN and DsRed2 were transcriptionally regulated by a truncated human GFAP promoter (Gfa104), which provides astrocyte-specific expression (Ortinski et al., 2010; Cui et al., 2014). Using confocal microscopy and/or immunodepletion assays, we previously showed that AAV-mediated expression of EGFP was driven exclusively in astrocytes (in mice and rats) when a similar Gfa2 promoter was used (Furman et al., 2012; Furman et al., 2016). Consistent with these observations, immunofluorescent

labeling of the DsRed2 tag in the present study was limited to astrocytes and showed no co-localization with the neuron-specific protein MAP2b (Figure 2.6B).

At 4 months post-AAV injection, brain slices from both hemispheres were harvested and processed in parallel for the electrophysiological assessment of basal CA3-CA1synaptic strength. Field EPSP slopes were recorded in CA1 *stratum radiatum* and plotted against corresponding FV amplitudes at 12 different stimulus intensities to generate synaptic strength curves (Figure 2.6C, D). Compared to slices from the DsRed2 control vector-treated hemisphere, slices from the ΔCN-treated side exhibited depressed synaptic strength curves (Figure 2.6D) with a corresponding reduction in the maximal EPSP/FV ratio (p <0.05, Figure 2.6E). Further analyses of synaptic strength curve parameters revealed a significant reduction in the maximal EPSP amplitude (p <0.05), but did not find any differences in the slope of the curve or in the FV amplitude necessary for half-maximal EPSP amplitude (Figure 2.6F). Finally, while the evoked field EPSP was reduced in slices from the ΔCN-treated hemisphere, these slices were also generally more excitable as indicated by a reduced population spike (PS) threshold (Figure 2.6G). A similar reduction in the PS threshold has been reported in APP/PS1 mice (Furman et al., 2012) and may be indicative of neuronal hyperexcitability. Together, these results suggest that the presence of ΔCN in astrocytes is sufficient to drive synaptic dysfunction in intact animals.

2.4 Discussion

CN proteolytic fragments show abnormally high levels of phosphatase activity under resting Ca^{2+} levels and are associated with numerous forms of neurologic injury and disease (Norris, 2014). Using a novel antibody generated to the ΔCN proteolytic

fragment, the present study has provided some of the first evidence that CN proteolysis can occur extensively in astrocytes associated with AD and small vessel pathology. Furthermore, overexpression of the ΔCN fragment in astrocytes of otherwise healthy adult animals causes synaptic deficits. The results demonstrate that proteolysis may be an important source of CN dysregulation in astrocytes leading to altered astrocyte function and neural dysfunction with the progression of neurodegenerative disease.

2.4.1 Importance of antibody selection for assessing CN expression/activity in disease. The proteolysis of CN was first shown under *in vitro* conditions, but has subsequently been demonstrated to occur in intact nervous tissue after cellular insult (Wu et al., 2004; Huang et al., 2005; Shioda et al., 2006; Shioda et al., 2007; Abdul et al., 2011; Rosenkranz et al., 2012). Using an antibody directed to the N terminus of CN A, Wu et al. (2004) showed that at least three distinct CN A fragments are generated *in vivo* in response to cellular injury and high levels of calpain activity. The 48 and 45 kDa fragments generated by calpain-dependent proteolysis are fully-functional enzymes that show high activity at low (resting) Ca^{2+} levels due to the absence of an AID that normally keeps CN activity in check. High levels of CN proteolysis can dramatically alter cellular function and viability (Wang et al., 1999; Wu et al., 2004; Abdul et al., 2011), which highlights the importance of choosing the appropriate antibody to investigate CN functions in CNS injury and disease. In particular, C-terminus directed antibodies to CN A only detect full length CN and may give the impression that CN expression is reduced, rather than proteolytically activated, under neurodegenerative conditions. The use of C-terminus antibodies may explain why early reports observed reductions in CN A levels and activity in AD tissue (Billingsley et al., 1994; Ladner et al., 1996; Lian et al., 2001; Karch et al., 2013).

While N-terminus antibodies are useful in Western blot applications for determining the extent of CN proteolysis in whole brain tissue, they do not specify which cell types give rise to CN proteolysis, nor do they determine whether proteolysis occurs selectively in the close proximity of specific pathological markers. Furthermore, because of the vast cellular heterogeneity of the CNS, changes in proteolysis for any one cell type may be masked or diluted in biochemical analyses of whole tissue homogenates. This problem severely limits mechanistic insights into the downstream consequences of CN proteolysis, primarily because CN is expressed in many different cell types (Goto et al., 1986; Kuno et al., 1992; Hashimoto et al., 1998; Norris et al., 2005; Celsi et al., 2007; Abdul et al., 2009), each of which can use CN for unique functions. For example, when expressed in neurons using gene delivery techniques, ΔCN causes alterations in synaptic function, Ca^{2+} channel dysregulation, degeneration of neurites, and apoptosis (Kromer Vogt et al., 1990; Celsi et al., 2007; Smith et al., 2012; Norris, 2014; Rojanathammenee et al., 2015; van Veluw et al., 2015; Kapasi and Schneider, 2016).

Astrocytes may also be an important source for CN dysregulation (Furman and Norris, 2014), which is notable given the increasing attention astrocytes have received for their contributions to neurologic dysfunction during aging, injury, and disease (Hamby and Sofroniew, 2010; Pekny and Pekna, 2014; Verkhratsky et al., 2012; Verkhratsky et al., 2015). Overexpression of ΔCN in astrocytes leads to the production and release of a variety of immune factors (*e.g.* cytokines and chemokines) linked to glial activation and neuroinflammation (Norris et al., 2005; Fernandez et al., 2007; Sama et al., 2008). While many of these cell-specific processes arise in neurodegenerative diseases, and are blocked by both calpain and CN inhibitors (Norris, 2014), it has been unclear if (and to what extent) CN proteolysis actually occurs in these cell types during the disease process.

The ΔCN antibody was designed with the intent to identify the cellular source for CN proteolysis in diseased and/or injured brain tissue. This antibody showed much greater selectivity to calpain-generated CN fragments than to full-length CN (Figure 2.1C) in Western blot applications and was associated with high-signal to background labeling in IHC applications (*e.g.* see Figures 2.2 and 2.4). When incubated with postmortem human brain sections from confirmed AD cases, the ΔCN antibody provided intense labeling of astrocyte clusters, many of which were in close juxtaposition to Aβ deposits and/or blood vessels (Figure 2.2). Previously, we observed a similar co-localization of CN to activated astrocytes in amyloidogenic mice and human AD brain tissue using N-terminus antibodies, which identify both full length and proteolyzed CN (Norris et al., 2005; Abdul et al., 2009). The findings of the present study suggest that the elevated activity of CN and/or CN-dependent signaling mediators (*e.g.* NFAT) reported earlier for AD mouse models and human AD cases (Reese et al., 2008; Abdul et al., 2009; Wu et al., 2010; Abdul et al., 2011) may arise, at least partly, from the calpain-dependent proteolysis of CN in astrocytes.

2.4.2 ΔCN and Microinfarcts. ΔCN labeling was also particularly intense for astrocytes in human cases characterized by extensive vascular pathology (Figure 2.4). Microinfarcts, in particular, are increasingly recognized as a key mechanism for dementia (Smith et al., 2012; Kapasi and Schneider, 2016). Though etiologically distinct from AD pathology, microinfarcts and other forms of vascular pathology show high comorbidity with AD, where they appear to exacerbate neurodegenerative processes and hasten cognitive decline (Kalaria et al., 2012; van Norden et al., 2012; Raz et al., 2016; Corriveau et al., 2016; Nelson et al., 2016; Vemuri and Knopman, 2016; Wilcock et al., 2016). Microinfarcts are often defined by extensive gliosis surrounding the core,

including profound astrocyte activation (Wang et al., 2012; van Veluw, 2015). Similar to Aβ plaque-associated astrocytes, we found that activated astrocytes surrounding microinfarcts were intensely labeled with the ΔCN antibody (Figure 2.4), suggesting that small vascular pathologies can result in aberrant CN proteolysis, which may, in turn, contribute to further glial activation and/or elevated levels of harmful neuroinflammatory factors (Sama et al., 2008). While many of the ΔCN-labeled cells around microinfarcts had activated astrocyte morphology, it's possible that GFAP-negative astrocytes, activated microglia, and/or infiltrating immune cells are also an important source of ΔCN. Microglia, in particular, express numerous CN-dependent substrates, including NFATs that play key roles in cytokine production and neuroinflammation (Nagamoto-Combs and Combs, 2010; Shiratori et al., 2010 Kim et al., 2011; Rosenkranz et al., 2012; Rojanathammenee et al., 2013). Other cells relevant to the vasculature, such as microvascular pericytes, can express high levels of NFAT4 (Filosa et al., 2007), which is intriguing given that ΔCN was also commonly observed in or around microvessels in the present study.

In addition to glial cells, we also observed ΔCN labeling in neurons, especially within close proximity to microinfarcts (Figure 2.5B). NeuN- ΔCN colocalization appeared most extensive within the microinfarct core region, which may be subject to marked hypoxic damage (Shih et al., 2013)—a well-characterized stimulus for CN proteolysis in brain tissue (Shioda et al., 2006; Shioda et al., 2007). As mentioned, ΔCN expression in neurons has been shown to activate both necrotic and apoptotic signaling pathways (Wang et al., 1999; Wu et al., 2004), suggesting that the neuronal expression of ΔCN within and near microinfarcts may also be a major contributor to neurodegeneration associated with vascular damage. Additional work directed at identifying all of the different cell types expressing ΔCN following microvessel damage and how CN

proteolysis in each cell type specifically contributes to neural function/dysfunction should provide important insights into the pathophysiology of AD and VCID.

2.4.3 ΔCN in Astrocytes and synapses. One of the major functions of astrocytes is to promote the structural and functional integrity of synaptic contacts (Allen, 2014). Deficits in synaptic function are usually found in animal models characterized by extensive astrocyte activation (Bachstetter et al., 2012; Furman et al., 2012; Rossi, 2015), suggesting that activated astrocytes directly damage and/or lose the capacity to protect synapses. We previously showed that the blockade of astrocytic CN/NFAT signaling, using AAV-Gfa vectors, ameliorated synaptic deficits in both basal synaptic transmission and plasticity and normalized the PS threshold in APP/PS1 mice (Furman et al., 2012). Similar levels of synaptoprotection were observed in brain-injured rats treated with the same AAV reagents (Furman et al., 2016). Consistent with these findings, the present study found that hippocampal synaptic strength was compromised in healthy adult rats following the forced overexpression of ΔCN in astrocytes. Together, the results are consistent with the possibility that proteolytic activation of CN in activated astrocytes is a crucial causative mechanism for the deterioration of synaptic function. However, our results do not rule out the possibility that full-length CN could mediate similar effects (in the absence of proteolysis), if the phosphatase was activated at high levels by normal binding to Ca^{2+}/calmodulin.

While the present study did not address how astrocytic CN activity disrupts synaptic function, there are many possible mechanisms that will need to be systematically investigated. For instance, CN signaling pathways help drive the production of numerous immune factors, including tumor necrosis factor and other cytokines, which are implicated in chronic neuroinflammation (Griffin et al., 1998; Mrak and Griffin, 2005; Van

Eldik et al., 2007; Sama et al., 2008) and widely regarded as causal factors of synaptic decline in animal models of aging, injury, and AD (Pickering and O'Connor, 2007; Sama and Norris, 2013; Rossi, 2015). Synaptic function is also strongly modulated by a variety of releasable factors (*e.g.* SPARC/SPARC-L, C3, and ephrin/Eph receptors) (Stevens et al., 2007; Jones et al., 2011; Murai and Pasquale, 2011), which are produced in activated astrocytes (Ridet et al., 1997; Frugier et al., 2012; Ingram et al., 2014) and sensitive to CN/NFAT activity (Norris et al., 2005; Furman et al., 2016), while other toxins, such as glutamate and Aβ peptides, can be released from activated astrocytes via the CN-dependent downregulation of glutamate transporters (Sama et al., 2008; Abdul et al., 2009) and the upregulation of β-secretases (Furman et al., 2012; Jin et al., 2012) respectively. But, regardless of the specific cellular mechanism, our data provide proof-of-concept that CN hyperactivity in astrocytes, especially in areas of amyloid and vascular pathology (as shown with the ΔCN antibody, see Figures 2.2-2.4), can have deleterious effects on synapses. Whether the proteolysis of CN is directly linked to the striking synapse loss that occurs with AD (Scheff et al., 2013; Scheff et al., 2015; Scheff et al., 2016) and VCID (Sinclair et al., 2015) is still unknown and will need to be determined.

2.4.4 ΔCN in Astrocytes: Deleterious vs Beneficial Effects on Neural Function. The electrophysiological findings in the present study are consistent with numerous studies that have found a deleterious role of CN signaling in rodent models of aging (Foster et al., 2001; Norris et al, 2005), AD (Norris et al., 2005; Kuchibhotla et al., 2008; Reese et al., 2008; Taglialatela et al., 2009; Wu et al., 2010; Furman et al., 2012; Hudry et al., 2012; Taglialatela et al., 2015), and injury (Wu et al., 2004; Huang et al., 2005; Shioda et al., 2006; Shioda et al., 2007; Furman et al., 2016). The data provided here also directly

supports our previous work (Furman et al., 2012; Furman et al., 2016) and work from others (Fernandez et al., 2016) showing that astrocyte-specific inhibition of CN signaling results in improved neuronal viability, synaptoprotection, and/or improved cognition. However, these results are apparently in disagreement with another study by the Torres-Aleman lab that showed a number of neurologic benefits in amyloidogenic mice when ΔCN was overexpressed in astrocytes (see Fernandez et al., 2012). The reason(s) for this discrepancy is not immediately clear. In many tissues, overexpression of ΔCN is associated with cellular toxicity (*e.g.* see Wang et al., 1999; Wu et al., 2004). It's therefore possible that the overexpression of ΔCN, in the context of an already toxic environment (*i.e.* high amyloid levels), leads to the death of activated astrocytes. The end result may be beneficial, if activated astrocytes are having a deleterious impact on neural function. Though we observed no evidence for astrocyte deterioration in adult rats treated with AAV-Gfa vectors, the viability of ΔCN -expressing astrocytes should be closely monitored in future studies, especially when ΔCN is expressed in animal models where neuropathology is already extensive. Alternatively, the beneficial vs. detrimental effects of ΔCN could be a further indication of the highly heterogeneous nature of astrocytes both within and across different brain regions. In the present study, forced overexpression of ΔCN was limited to astrocytes in the hippocampus, which is also where we observed beneficial effects of CN/NFAT inhibition using AAV-Gfa vectors (Furman et al., 2012; Furman et al., 2016). In contrast, Fernandez et al. 2012 induced ΔCN expression in astrocytes across the entire forebrain. The specific outcome of ΔCN expression may therefore depend critically on the brain region examined. It's also possible that ΔCN generates some neurologic benefits, including improved cognition, at the cost of other functions, like synaptic transmission and plasticity, though this would be contrary to numerous other studies where synaptic deficits and cognitive impairments

run in parallel. Finally, it is interesting to note that a more recent study by the Torres-Aleman lab (Fernandez et al., 2016) reported a number of functional benefits in AD transgenic mice following treatment with reagents that disrupt astrocytic CN signaling, which is more consistent with our present findings and previous research. Regardless, it would appear that astrocytic CN signaling is highly complex and additional research will be necessary to fully characterize the molecular, cellular, and behavioral phenotypes of animals that show elevated levels of ΔCN in brain astrocytes.

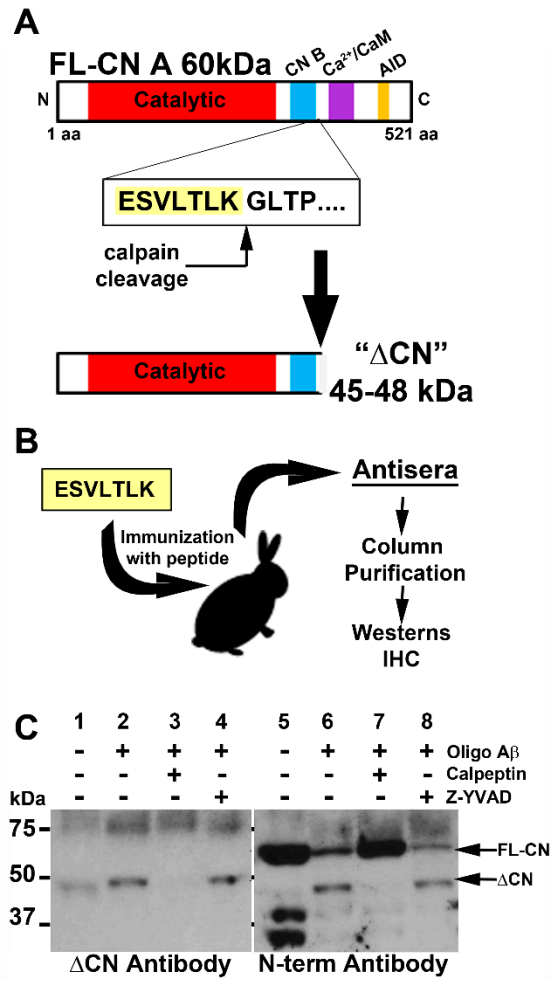
A
FL-CN A 60kDa
CN B
Ca2+/CaM
AID
N
Catalytic
C
1 aa
521 aa
ESVLTLK GLTP....
calpain cleavage
Catalytic
"ΔCN"
45-48 kDa
B
ESVLTLK
Immunization with peptide
Antisera
Column Purification
Westerns
IHC
C
1 2 3 4 5 6 7 8
- + + + - + + + Oligo Aβ
- - + - - - + - Calpeptin
kDa - - - + - - - + Z-YVAD
75
50
37
FL-CN
ΔCN
ΔCN Antibody
N-term Antibody

Figure 2.1 Production of ΔCN antibody.

(A) Calpain-dependent cleavage between lysine 424 and glycine 425 generates a 45–48 kDa fragment (ΔCN). (B) The peptide immediately upstream from the ΔCN cleavage site (ESVLTLK) was used to immunize rabbits. Antisera were column-purified to enrich the ΔCN antibody. (C)Western blot showing proteolysis of CN in primary rat hippocampal cultures treated for 24 h with oligomeric Aβ1–42 peptides (65 nM) in the presence or absence of the CP inhibitor, calpeptin (10 μM) or caspase-1 inhibitor, Z-YVAD. The ΔCN antibody (left panel) detects the 45–48 kDa fragment but not full-length CN. Commercial N terminus antibodies (right panel) recognize both full-length (60 kDa) CN and the 45–48 kDa fragment. Blockade of CP activity with calpeptin prevents Aβ-dependent proteolysis while inhibition of caspase activity does not.

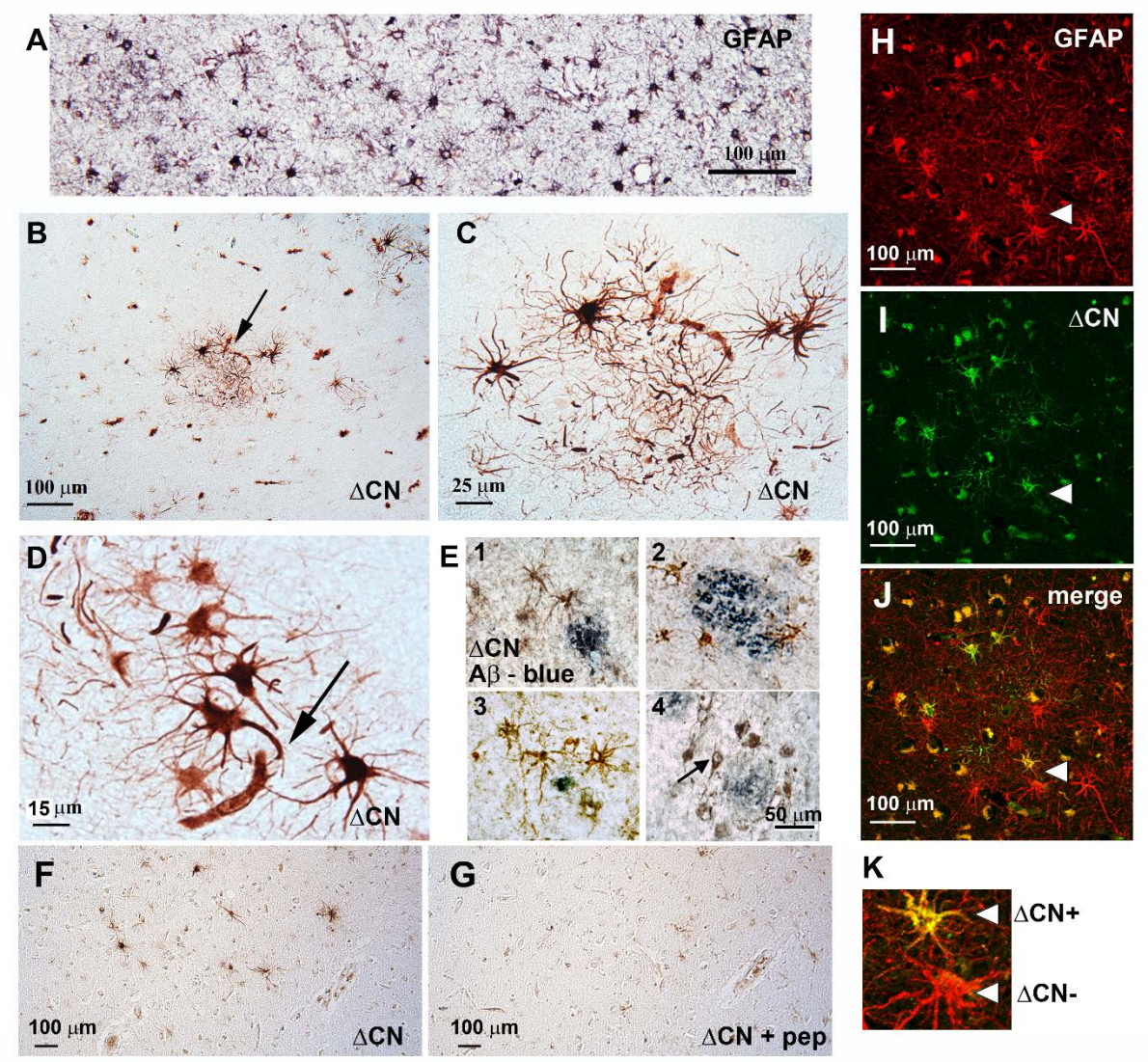
A
GFAP
100 μm
B
100 μm
ΔCN
C
25 μm
ΔCN
D
15 μm
ΔCN
E
1
ΔCN
Aβ - blue
2
3
4
50 μm
F
100 μm
ΔCN
G
100 μm
ΔCN + pep
H
GFAP
100 μm
I
ΔCN
100 μm
J
merge
100 μm
K
ΔCN+
ΔCN-

Figure 2.2 ΔCN antibody labels astrocytes in human tissue.

(A) GFAP labeling in an AD section from a subject with confirmed AD. (B–C) Low and high power photomicrographs of human AD amygdala showing intense labeling of astrocyte clusters and (D) astrocytes in close proximity to microvessels using the ΔCN antibody. (E1–4) Co-labeling reveals that ΔCN-positive cells (brown) appear around amyloid deposits (blue). Though most cells contained within clusters exhibited a clear astrocyte morphology, some cells showed neuron-like characteristics (see arrow in E4). (F, G) Serial sections of amygdala labeled with ΔCN antibody alone (F) or ΔCN antibody plus ESVLTLK blocking peptide (G). (H–K) Confocal micrographs showing labeling with a GFAP antibody (red) and the ΔCN antibody (green). The merged image shows areas of colocalization, indicating that most GFAP-positive astrocytes have regions that are also occupied by the ΔCN fragment (arrows). However; some GFAP-positive astrocytes (indicated by arrowheads and shown at larger magnification in K) were devoid of ΔCN.

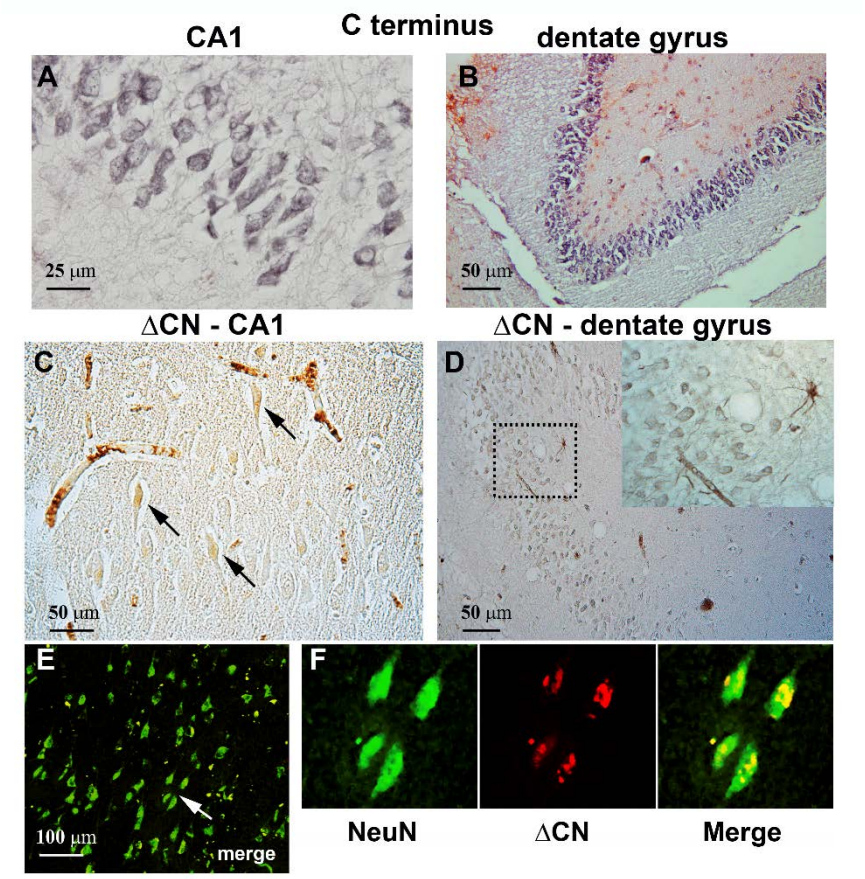

Figure 2.3 ΔCN antibody shows faint labeling in NeuN positive neurons.

(A–B) Photomicrographs of human AD hippocampus in CA1 (A) and in the dentate gyrus (B) show strong labeling of neurons using a commercial antibody to the C-terminus of CN. (C–D) Labeling of the CA1 and dentate granule layers with the ΔCN antibody. Neuronal labeling with the ΔCN antibody was relatively faint and limited to the cell body region and proximal apical dendrites (for pyramidal neurons). Inset in D shows an intensely labeled astrocyte and blood vessel near weakly labeled dentate granule cells. (E–F) Low (E) and higher-powered (F) confocal micrographs of NeuN and ΔCN double-labeling in area CA1 of an AD subject. Merged low-power images from the region denoted by the arrow in panel E shows punctate localization of ΔCN (red) to NeuN positive cell bodies (green).

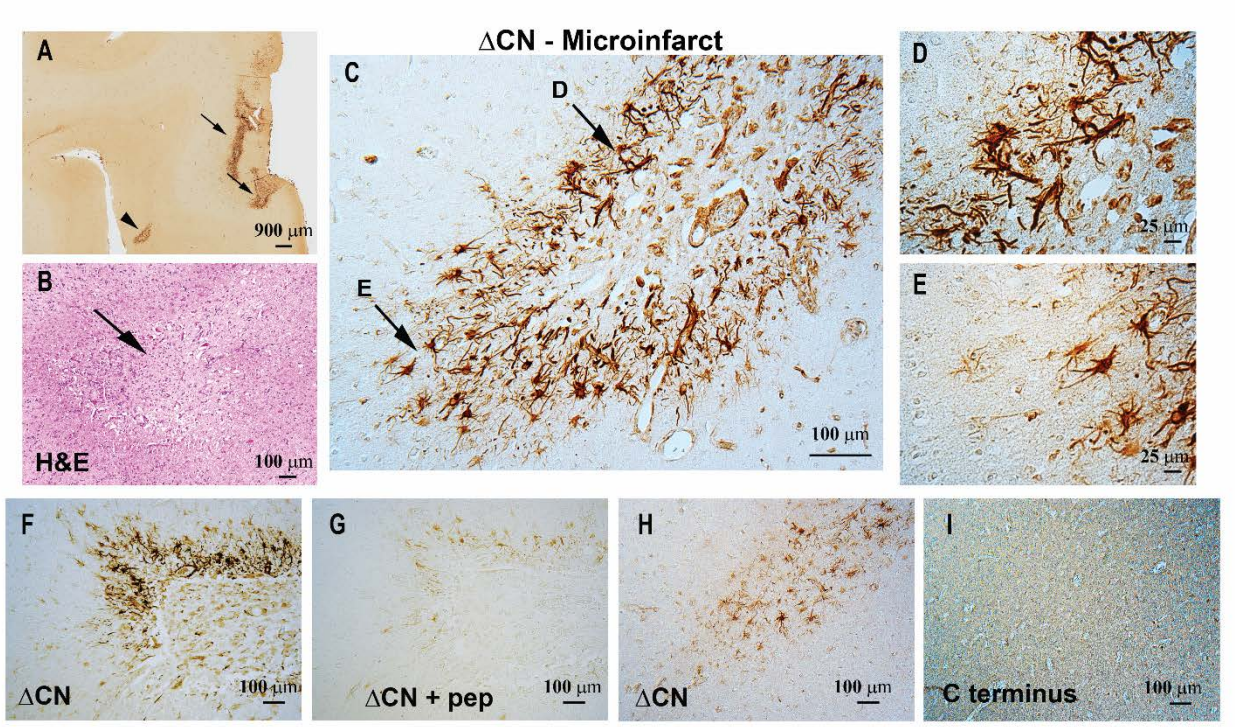

Figure 2.4 ΔCN antibody labels microinfarcts.

Representative low magnification photomicrograph (A) that shows ΔCN labeling around several microinfarcts (arrows and arrowhead) in neocortex. (B) Serial section through neocortex stained by H&E to confirm the presence of microinfarcts. The image shown is a high magnification of the region denoted by the arrowhead in Panel A. (C) High power photomicrograph of the region in A (arrowhead) showing intense ΔCN antibody labeling of astrocytes. Higher magnification of the areas denoted by arrows are shown in panels D and E. (F, G) Serial sections of neocortex labeled with ΔCN antibody alone (F) or ΔCN antibody plus ESVLTLK blocking peptide (G). The blocking peptide greatly reduced the labeling intensity of the ΔCN antibody. (H, I) Serial sections of human cortical tissue treated with the ΔCN antibody (H), or a commercial C-terminus antibody (I) that detects FL-CN, but not proteolyzed CN (G). Little to no labeling in the microinfarct region is observed with the C-terminus antibody.

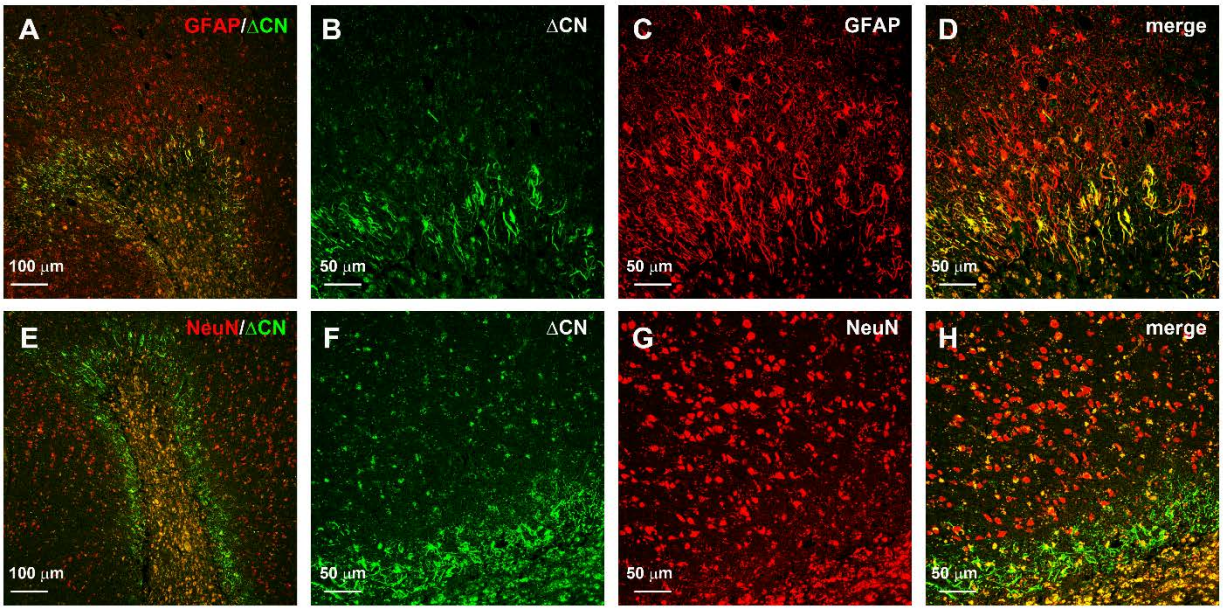

Figure 2.5 ΔCN localizes to astrocytes and neurons around microinfarcts.

(A) Merged confocal micrograph showing the colocalization of ΔCN (green)with GFAP (red). B–D, high magnification images of the infarct in Panel A shown in individual channels (B, C) and merged (D). Co-localization of ΔCN with GFAP was most extensive in the region immediately adjacent to the infarct. (E) Merged confocal micrograph showing the colocalization of ΔCN (green) with NeuN (red). Note, this image is a serial section of the region shown in Panel A. F–H, high magnification images of the infarct in Panel E shown in individual channels (F, G) and merged (H). Co-localization of ΔCN with NeuN was most extensive in the microinfarct core, but could also be observed for numerous cells adjacent to the insult.

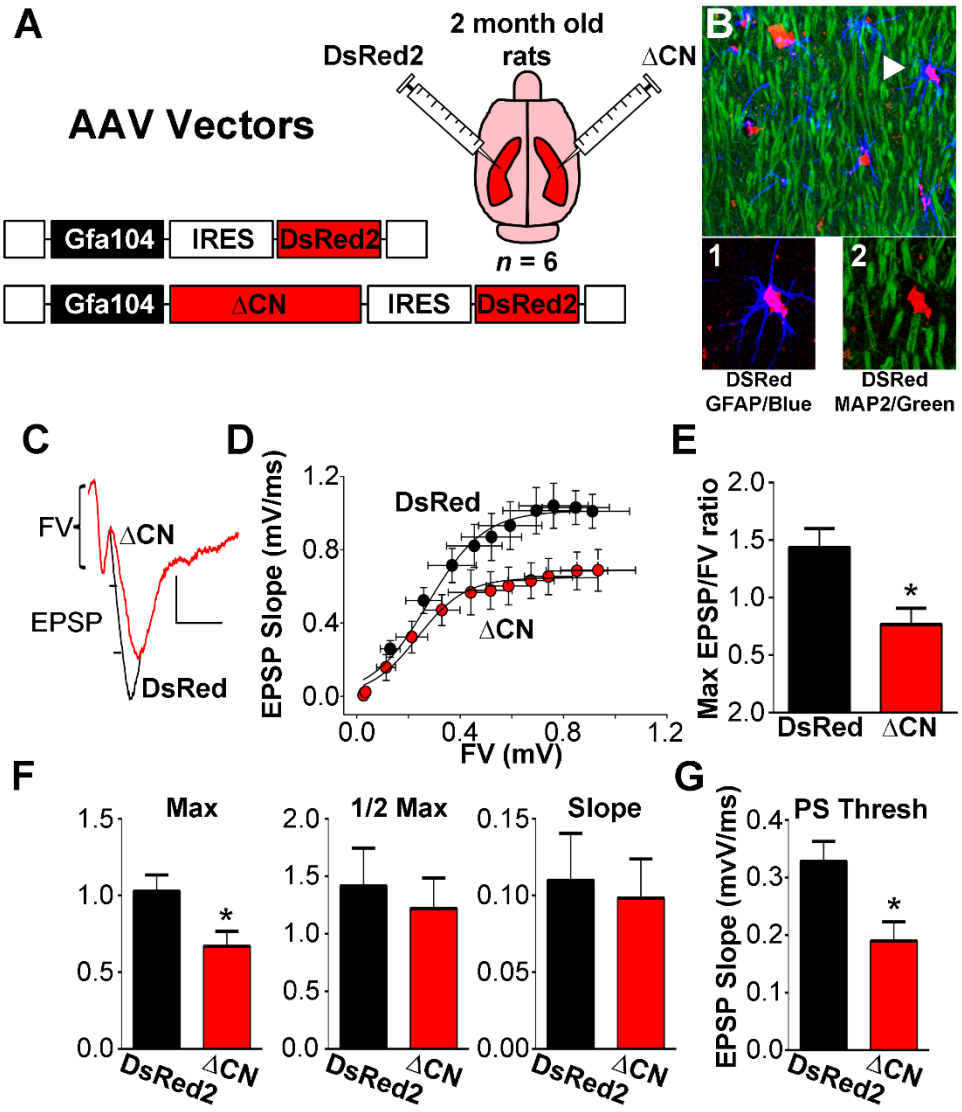
A
AAV Vectors
Gfa104
IRES
DsRed2
Gfa104
ΔCN
IRES
DsRed2
2 month old
rats
DsRed2
ΔCN
n = 6
B
1
2
DSRed
GFAP/Blue
DSRed
MAP2/Green
C
FV
ΔCN
EPSP
DsRed
D
DsRed
ΔCN
EPSP Slope (mV/ms)
FV (mV)
E
Max EPSP/FV ratio
DsRed
ΔCN
F
Max
1/2 Max
Slope
DsRed2
ΔCN
G
PS Thresh
EPSP Slope (mvV/ms)
DsRed2
ΔCN

Figure 2.6 ΔCN expression and hippocampal synaptic function.

(A) AAV2/5 vectors encoding a DsRed2 control construct or a ΔCN construct under the control of the astrocyte-specific promoter, Gfa104, were injected into alternate hemispheres (intrahippocampal) of intact adult rats (n = 6). B, Confocal micrograph of the *stratum radiatum* region of area CA1 showing MAP2b (green), GFAP (blue), and DsRed2 (red). Arrow points to a DsRed2-positive astrocyte shown in higher magnification images below. While many astrocytes labeled positive for DsRed2, there was no overlap in labeling for DsRed2 and MAP2b. C, representative waveforms recorded in *stratum radiatum* of CA1 in response to electrical orthodromic stimulation of Schaffer collaterals illustrating a reduced EPSP in slices from the ΔCN-treated hemisphere relative to the DsRed2-treated hemisphere, given a similar FV amplitude. Calibration bars: vertical 0.5 mV; horizontal 5 msec. D, Synaptic strength curves showing the mean ± SEM EPSP slope values plotted against the mean ± SEM FV amplitude values at increasing stimulus intensities. The average synaptic strength curve for the ΔCN-treated hemisphere exhibited a downward shift, consistent with reduced basal synaptic strength. E, Mean ± SEM maximal EPSP-to-FV ratio in each AAV-treated hemisphere. F, Synaptic strength curve parameters (Mean ± SEM maximal EPSP, curve slope, and half-maximal activation) from the data shown in panel C. G, Mean ± SEM PS threshold in ΔCN- and DsRed2-treated slices. *p b 0.05, paired t-test.

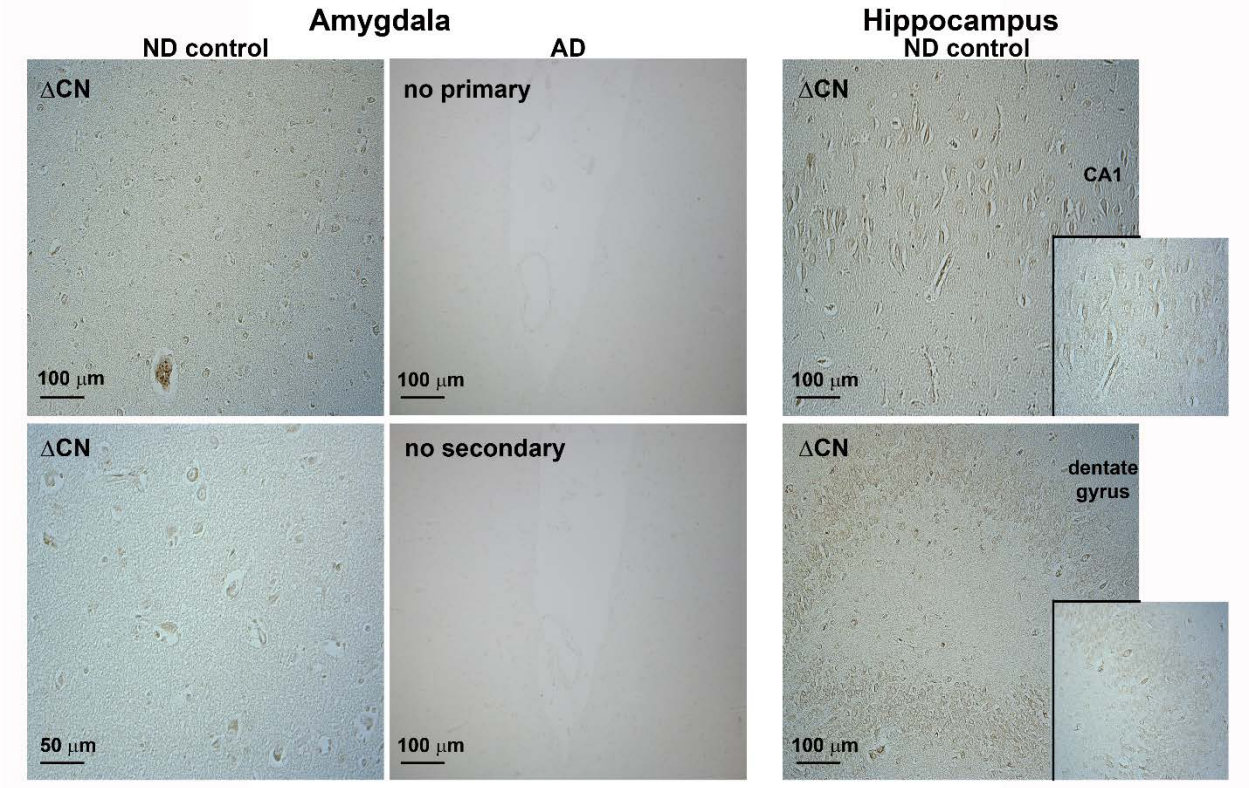

Figure 2.7 ΔCN labeling controls.

Labeling with the ΔCN antibody in both amygdala (far left column) and hippocampus (far right column) from non-demented control subjects reveals little-to-no labeling across the sections. Furthermore, sections were labeled in the absence of primary antibody and secondary antibody as additional controls to confirm antibody specificity.

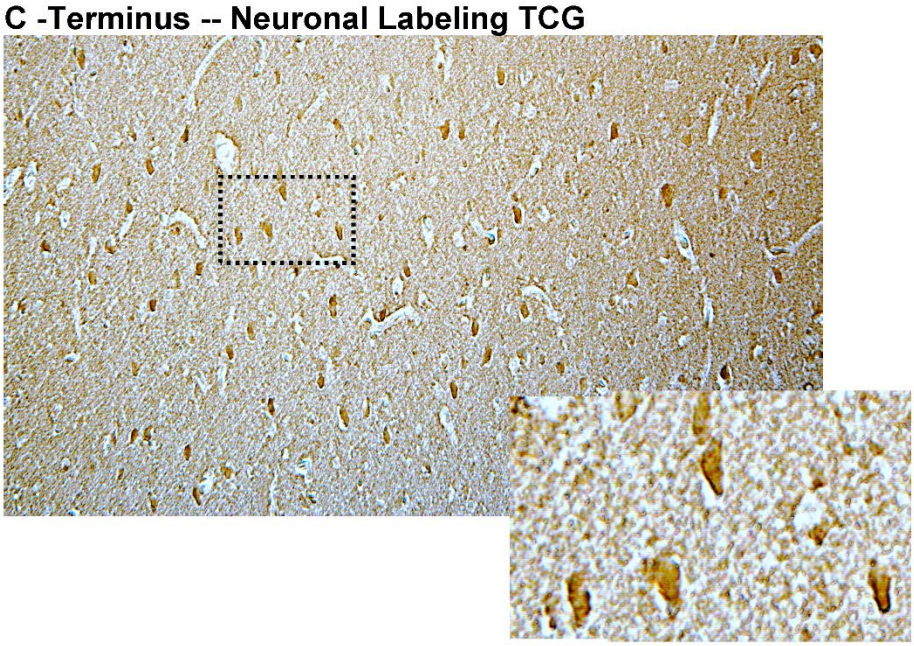

Figure 2.8 Commercial C-terminus CN antibody reveals labeling of neurons.

A cortical section labeled with a commercial C-terminus CN antibody reveals labeling of neurons.

CHAPTER III: INHIBITION OF CN/NFAT SIGNALING IN A MOUSE MODEL OF VASCULAR COGNITIVE IMPAIRMENT AND DEMENTIA

Melanie M. Pleiss[a], Pradoldej Sompol[b], Irina Artiushin[b], Susan D. Kraner[b], David K. Powell[c], Vikas Bakshi[b], Ai-Ling Lin[b], Peter T. Nelson[b], Donna M. Wilcock[b], Christopher M. Norris[b]

[a]Department of Pharmacology and Nutritional Sciences, University of Kentucky, Lexington, KY, 40536

[b]Sanders Brown Center on Aging, Lexington, KY, 40536

[c]Magnetic Resonance Imaging and Spectroscopy Center, University of Kentucky, Lexington, KY, 40536

3.1 Introduction

Astrocytes are one of the most abundant cell types in the brain (Chen and Swanson, 2003), and play a vital role in maintaining healthy nervous tissue. Calcineurin (CN), an exquisitely Ca^{2+}-sensitive Ser/Thr protein phosphatase, is profuse in neurons under normal conditions (Klee, 1991) but with neurodegenerative diseases (*e.g.* Alzheimer's disease and vascular cognitive impairment and dementia) CN can be highly expressed in a subset of activated astrocytes (Hashimoto et al., 1998; Norris et al., 2005; Celsi et al., 2007; Abdul et al., 2009). Activated astrocytes exhibit an increased production of pro-inflammatory cytokines, a decreased production of glutamate transporters, and a hypertrophic morphological change, and they have been implicated as a major component of neuroinflammation (Sama et al., 2008; Fuller et al., 2009; Sofroniew, 2009; Fuller et al., 2010; Sofroniew and Vinters, 2010).

Work from our lab and others has shown that changes in signaling pathways in activated astrocytes-- including CN signaling pathways-- can contribute to neural dysfunction (Abdul et al., 2009). One pathway in particular, the CN/nuclear factor of activated t-cells (NFAT) pathway, has been implicated in the initiation and/or progression of Alzheimer's disease (AD) (Abdul et al., 2009; Abdul et al., 2010; Wu et al., 2010; Hudry et al., 2012). Moreover, inhibition of the CN/NFAT pathway using a small inhibitory peptide (VIVIT) ameliorates synaptic deficits and glial activation in a mouse model of AD (Furman et al. 2012). To our knowledge, however, inhibition of CN/NFAT signaling has not been well-studied in the context of vascular cognitive impairment and dementia (VCID).

Pathological features of VCID include but are not limited to macro- and micro-infarctions, micro-hemorrhages, and arteriolosclerosis (Kapasi and Schneider, 2016). Buildup of homocysteine, a non-essential amino acid that is a transient, intermediate step in the transsulfuration pathway, either by genetic mutation (*e.g.* cystathionine β-

synthase) or dietary modifications (*e.g.* a deficiency of folate or excess of methionine) can result in an accumulation of homocysteine known as HHcy (Stipanuk and Ueki, 2011). HHcy is a risk factor not only for cardiovascular conditions (*i.e.* atherosclerosis and stroke) (Graham et al., 1997), but it is also an independent risk factor for AD (Seshadri et al., ,2002) and VCID (Brattstrom et al., 1984). In this study, we used a Teklad custom research diet (Harlan Laboratories) that was deficient in folate, B_6, and B_{12}, and also had excess methionine (7.7 g/kg) versus control diet (3.0 g/kg) in order to induce a moderate HHcy (as described by Ernest et al., 2005). Levels of other vitamins and minerals, as well as protein (195 g/kg) were uniform across the HHcy and control diets. A previous study using this diet to induce HHcy revealed significant cognitive deficits on the radial arm water maze, increased number of microhemorrhages, and increased expression of proinflammatory cytokines after just 11 weeks on the diet (Sudduth et al., 2013b).

To determine the role of astrocytic CN/NFAT signaling in HHcy-dependent VCID, we directed expression of a potent NFAT inhibitor, VIVIT, to wild type mice treated with either control or HHcy diet using adeno-associated virus (AAV) with an astrocyte-specific promoter. Results revealed that NFAT-DNA binding activity was greater in HHcy mice compared to mice on control diet. Moreover, consistent with our previous work (Furman et al., 2016), very preliminary NFAT4 labeling in HHcy tissue exhibited an astrocyte bias. Treatment of HHcy mice with AAV-Gfa2-VIVIT to inhibit astrocytic NFAT activity ameliorated deficits in synaptic strength and plasticity. Furthermore, VIVIT had favorable effects on cerebral blood flow (CBF) and several critical brain metabolites. Taken together, results suggest that inhibition of CN/NFAT in astrocytes is synaptoprotective in a mouse model of VCID.

3.2 Methods

3.2.1 Animals. Female C57Bl/6 (10 weeks of age) were housed in groups, provided access to food and water *ad libitum*, and used in accordance with International Animal Care and Use Committee of University of Kentucky.

3.2.2 Stereotaxic surgery. Mice underwent surgery as previously described (Furman et al., 2012). Briefly, mice were anesthetized with 2.5% isoflurane throughout the duration of the surgery. Once immobilized in the stereotaxic frame, AAV vectors (Gfa2-VIVIT or Gfa2-EGFP) were delivered bilaterally into the hippocampus (4uL/hemisphere) at a rate of 0.2uL/min using a sterotaxic injector (Stoelting). Coordinates for injection relative to bregma were +2.0 mm anteroposterior, ±1.5 mm mediolateral, and -1.5 mm dorsoventral.

3.2.3 Diet. One week post-AAV injection, mice were switched from normal chow diet to a custom research diet. Mice either went onto control diet (Harlan Teklad 5001 C) or HHcy diet (deficient in folate, B6, B12; enriched in methionine) (Harlan Teklad TD97345). Mice were maintained on custom diets *ad libitum* for a minimum of 11 weeks up to euthanasia.

3.2.4 Hippocampal slice preparation. Briefly, mice were deeply anesthetized with CO_2 and decapitated. Brains were removed and stored briefly in Ca^{2+}-free, ice-cold, oxygenated (95% O_2, 5% CO_2) artificial CSF (ACSF) containing the following (in mM): 124 NaCl, 2 KCl, 1.25 KH_2PO_4, 2 $MgSO_4$, 26 $NaHCO_3$, and 10 dextrose, pH 7.4. 400µm-thick sections from one hemisphere were cut on a vibrating microtome (Leica). Slices were then quickly transferred to netting in a custom Plexiglas holding chamber and maintained in CaCl2-containing (2 mM) ACSF at an interface with warm (32°C),

humidified air. Slices were permitted to equilibrate for at least 1.5 h before beginning electrophysiological analysis.

3.2.5 Synaptic strength and LTP measurements. For each slice, dual-stimulus pulses (S1 and S2), separated by 50 ms, were delivered at eleven different intensity levels (range of 25 –500 mA) at a rate of 0.1 Hz to establish a synaptic strength curve. Three field potentials at each stimulus level were averaged and measurements of fiber volley (FV) amplitude (in millivolts) and EPSP slope (millivolts per milliseconds) were performed offline using Clampfit software (Molecular Devices). Averaged EPSP slope measures were plotted against their corresponding FV amplitudes to estimate the strength of CA3–CA1 synaptic contacts. Paired-pulse facilitation (PPF) of the EPSP slope was calculated along the linear portion of the synaptic strength curve by dividing the EPSP slope of S1 by the EPSP slope of S2 and multiplying by 100. Following measurements of synaptic strength, stimulation intensity was readjusted to elicit an EPSP of 1 mV, and stimulus pulses were delivered at 0.033 Hz until a stable 20 min baseline was established. High-frequency stimulation (two 100 Hz trains, 1 s each, 10 s intertrain interval) was then delivered at the baseline stimulation intensity to induce long-term potentiation (LTP), followed by an additional 60 min baseline. Within each group, EPSP slope measures from the last 10 min of the post-LTP baseline were averaged across slices within animal and compared with the pre-LTP baseline slope average. For each animal, electrophysiological parameters were averaged across all slices within each animal (one to three slices), and the n used for statistical comparisons reflects the number of animals per diet and treatment group. All electrophysiological recordings were conducted and analyzed by personnel who were blind to diet and treatment conditions.

3.2.6 Cerebral blood flow and magnetic resonance spectroscopy. MRI experiments were performed on a 7T Clinscan MR scanner (Siemens) at the Magnetic Resonance Imaging & Spectroscopy Center of the University of Kentucky. Mice were anesthetized with 4.0% isoflurane for induction and then maintained in a 1%–2.5% isoflurane and air mixture using a nose cone. Heart rate (90–110 bpm), respiration rate (50–80 breaths/min), and rectal temperature (36±1 °C) were continuously monitored. A water bath with circulating water at 50–55 °C was placed outside the room and used to maintain body temperature.

Cerebral blood flow (CBF) was measured using a pseudocontinuous arterial spin labeling technique. Paired images were acquired with field of view (FOV) = 40×30mm^2, matrix = 128×128, slice thickness = 1mm, slice = 4, 120 measurements, labeling duration = 2,100ms, repetition time (TR) = 4,000ms, and echo time (TE) = 20ms. Quantitative CBF (mL/g/min) was computed employing codes written in Matlab. Following CBF measurements, we acquired proton (^{1}H) MR spectra (MRS) to determine brain metabolite levels. In vivo ^{1}H-MRS were obtained using a point-resolved spectroscopy sequence. Water-suppressed spectra were acquired with following parameters: TR = 1,500ms, TE = 135ms, spectral width = 60 Hz and average = 400. A voxel of interest of 18.2mm^3(2.0×7.0×1.3mm) covered bilateral hippocampus. An acquisition of nonwater suppressed spectrum with 10 averages was followed (the rest of the parameters were kept the same). Both with- and without-water suppression spectra were then processed using LCModel to determine the concentrations of the metabolites. LCModel uses a linear combination of model spectra of metabolite solutions in vitro to analyze the major resonances of in vivo spectra as previously reported (Provencher, 1993). The protocol, including MRI and MRS, took approximately 60 minutes for each mouse.

3.2.7 Radial arm water maze. Behavior testing was performed at the University of Kentucky Rodent Behavior Core. The 2-day radial arm water maze (RAWM) protocol was carried out as previously described in Alamed et al., 2006. Briefly, a six-arm maze was submerged in a pool of water maintained at 20.5°C, and a platform was placed at the end of one arm (equipment and tracking software from Noldus Information Technology). Each mouse was subjected to 15 trials per day for 2 days. Each mouse began each trial in a different arm while the arm containing the platform remained the same. The number of errors (incorrect arm entries) and time to platform was counted over a 1-minute period. The errors were averaged over three trials, resulting in ten blocks for the 2-day period.

3.2.8 Electrophoretic mobility shift assay. EMSAs were performed to determine NFAT-DNA binding as described previously in Furman et al., 2016. Briefly, whole cell extracts from frozen cortical brain tissue were made using a kit from Active Motif following the manufacturer's instructions. Images were obtained and fluorescent bands were quantified using the Licor Odyssey scanner. Control diet and HHcy tissue samples were run on the same gel for direct statistical comparisons.

3.2.9 Immunofluorescence. Immunofluorescent labeling was performed as described previously (Furman et al., 2016; Pleiss et al., 2016). In brief, human cortical samples were labeled using a 1:20 dilution of anti-mouse NFAT4 (Santa Cruz), amplified and labeled using tyramide-Alexa 594 from a tyramide signal amplification kit (Invitrogen). Sections were further labeled using a 1:100 dilution of anti-rat GFAP (Life Technologies) and labeled using the secondary rabbit anti-rat Alexa 488 (Invitrogen). Images were obtained using confocal microscopy (Nikon Eclipse Ti).

3.2.10 Immunohistochemistry. Immunohistochemistry was performed as described previously (Pleiss et al., 2016). In brief, human cortical sections were labeled primarily with a 1:25 dilution of ΔCN (custom, see Chapter II) or 1:20 dilution of NFAT4 (Santa Cruz). Following primary antibody incubation, secondary antibodies and ABC kits (Vector Laboratories) were used to amplify the signal, followed by detection with DAB substrate kit (Vector Laboratories). Images were obtained using X scope.

3.2.11 Statistics. Unless otherwise noted, outcome measures were assessed for both the control diet and HHcy diet animals and compared across treatment groups using two-way ANOVA. When appropriate, Fisher's protected least significant difference test was used for *post hoc* analyses. Significance for all statistical comparisons was set at $p \leq 0.05$.

3.3 Results

3.3.1 Elevated NFAT4-DNA binding and labeling is seen in mouse and human tissue with vascular-associated pathologies.

We have previously shown that NFAT-DNA binding is elevated in a rat model of TBI, and the NFAT4 isoform in particular exhibits a strong astrocyte bias (Furman et al., 2016). Consistent with previous findings, using electrophoretic mobility shift assays (EMSAs) we found that NFAT-DNA binding was increased cortical tissue from mice on an HHcy-diet induced model of VCID compared to tissue from mice on the control diet (Fig 3.1A-B). Previous studies have observed ΔCN fragments in neurodegenerative conditions with significant vascular contributions (Shioda et al., 2006; Shioda et al., 2007; Rosenkranz et al., 2012). Moreover, elevated NFAT levels have been implicated in neurodegenerative conditions like MCI (Abdul et al., 2009). Using human cortical tissue

from a case of VCID with confirmed microinfarct pathology, we found intense labeling of ΔCN (See Chapter II, Fig 2.4) as well as NFAT4 (Fig 3.1 C, E, F) surrounding the microinfarct core. Studies have recently, suggested that microinfarcts are the most common and significant contributor to vascular cognitive impairment and dementia (Smith et al., 2012; Kapasi and Schneider, 2016). Moreover, activated astrocytes often envelope the microinfarct core (Wang et al., 2012; van Veluw et al., 2015). Double labeling with NFAT4 and GFAP, an intermediate filament that is found almost exclusively in astrocytes (Eng, 1985), revealed co-labeling in human cortical tissue from a confirmed case of VCID (Fig 3.1 F). Together, these results suggest that CN/NFAT4 signaling is elevated in astrocytes in both human and mouse tissue with cerebrovascular-associated pathologies.

3.3.2 Inhibition of CN/NFAT using AAV-Gfa2-VIVIT improves synaptic strength and plasticity in an HHcy diet-induced model of VCID.

Previous studies have shown that selective inhibition of CN/NFAT in models of AD (Furman et al., 2012) and TBI (Furman et al., 2016) using adeno-associated virus (AAV) with an astrocyte-specific promoter (Gfa2) has many protective benefits including improved synaptic parameters. Moreover, astrocytes play a major role in the regulation and maintenance of synaptic transmission and plasticity (Allen, 2014). Together, this suggests that elevated CN/NFAT signaling in astrocytes can significantly contribute to disease pathophysiological processes and selective inhibition of CN/NFAT provides many benefits. To our knowledge the role CN/NFAT signaling in a mouse model of VCID has not been well-investigated.

To determine if selective inhibition of CN/NFAT could improve synaptic parameters in a diet-induced model of VCID, we delivered AAV 2/5 vectors expressing VIVIT-EGFP or EGFP alone (control) into the hippocampus of 10 week old C57BL/6 mice. VIVIT has

been previously shown to potently and selectively inhibit CN/NFAT interactions (Aramburu et al., 1999). One hippocampus received VIVIT-EGFP and the other hippocampus received EGFP control for a within-subject experimental design (see Fig 3.2). Both VIVIT-EGFP and EGFP control vectors were transcriptionally regulated by a human GFAP promoter (Gfa2) which provides astrocyte-specific expression (Lee et al., 2008), which we have previously shown drives AAV-mediated expression of EGFP exclusively in astrocytes in both mice and rats (Furman et al., 2012; Furman et al., 2016).

At 12 weeks post-injection, brain slices from both hemispheres were harvested and processed in parallel for the electrophysiological assessment of basal CA3-CA1synaptic strength. Field EPSP slopes were recorded in CA1 *stratum radiatum* and plotted against corresponding FV amplitudes at 12 different stimulus intensities to generate synaptic strength curves. Compared to slices from the EGFP alone control vector-treated hemisphere, slices from the VIVIT-treated side exhibited improved synaptic strength curves (Figure 3.3A). Furthermore, following a 20 minute baseline recording, high-frequency stimulation was then delivered at the baseline stimulation intensity to induce long-term potentiation (LTP), followed by an additional 60 min baseline recording. Comparted to slices from the EGFP alone control vector-treated hemisphere, slices from the VIVIT-treated side exhibited improved LTP (Figure 3.3B) Together, these results suggest that selective inhibition of CN/NFAT signaling in astrocytes is sufficient improve synaptic parameters and plasticity in an animal model of VCID.

3.3.3 Inhibition of CN/NFAT using AAV-Gfa2-VIVIT favorably improves cerebral blood flow and brain metabolite levels in an HHcy diet-induced model of VCID.

Previous studies have shown significant deficits in cerebral blood flow (CBF) in mice on an HHcy diet versus mice on control diet. Decreased CBF has been associated with increased vascular risk factors (*e.g.* hypertension) (Muller et al., 2012; Bangen et al., 2014). Moreover, changes in several brain metabolites has been implicated in neurodegenerative conditions such as AD. Specifically, in healthy tissue, levels of N-acetylaspartate (NAA) are normally elevated with reductions in NAA levels being indicative of increased neuronal loss. Additionally, levels of myo-Inositol (mI) are normally low but indicate increased glial activation when elevated (Parnetti et al., 1997; Zhu et al., 2006; Chang et al., 2013; Lin and Rothman, 2014; Lin et al., 2016). To our knowledge, selective inhibition of CN/NFAT to observe its effects on CBF and brain metabolite levels has not been well-investigated.

At 14 weeks post-initiation of HHcy diet, we performed arterial spin labeling (ASL) magnetic resonance imaging (MRI) to measure CBF. We also used magnetic resonance spectroscopy (MRS) normalized to a water peak to obtain brain metabolite levels (see Fig 3.2). In mice on the HHcy diet, we found that treatment with AAV-Gfa2-VIVIT compared to treatment with AAV-Gfa2-EGFP control improved CBF ($p = 0.045$ [1-tailed T-test]) (Fig 3.4A). Moreover, treatment with AAV-Gfa2-VIVT compared to treatment with AAV-Gfa2-EGFP control favorably elevated levels of NAA ($p = 0.03$ [1-tailed T-test]) (Fig 3.4B) and appeared to favorably reduce levels of mI (n.s) (Fig 3.4C). Although a large spectrum of metabolites was obtained, we did not see any significant change in other metabolite levels (*e.g.* glutamate) in VIVIT-treated versus EGFP control-treated mice on the HHcy diet. Together, these results suggest that selective inhibition of CN/NFAT in mice on an HHcy diet favorably improves both CBF and levels of brain metabolites.

3.3.4 Inhibition of CN/NFAT using AAV-Gfa2-VIVIT did not significantly improve performance on the radial arm water maze.

The 2-day radial arm water maze (RAWM) task can expose deficits in spatial learning and memory as described by Alamed et al., 2006. Previous studies have revealed a significant deficit on the RAWM with mice on the HHcy diet versus mice on a control diet (Sudduth et al. 2013b). Additionally, inhibition of CN/NFAT signaling in an aggressive 5xFAD model of AD shows improved performance on the RAWM (Sompol et al., *in preparation*). To our knowledge, selective inhibition of CN/NFAT and its effect on spatial learning has not been well-studied in a mouse model of VCID.

At 16 weeks post-initiation of HHcy diet, mice were run on the 2-day RAWM task (see Fig 3.2). We observed a significant deficit on the task in mice on HHcy diet versus those on the control diet (Fig 3.5). Within mice on HHcy diet, treatment with AAV-Gfa2-VIVIT (Fig 3.5, green line) did not significantly improve performance on the task compared to treatment with AAV-Gfa2-EGFP (Fig 3.5, red line). While results did not show a significant improvement, treatment with AAV-Gfa2-VIVIT may improve performance on an executive function task, which tends to be more impaired in VCID as opposed to learning and memory in AD, and will be elaborated in the Chapter III discussion.

3.4 Discussion

An overarching hallmark of neurodegeneration is neuroinflammation that is driven in part by CN/NFAT signaling (Griffin et al. 1998; Mrak and Griffin, 2005a). Inhibition of this pathway has been shown to be beneficial in several mouse models of injury and neurodegenerative disease (Furman et al., 2012; Furman et al., 2016). Using a potent NFAT inhibitor specifically targeted to astrocytes, AAV-Gfa2-VIVIT, the present study has provided some of the first evidence that inhibition of CN/NFAT interactions in a diet-induced mouse model of VCID is synaptoprotective. Moreover, blockade of CN/NFAT

appears to improve parameters of cerebral blood flow and brain metabolism. The results suggest that elevated CN/NFAT signaling may contribute to detrimental alterations in synaptic and cerebrovascular function in VCID, and inhibition of this pathway may have potential therapeutic benefits.

3.4.1 Elevations in NFAT4 in tissue with vascular pathology: a good target?

The biochemical findings in this study are consistent with previous studies that show elevated levels of NFATs in tissue following injury and disease (Serrano-Perez et al., 2011; Neria et al., 2013; Yan et al., 2014; Furman et al., 2016). Our previous work has found elevated levels of NFAT1 activation in human hippocampus in the early stages of AD (Abdul et al., 2009) Furthermore, our group recently found elevated levels of NFAT4-DNA binding activity in the hippocampus of traumatic brain injured rats that was confirmed using immunofluorescence and confocal microscopy (Furman et al., 2016). Consistent with these reports, the present study found elevated NFAT-DNA binding in cortical tissue from mice on HHcy diet versus those on control diet. Moreover, using immunohistochemical techniques in human tissue from confirmed cases of VCID, we found elevated labeling of ΔCN (see Chapter II, also see Fig 2.4) and NFAT4, especially around microinfarcts (Fig 3.1 C, E, F). The elevations in both CN (see Chapter II) and NFAT4 suggest that these proteins may be playing a significant role in HHcy-induced VCID.

What is the role of NFATs and why do we see elevations with CNS injury and disease? NFATs are transcription factors that are activated by CN in response to Ca^{2+} influx into cells, and are intimately involved in the immune/inflammatory response (Crabtree and Olson, 2002). Once in the nucleus, NFATs coordinate the transcription of pro-inflammatory cytokines and chemokines such as TNFα or IFNγ (McCaffrey et al.,

1994; Stankunas et al., 1999; Avni et al., 2002; Palanki, 2002; Kitazawa et al., 2004; Demuro et al., 2005; White et al., 2005; Shankar et al., 2008) (refer to Fig 1.2), which can have a detrimental effect if chronically activated. Furthermore, we have shown that both levels of CN and NFATs are robustly elevated in activated astrocytes with CNS injury and disease (Norris et al., 2005; Furman et al., 2016; Pleiss et al., 2016). Thus, an ideal therapeutic agent would need to inhibit CN/NFAT interactions specifically in astrocytes.

Using a potent NFAT inhibitor (VIVIT) targeted directly to astrocytes using a GFAP promoter (Gfa2) in an adeno-associated virus vector, we have previously shown that inhibition of CN/NFAT in astrocytes in mouse models of CNS injury and disease is synaptoprotective (Furman et al., 2012; Furman et al., 2016; Sompol et al., *in preparation*), shows cognitive benefits (Furman et al., 2012; Sompol et al., *in preparation*), and shows reduced glial activation (Furman et al., 2012). Although AAV-Gfa2-VIVIT treatment reveals numerous benefits- and AAV vectors in general are associated with low immunogenicity (Zaiss and Muruve, 2005)- our AAV2/5 constructs cannot cross the blood-brain barrier (BBB) and therefore must be directly injected into the brain. Future studies using a less invasive strategy (*e.g.* AAV9 that can cross the BBB; Manfredsson et al., 2009) should be considered. However, from a translational viewpoint, when looking at the benefits of specific CN/NFAT inhibition versus the cost of invasiveness, AAV-Gfa2-VIVIT should not be ruled out as a viable therapeutic agent.

3.4.2 Astrocytic CN/NFAT and synapses

Astrocytes play a critical role in maintaining the structural and functional integrity of synapses (Allen, 2014). Animal models characterized by extensive astrocyte activation often have deficits in synaptic function (Bachstetter et al., 2012; Rossi, 2015), suggesting that activated astrocytes lose the ability to protect and/or directly disrupt

synapses. We have previously shown that inhibition of astrocytic CN/NFAT in APP/PS1 mice (Furman et al., 2012), 5xFAD mice (Sompol et al., *in preparation*), and rats with traumatic brain injury (TBI) (Furman et al., 2016) ameliorates deficits in basal synaptic transmission as well as plasticity. Consistent with these findings, the present study found that hippocampal synaptic strength and plasticity was normalized in mice on an HHcy diet treated with AAV-Gfa2-VIVIT versus those treated with AAV-Gfa2-EGFP control (Fig 3.3). These results are consistent with the idea that CN/NFAT activation in astrocytes can help drive synaptic deficits, and inhibition of this pathway can ameliorate these deficits.

While the results revealed striking synaptoprotection in a mouse model of VCID, it did not address the mechanisms by which the synaptic deficits occur. One possible mechanism is the CN-dependent production of numerous immune factors (*e.g.* TNFα or IL-6) that are associated with neuroinflammation (Griffin et al., 1998; Mrak and Griffin, 2005a; Van Eldik et al., 2007; Sama et al., 2008) and implicated as causal factors of synaptic decline in models of CNS injury and disease (Pickering and O'Connor, 2007; Sama and Norris, 2013; Rossi, 2015). Alternatively, pathogenic toxins associated with neurodegenerative diseases (*e.g.* Aβ peptides and glutamate) can be released from activated astrocytes by upregulation of β-secretases (Furman et al., 2012; Jin et al., 2012) or downregulation of glutamate transporters (Sama et al., 2008; Abdul et al., 2009). Regardless of mechanism, this study in combination with our previous studies shows that astrocytic-specific inhibition of CN/NFAT provides overarching synaptoprotection in animal models of CNS injury and disease.

3.4.3 Astrocytic CN/NFAT and cerebral blood flow and metabolism

Maintenance of cerebral blood flow is critical for delivering crucial oxygen to brain tissue (Cipolla, 2009) This may be mediated, in part, by astrocyte endfeet that project onto

cerebral blood vessels and participate in regulation of blood flow via release of vasoactive metabolites (Howarth, 2014; MacVicar and Newman, 2015). Under conditions of injury and disease, increased astrocyte activation- driven in part by CN/NFAT activation- disrupts normal astrocyte physiology and may lead to compromised cerebral blood flow (CBF) which can have detrimental effects on cells. Previous studies have revealed impairments in cerebral blood flow (cerebral hypoperfusion) in several neurodegenerative disorders including AD (Lin et al., 2015; Dai et al., 2016) as well as VCID (Ighodaro et al., 2016; Sun et al., 2016). Consistent with these findings, the present study revealed a deficit in CBF in mice on an HHcy diet-induced model of VCID that was normalized by treatment with AAV-Gfa2-VIVIT (Fig 3.4). These results suggest that targeting a mechanism that can help drive astrocyte activation *(i.e.* CN/NFAT) may restore normal astrocyte regulation of cerebral vessels and thus restore CBF.

Additionally, shifts in brain metabolism have been implicated in neurodegenerative diseases (Herminghaus, 2003; Graff-Radford and Kantarci, 2013). Metabolites of interest include N-acetylaspartate (NAA), a marker of neuronal viability, and myo-inositol (mI), a marker of glial activation (Zhu et al., 2006). Previous studies in both mouse models of neurodegeneration and humans have revealed alterations in brain metabolites including NAA and mI (Chang et al., 2013; Lin et al., 2015). Consistent with previous findings, the present study found reduced levels of NAA in mice on the HHcy diet that was improved by treatment with AAV-Gfa2-VIVIT. Moreover, we found increased levels of mI in mice on the HHcy diet that was improved by treatment with AAV-Gfa2-VIVIT (Fig 3.4). Surprisingly, we did not see any significant differences in levels of glutamate-glutamine.

One possible explanation for the lack of change in glutamate levels could be that inhibition of CN/NFAT has a stronger effect on brain metabolites associated with

neuroinflammation (*i.e.* NAA and mI) than those associated with glutamate synthesis/release. Additionally, our measurements were done in the hippocampus, but it would be interesting to determine if significant changes in CBF and/or brain metabolism occurs in the cortex. Regardless, this study provides proof that astrocyte-specific inhibition of CN/NFAT can have beneficial effects on cerebral blood flow as well as brain metabolism.

3.4.4 Spatial memory and VCID: is there a better behavior test?

Consistent with previous studies (Sudduth et al., 2013b) mice on the HHcy diet exhibited a significant deficit on the radial arm water maze (RAWM) (Fig 3.5). The RAWM consists of six arms in a round pool, with the platform fixed in the same "goal" arm throughout the entire paradigm (Alamed et al., 2006) and is designed to elicit impairments in spatial learning and memory (Shukitt-Hale et al., 2004). Mouse models of AD exhibit striking deficits in spatial learning and memory (Ashe, 2001; Scearce-Levie, 2011; Yin et al., 2011). Moreover, we have previously shown that inhibiting CN/NFAT in astrocytes improves spatial learning and memory in 5xFAD mice treated with the potent NFAT inhibitor VIVIT versus those treated with our control construct (Sompol et al., *in preparation*). However, in the present study, mice on the HHCy diet treated with AAV-Gfa2-VIVIT did not exhibit a significant improvement in performance on the RAWM versus those treated with control EGFP (Fig 3.5, green line).

While this is surprising, it is possible that cerebrovascular pathology does not affect spatial learning and memory in VCID to the same capacity as Aβ plaque and NFT pathology does in AD. This is plausible because Aβ plaques and NFT accumulate in the hippocampus in the earliest stages of the disease, and spatial learning and memory is largely a hippocampal-dependent function. On the other hand, if vascular pathology (*e.g.* microinfarcts or microhemorrhages) tends to affect the cortex or other brain regions in

VCID, perhaps using a treatment targeted to the hippocampus may not be the most effective strategy. Future studies could explore delivering AAV-Gfa2-VIVIT to astrocytes in the cortex as opposed to the hippocampus in order to see improvement on the RAWM. However, if AAV-Gfa2-VIVIT is injected into the cortex, it is likely that protective effects on hippocampal synaptic function and plasticity will be lost. Alternatively, different behavioral tests such as the puzzle box or set shifting (Birrell and Brown, 2000; McAlonan and Brown, 2003; Ben et al., 2011) could be used to elucidate the effects of CN/NFAT inhibition on executive function. Together, both additional approaches should help to improve understanding of how inhibition CN/NFAT signaling in VCID affects behavioral and cognitive performance.

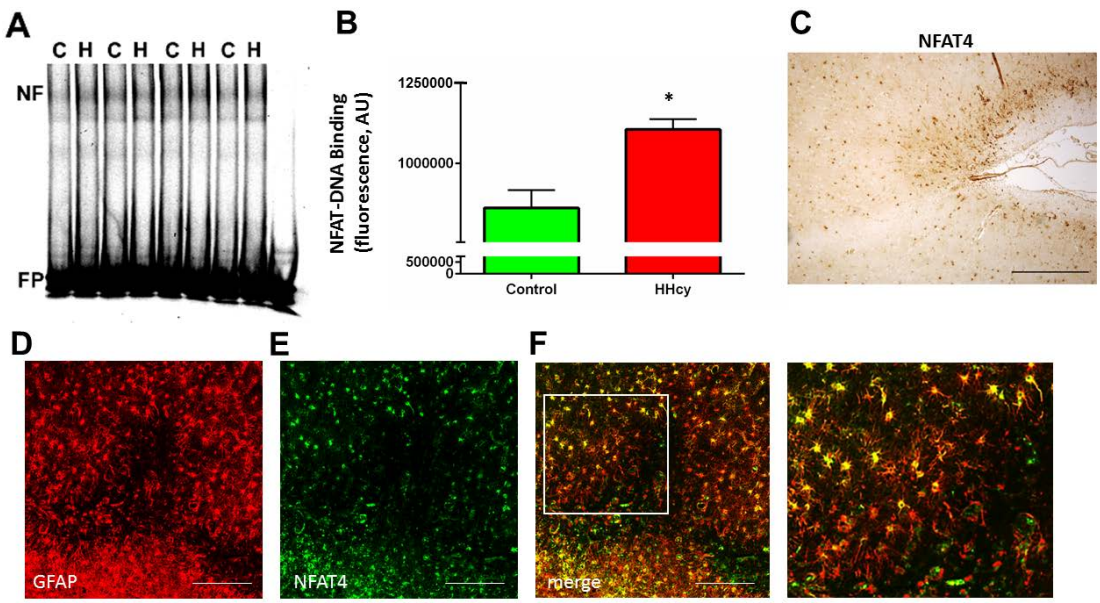

Figure 3.1 Elevated NFAT4 DNA binding and labeling are seen in mouse and human tissue with vascular-associated pathology.

(A) Representative gel showing NFAT band (NF) for control [C] and HHcy [H] mouse cortical tissue. (B) Fluorescence-quantified (AU) NFAT-DNA binding activity for control tissue vs. HHcy tissue. (C) Photomicrograph of human cortical tissue from confirmed VCID case reveals intense labeling of NFAT4 surrounding a microinfarct. 10x photomicrographs of double-labeling with GFAP (D) and NFAT4 (E) reveals co-labeling (F) between GFAP and NFAT4, and confirms that the NFAT4 isoform has a strong astrocyte bias.

COHORT 1

CT diet	HHcy diet
n=10	n=10

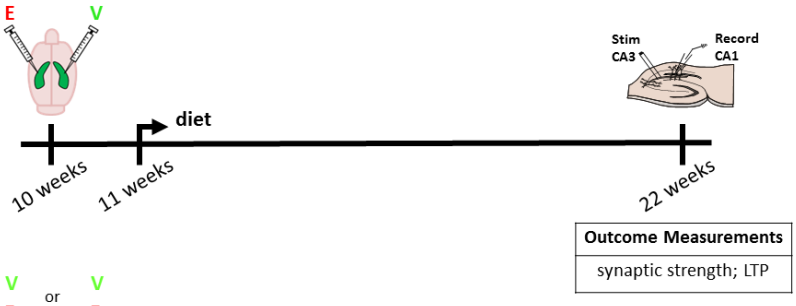

Outcome Measurements
synaptic strength; LTP

COHORT 2

	CT diet	HHcy diet
Egfp	n=10	n=10
VIVIT	n=10	n=10

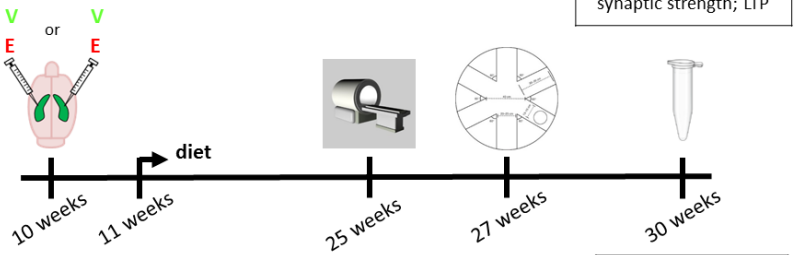

Outcome Measurements
CBF; MRS

Outcome Measurements
RAWM

Outcome Measurements
EMSA; immunofluorescence

Figure 3.2 Experimental design and timeline.

The first cohort of animals was injected bilaterally with both AAV-Gfa2-EGFP (left hemisphere) and AAV-Gfa2-VIVIT-EGFP (right hemisphere) at 10 weeks of age. One week post-injection, mice were started on either control diet (n=10) or HHcy diet (n=10). Mice remained on diet for 11 weeks until sacrifice for slice electrophysiology recordings (synaptic strength and LTP). A second cohort of mice were injected bilaterally with either AAV-Gfa2-EGFP (n=20) or AAV-Gfa2-VIVIT-EGFP (n=20) at 10 weeks of age. One week post-injection, mice were started on either control diet (EGFP, n=10; VIVIT, n=10) or HHcy diet (EGFP, n=10; VIVIT, n=10). After 14 weeks on the diet, mice were imaged using MRI to obtain cerebral blood flow (CBF) and metabolite measurements. Two weeks following MRI measurements, mice underwent radial arm water maze (RAWM) behavioral testing. Three weeks post-behavior, mice were sacrificed via saline-perfusion. One hemisphere was immediately snap-frozen at -80°C using liquid nitrogen for electrophoresis mobility shift assays (EMSAs) and other biochemical measurements; the other hemisphere was immediately post-fixed in 4% paraformaldehyde and later sectioned for histochemical measurements.

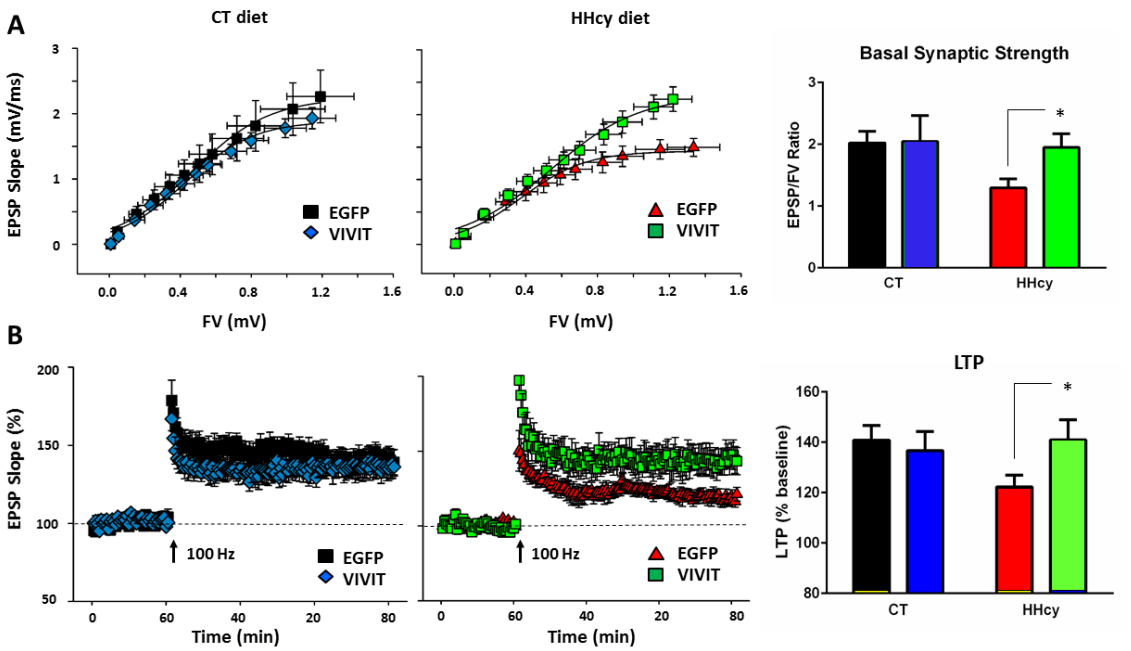

Figure 3.3 AAV-Gfa2-VIVIT improves synaptic function in mice on HHcy diet

Synpatic strength curves are shown for mice on control diet (A, left) and HHcy diet (A, center) in which mean EPSP slope (millivolts per milliseconds) amplitudes (SEM, vertical error bars) are plotted against FV (millivolts) amplitudes (SEM, horizontal error bars) across nine stimulus intensity levels. Quantified EPSP/FV ratio (A, right) shows that VIVIT-treated HHcy mice have normalized synaptic strength relative to control-treated HHcy mice. Similarly, Gfa2-VIVIT improves LTP in mice on HHcy diet. LTP plots are shown for mice on control diet (B, left) and HHcy diet (B, center) in which EPSP slope (% baseline) is plotted against time. Quantified LTP (B, right) revealed that VIVIT-treated HHcy mice have improved LTP relative to control-treated HHcy mice.

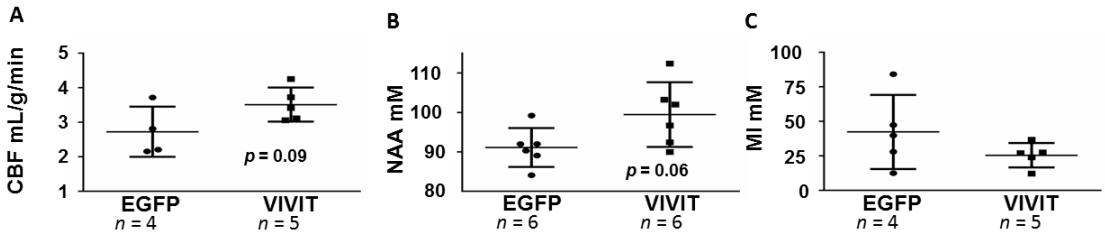

Figure 3.4 AAV-Gfa2-VIVIT improves CBF/MRS parameters in HHcy mice.

Mice at 25 weeks of age on the HHcy diet treated with EGFP control construct exhibited a reduction in cerebral blood flow that was improved in mice treated with VIVIT (A). A reduction in levels of N-acetylaspartate (NAA), indicative of neuronal loss, was seen in mice treated with EGFP; levels were normalized in mice treated with the VIVIT construct (B). An increase in levels of myo-inositol (mI), indicative of increased astrocyte activation, was seen in mice treated with EGFP; levels were normalized in mice treated with the VIVIT construct (C).

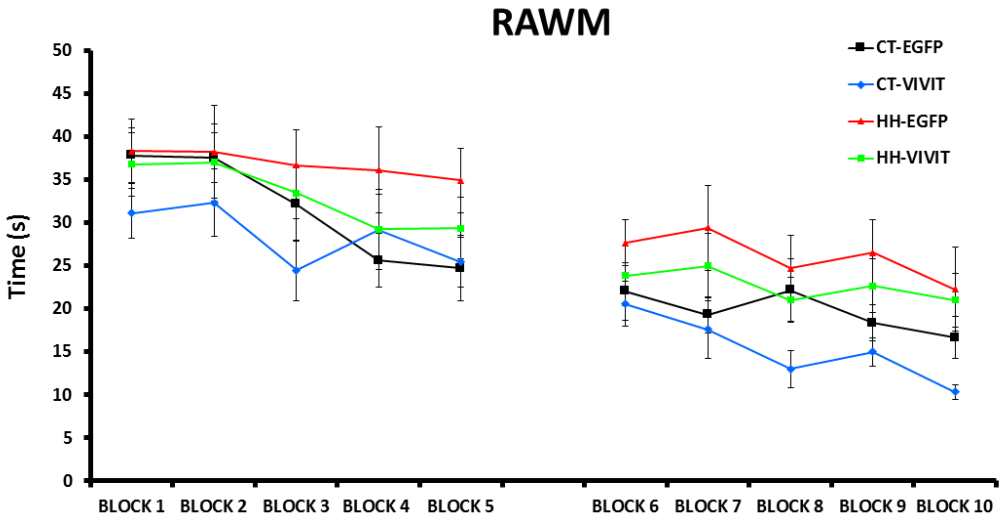

Figure 3.5 Radial arm water maze behavioral testing did not reveal a significant improvement in HHcy mice treated with AAV-Gfa2-VIVIT.

Mice were run through radial arm water maze (RAWM) at 27 weeks of age. Analysis by time (s) revealed a significant deficit in mice on HHcy diet (red and green lines) versus those on the control diet (blue and black lines). However, analysis by either parameter did not reveal a significant improvement in mice treated with AAV-Gfa2-VIVIT (green line) versus those treated with AAV-Gfa2-EGFP (red line).

CHAPTER IV: CALCINEURIN-MEDIATED DEPHOSPHORYLATION OF CONNEXIN43 IN ASTROCYTES: IMPLICATIONS FOR HEMICHANNEL FUNCTION IN THE PROGRESSION OF ALZHEIMER'S DISEASE

Melanie M. Pleiss[a], Hafiz Mohmmad Abdul[b], Jennifer L. Furman[a], Christopher M. Norris[b]

[a]Department of Pharmacology and Nutritional Sciences, University of Kentucky, Lexington, KY 40536

[b]Sanders Brown Center on Aging, University of Kentucky, Lexington, KY 40536

4.1 Introduction

Astrocytes are one of the most abundant cell types in the brain and perform many critical functions in healthy brain tissue (Chen and Swanson, 2003). With aging, injury, and disease- including neurodegenerative conditions such as Alzheimer's disease (AD)- astrocytes become activated which includes a hypertrophic change in morphology, increased production of pro-inflammatory cytokines, and a decreased regulation of glutamate transport (Sama et al., 2008; Fuller et al., 2009; Sofroniew, 2009; Fuller et al., 2010; Sofroniew and Vinters, 2010). Astrocyte activation has been identified as a profound and key component of neuroinflammation (Colombo and Farina, 2016).

Changes in several signaling pathways in activated astrocytes have been implicated in neural dysfunction, one of which being the calcineurin (CN) signaling pathway (Abdul et al., 2009). CN is an exquisitely calcium-sensitive serine/threonine phosphatase (Klee, 1991), and studies in both human AD tissue and transgenic AD mouse tissue have revealed intense labeling of CN in activated astrocytes, especially surrounding amyloid deposits (Norris et al., 2005; Furman et al., 2012; Pleiss et al., 2016). Astrocytic CN has been shown to mediate many of its effects on neurons and other cell types via activation of downstream transcription factors, including nuclear factor of activated T cells (NFAT) and NFκB, both of which have been well-characterized (Fernandez et al., 2007; Abdul et al., 2009; Abdul et al., 2010). Another potential downstream target in astrocytes is connexin43 (Cx43), whose interaction with CN has not been extensively investigated.

Hemichannels (HCs) are composed of connexin protein hexamers (Takeuchi and Suzumura, 2014; Olsen et al., 2015; Moore and O'Brien, 2015), with Cx43 being the most abundant isoform in astrocytes (Orellana et al., 2009; Koulakoff et al., 2012; Orellana et al., 2012). These HCs play a vital role in normal astrocyte function, including maintenance of synapses and neuronal viability. Studies from our lab and others

suggest that levels of Cx43 may change during the progression of AD (Nagy et al., 1996; Mei et al., 2010). The C-terminus of Cx43 is modulated by several protein kinases that are associated with neuroinflammation *e.g.* mitogen-activated protein kinase (MAPK) (Lampe and Lau, 2004; Solan and Lampe, 2009; Solan and Lampe, 2014). A few recent studies have shown that serine 368 in the C-terminus tail is strongly dependent on CN activity (Li and Nagy, 2000; Tence et al., 2012). Here, we found that levels of dephosphorylated connexin43 (dCx43) were increased in human hippocampus in parallel with CN activity in the mild cognitive impairment (MCI) stage of AD. Similarly, elevations in dCx43 were observed in rat primary astrocyte cultures treated with the endogenous inflammatory mediator IL-1β, and this effect was blocked by inhibition of CN with cyclosporin A (CsA) or by the addition of a decoy mimetic peptide to the C-terminus of Cx43, ^{43}Gap52. The ^{43}Gap52 peptide did not inhibit NFAT activity, suggesting that the peptide is relatively selective for Cx43/CN interactions although there was a high amount of variability between the samples. Lastly, application of CsA or ^{43}Gap52 in primary astrocyte cultures reduced EtBr uptake in response to IL-1β, suggesting that CN/Cx43 interactions increase astrocytic membrane permeability via HCs under neuroinflammatory conditions. Together, these results suggest that CN/Cx43 interactions may have a major impact on the function of activated astrocytes and their maintenance of neural and synaptic function.

4.2 Methods

4.2.1 Human biospecimens. Post-mortem brain samples from the hippocampus were provided by the Neuropathology Core of the Alzheimer's Disease Center (ADC) at the University of Kentucky Sanders-Brown Center on Aging and have been previously characterized for the status of multiple CN signaling properties including protein levels, proteolysis, and nuclear localization of NFAT transcription factors (Abdul et al., 2009;

Mohmmad Abdul et al., 2011). Briefly, specimens from individuals with mild cognitive impairment (n = 9), with confirmed AD (n = 15), or with low pathology and no dementia (n = 12) were obtained at autopsy and snap-frozen in liquid nitrogen until use. Diagnostic criteria have been described in detail elsewhere (Mirra et al., 1991; Nelson et al. 2007; Hyman et al., 2012; Montine et al., 2012; Nelson et al., 2012). Multiple case descriptors including age, sex, Braak stage, postmortem autopsy interval, and mini-mental status are provided for each diagnostic category.

4.2.2 Preparation of cell extracts from human brain tissue. Membrane, cytosolic and nuclear fractions from hippocampal tissue samples were prepared as described previously (Abdul et al. 2009). The membrane fractions obtained were resuspended in sucrose buffer [in mM: 300 sucrose, 75 Nacl, 10 Tris (pH 7.4), 20 EDTA, 20 EGTA] containing phosphatase, protease, and CP inhibitor cocktails (EMD Chemicals). Cytosolic and nuclear fractions were resuspended in buffer C [in mM: 50 HEPES (pH 7.6), 50 KCl, 0.1 EDTA, 10% glycerol, 1 dithiothreitol (DTT)], containing phosphatase, protease, and CP inhibitor cocktails and stored at −80° C until use.

4.2.3 Western blot analysis- human biospecimens. Samples were loaded in equal amounts onto pre-cast 4-20% gradient gels (Bio-Rad), resolved using SDS-PAGE and electrophoresis, and transferred onto polyvinylidene difluoride membranes (PVDF) for semiquantitative Western blot. In brief, membranes were blocked using I-Bloc (Tropix) and incubated overnight at 4°C in the following primary antibodies. mouse anti-total Cx43 (1:5,000; Santa Cruz), mouse anti-dephosphorylated Cx43 (1:500; Invitrogen), and mouse anti-Na+,K+-ATPase (1:10,000; Abcam). The Invitrogen antibody is a particularly useful tool as it specifically recognizes connexin43 that is dephosphorylated at Ser368, which has been shown to be a CN-sensitive target and is our primary residue of interest.

Primary antibodies were tagged with HRP-conjugated secondary antibodies (1:10,000), and developed using ECL-plus Western kit (GE Healthcare). Protein levels were quantified on the Storm Phosphor Imager (GE Healthcare). Signal intensity for resultant bands was calculated, and all protein signals were normalized to internal control (i.e. Na+,K+) bands.

4.2.4 Primary astrocyte culture. Primary astrocyte cultures were prepared from E18 Sprague Dawley rat pups similar to that described previously (Sama et al. 2008; Furman et al., 2010). Animals were treated in accordance with the National Institute of Health Guide for the Care and Use of Laboratory Animals. In brief, fetal cortical tissue was harvested and washed in Hanks Balanced Salt Solution before trypsinization and mechanical dissociation by trituration. Cells were plated in culture flasks in Minimal Essential Medium (MEM), buffered by NaHCO3, and supplemented with L-glutamine, 1% antibiotics/antimitotics, and 10% fetal bovine serum. Astrocyte cultures were grown to 80–90% confluency (typically 10–12 days), and microglia were removed by vigorously shaking the flasks at room temperature for 30 min on an orbital shaker [Keller et al. 1996]. Cells were trypsinized and replated with fresh medium in 35-mm culture dishes and grown to ~90% confluency. Previous immunocytochemical analyses of our cultures have indicated that fewer than 5% of plated cells label positively for the microglial marker Iba-1 (data not shown). For a serum-free environment, regular medium was replaced with serum-free medium (MEM, N2, and gentamicin) immediately prior to the start of experiments.

4.2.5 Culture treatments and collection. At approximately 24 h before collection, astrocyte culture dishes were washed 2x with phosphate-buffered saline and switched into serum-free media. For all culture experiments, approximately 16 h prior to collection,

either CsA (10μM; Millipore) or ^{43}Gap52 (1μM; RS Synthesis [described further in background]) were added to inhibitor condition dishes. For EtBr uptake assay, either CN auto-inhibitory peptide (CNAIP) (50μM; Millipore) was added in addition to CsA or ^{43}Gap52. Approximately 3-5 h prior to collection, dishes in CN-stimulating conditions were exposed to 10ng/mL IL-1β. For Western blot analysis, the exogenous Ca^{2+}-mobilizers ionomycin (Ion) (1μM; Sigma) and phorbol ester (PE) (1μM; Sigma) were also applied to culture dishes.

For Western blot analysis, cultures were homogenized in 30% sucrose buffer containing a panel of phosphatase and protease inhibitors as described (Sama et al., 2009; Furman et al, 2010) and scraped free into Eppendorf tubes. Cell lysates from each dish were stored at -80°C until use.

For NFAT-Luciferase assay endpoint measurements, cells were infected with Ad-NFAT-Luc approximately 24 h prior to collection at multiplicity of infection (MOI) of 100. At an MOI of 100, more than 90% of all astrocytes are infected within each dish, ensuring uniform distribution of the NFAT-reporter construct across treatment groups. To collect cell lysates, each culture dish was washed two times with phosphate-buffered saline, and then cells were scraped free in mammalian protein extract reagent (M-PER) buffer (Thermo Fisher) into Eppendorf tubes. Cell lysates from each 35-mm dish were stored at -20°C until use.

4.2.6 Western blot analysis- primary astrocyte culture. Equal amounts of protein using the Lowry method were loaded into individual wells of Criterion TGX pre-cast 4–20% gradient gels (Bio-Rad) and resolved using SDS-PAGE. Proteins were then transferred to polyvinylidene difluoride membranes for semi-quantitative Western blot analysis using the Odyssey Sa Imager System. Membranes were pre-blocked with Odyssey Blocking Buffer and incubated overnight in blocking buffer plus primary

antibodies as described above for the blots with human samples. Primary antibodies were tagged with IRDye-conjugated fluorescent secondary antibodies (1:15,000 [800] or 1:20,000 [680]; Li-Cor), and near-infrared signal was detected on the Odyssey Sa Imager System (Li-Cor). Signal intensity for resultant bands was calculated, and all protein signals were normalized to internal control (i.e. Na+,K+) bands.

4.2.7 NFAT-luciferase reporter assay. As a control for potential between-group variability in NFAT-luciferase expression, all sample volumes were normalized to the same protein concentration with TCM buffer using the Lowry method. Luciferase expression was quantified using a luciferase detection kit (Luc Screen; Tropix) and a plate reader. Typically, six or more dishes were analyzed per treatment condition and experiment was repeated in triplicate, resulting in a well powered experimental design.

4.2.8 Ethidium bromide dye uptake assay. To assess hemichannel permeability, cells were exposed to 5µM ethidium bromide (EtBr; Fisher) for 10 min, washed 2x with phosphate-buffered saline, and immediately imaged on an inverted fluorescent microscope [Nikon Eclipse TE200 with Nuance FX Multispectral Imaging System]. Typically, three or more dishes were analyzed per treatment condition and experiment was repeated in triplicate, resulting in a well powered experimental design. For analysis, total fluorescence intensity was calculated using Adobe Photoshop.

4.2.9 Statistics. ANOVA was used to compare differences in Western blot protein levels. Average luciferase and ethidium bromide values were compared with repeated measures ANOVA. When appropriate, Fisher's protected least significant difference test was used for *post hoc* analyses. Significance for all statistical comparisons was set at $p \leq 0.05$.

4.3 Results

4.3.1 Levels of dephosphorylated Cx43 are elevated early in the progression of AD and are positively correlated with increased CN activity.

Studies from other labs have demonstrated raised levels of dephosphorylated Cx43 with neuroinflammation or other insults e.g. hypoxia. To assess levels of dCx43 through the progression of AD, we used human hippocampal biospecimens from confirmed cases of Mild Cognitive Impairment (MCI), AD, as well as age-matched non-demented controls (ND). All samples were obtained with a rapid post-mortem autopsy interval (approx. 3 hours) and were extensively characterized for AD pathology i.e. Braak stage, MMSE score by a neuropathologist. Using an antibody that recognizes the entire Cx43 protein, Western blot analyses revealed a small, non-significant reduction in total Cx43 levels in MCI cases relative to ND control cases (Fig 4.1A). Further, using an antibody that specifically recognizes the Cx43 protein when it's dephosphorylated at serine368 (CN-sensitive residue), Western blot analyses revealed a significant increase ($p < 0.01$) in dCx43 levels in samples from MCI cases relative to ND control samples (Fig 4.1B). Thus, comparing the ratio of dCx43 to total Cx43 we see a significant increase ($p < 0.001$) in MCI cases relative to ND control cases (Fig 4.1C).

Using samples from the same cases, we measured protein levels of ΔCN, a constitutively active CN fragment, in cytosolic fractions as well as protein levels of NFAT1, a downstream CN target, in nuclear fractions. With ranked levels of dCx43, we observed significant positive correlations with both CN activation (ΔCN) ($p < 0.05$) (Fig 4.1D) and CN activity (NFAT1 translocation) ($p < 0.01$) (Fig 4.1E). These results indicate that dCx43 are elevated in early stages of AD in a CN-dependent manner.

4.3.2 Levels of dephosphorylated Cx43 are elevated under CN-stimulating conditions in rat primary astrocyte cultures, and are blocked with the use of CN inhibitors.

To mimic the results we observed in the human biospecimens, we performed Western blot analyses using rat primary astrocyte cultures. Conditions of elevated CN activation were achieved with the application of exogenous Ca2+ mobilizers, ionomycin (Ion) and phorbol ester (PE), as well as the endogenous neuroinflammatory factor, interleukin 1 beta (IL-1β). Similar to our human data, with both Ion/PE (Fig 4.2, left panels) and IL-1β (Fig 4.2, right panels) we saw a reduction in levels of total Cx43 (Fig 4.2 A,D) and a rise in levels of dCx43 (Fig 4.2, B,E) under conditions of CN stimulation relative to untreated controls. This resulted in significant increase ($p < 0.05$) in dephosphorylated-to-total Cx43 ratio after treatment with both Ion/PE and IL-1β (Fig 4.2 C,F). This effect was inhibited using the CN inhibitor, cyclosporin A (CsA) (Ion/PE, data not shown; IL-1β, see Fig 3). These results reinforce that the trends we see in our human data i.e. levels of dCx43 increase in tandem with CN proteolysis and activity, and can be replicated using a primary astrocyte culture system.

4.3.3 A mimetic peptide that encompasses Serine 368 on the C-terminus of Cx43 blocks dephosporylation of Cx43 but does not interfere with other CN substrates.

To determine if our mimetic peptide (^{43}Gap52) could prevent dephosphorylation of Cx43 we performed Western blot analyses using rat primary astrocyte cultures stimulated IL-1β. Inhibition of the inflammatory mediatior, IL-1β, with both CsA and ^{43}Gap52 blocked dephosphorylation of Cx43 ($p < 0.05$) (Fig 4.3 A,B). Moreover, to ensure that ^{43}Gap52 does not interfere with other CN substrates e.g. Nuclear factor of activated T cells, we did an NFAT-luciferase reporter assay. Application of CsA to primary astrocyte cultures treated with IL-1β revealed a significant reduction in luciferase expression ($p < 0.05$) (Fig

4.3 C), but application of ^{43}Gap52 did not reduce luciferase expression (Fig 4.3 D). Together, these results suggest that ^{43}Gap52 sufficiently reduces dephosphorylation of Cx43, and is relatively selective for CN/Cx43 interactions.

4.3.4 Hemichannel permeability is reduced using CN-AIP and ^{43}Gap52 in primary astrocyte cultures treated with IL-1β.

To assess hemichannel permeability, we performed ethidium bromide (EtBr) dye uptake assays in primary astrocyte cultures treated with IL-1β. Culture dishes with no EtBr treatment served as a negative control, and imaging revealed uniform auto-fluorescence but no uptake into the nuclei of cells (data not shown). Application of IL-1β resulted in significant EtBr uptake into cells (Fig 4.4 A, top right) versus untreated (UT) conditions ($p < 0.001$) while pre-treatment with both the CN-AIP ($p < 0.01$) or ^{43}Gap52 ($p < 0.001$) had reduced EtBr uptake into cells (Fig 4.4 A, bottom panels). These results suggest that CN/Cx43 interactions lead to increased hemichannel permeability in astrocytes which may negatively impact synaptic function and neuronal viability.

4.4 Discussion

In this present study, levels of connexin43 dephosphorylation were elevated in both human MCI tissue and rat primary astrocyte cultures that had been treated with CN stimulators. Further, a novel mimetic peptide (^{43}Gap52) was used as a potentially selective inhibitor for CN/Cx43 interactions. Lastly, ethidium bromide uptake assays revealed increased dye uptake under conditions of CN activation. Together, results suggest that CN/Cx43 interactions may have a major impact on the function of activated astrocytes and their role in synaptic maintenance.

4.4.1 Dephosphorylation of Cx43 in AD progression

CNS injury and disease (*e.g.* Alzheimer's disease) are associated with changes in connexins, including connexin43 (Cx43), which is the most abundant connexin expressed in astrocytes (Orellana et al., 2009; Koulakoff et al., 2012; Orellana et al., 2012). Moreover, a specific residue on the C-terminus of Cx43, Ser368, is sensitive to CN (Li and Nagy, 2000; Tence et al., 2012). Work from our lab, and others, have shown CN expression and activation of downstream targets (*i.e.* NFATs) is elevated with Alzheimer's disease (Hashimoto et al., 1998; Norris et al., 2005; Celsi et al., 2007; Abdul et al., 2009; Serrano-Perez et al., 2011; Neria et al., 2013; Furman et al., 2016; Pleiss et al., 2016). Consistent with these findings, the present study found elevated levels of dephosphorylated Cx43 in both primary astrocyte cultures and human MCI hippocampus in tandem with elevations in CN activity (Figs 4.1 and 4.2). These results suggest CN/Cx43 interactions may play a significant role in the initiation or progression in the early stages of AD (*i.e.* MCI).

Surprisingly, in human tissue, levels of dephosphorylated connexin43 were reduced to control levels (Fig 4.1 B). One possibility for this reduction is that AD tissue can have variable levels of both Aβ and NFT pathology, which could mask any trends in levels of dephosphorylated Cx43. Future studies to measure protein levels of dephosphorylated Cx43 across the course of AD (*i.e.* mild, moderate, severe) could help elicit the trend in Cx43 dephosphorylation. An alternative possibility is that tissue is too severely degenerated in AD cases to get a true measurement of dephosphorylated Cx43 levels. Regardless, the elevations in dephosphorylated Cx43 in MCI tissue suggest that potential therapeutics should be delivered early in the disease progression.

4.4.2 Use of the novel mimetic peptide, ^{43}Gap52

Inhibition of CN using general inhibitors (*e.g.* cyclosporin A or FK506) can have beneficial effects for neurons and astrocytes, such as improved synaptic function (Taglialatela et al., 2009). However, not only is general inhibition of CN non-specific, there are also many adverse side effects, including nephrotoxicity and immunosuppression (Reese and Taglialatela, 2011; Taglialatela et al., 2015). We have previously shown that use of a selective CN/NFAT inhibitor (VIVIT) delivered to astrocytes in models of CNS injury and disease results in improved synaptic function (Furman et al., 2012; Furman et al., 2016; Sompol et al., *in preparation*), improved cognitive performance (Furman et al., 2012; Sompol et al., *in preparation*), and reduced glial activation (Furman et al., 2012). Using this rationale, in the present study we developed a small mimetic peptide to the C-terminus of Cx43 encompassing the CN-sensitive residue, Ser368 (named ^{43}Gap52) to act as a "decoy" substrate. While ^{43}Gap52 significantly reduced levels of dephosphorylated Cx43 in primary astrocyte culture ($p < 0.05$) (Fig 4.3 B), it did not inhibit expression of NFAT-luciferase (Fig 4.3 D), suggesting the ^{43}Gap52 is relatively selective at inhibiting CN/Cx43 interactions.

While the preliminary evidence is encouraging, the peptide is 52 residues in length (including 11 poly-Arg and 3 Gly linker residues to facilitate cellular uptake). Additionally, studies were performed in primary astrocyte culture and human tissue, but no *in vivo* studies using ^{43}Gap52 have been performed. Future studies should first focus on refining ^{43}Gap52 to reduce the peptide length but only to the extent that it is still effective at inhibiting CN/Cx43 interactions. Next, ^{43}Gap52 could be put into an AAV vector with a Gfa2 promotor so that it could be delivered specifically to astrocytes in transgenic AD mouse models or HHcy diet-induced mouse models of VCID. The *in vivo* studies using ^{43}Gap52 could measure synaptic function and plasticity, cognition, and

protein levels of dephosphorylated Cx43. Overall, the preliminary evidence for selective CN/Cx43 inhibition in the present study is encouraging for future *in vivo* studies.

4.4.3 Modulation of Cx43 hemichannes: implications for synaptic function

Hemichannels (HCs) are composed of connexin hexamers that are unopposed in the plasma membrane, and facilitate critical cross-talk between the cytosol and the extracellular milieu. Normally maintained in a closed state, HCs can significantly alter the composition of the astrocyte cytosol (via passage of glutamate, ATP, Ca^{2+}) when open (Takeuchi and Suzumura, 2014; Moore and O'Brien, 2015; Olsen et al., 2015). Alterations in HCs in astrocytes have been implicated in several neurological disorders, including epilepsy (Seifert et al., 2010; Steinhauser et al., 2012) and neurodegeneration (Seifert et al., 2006; Rossi and Volterra, 2009; Quintanilla et al., 2012). Moreover, previous studies have not only found that AD-relevant factors can increase hemichannel activity in astrocytes but these astrocyte hemichannels also release neurotoxic factors such as glutamate (Orellana et al., 2011 a,b). Consistent with these findings, the present study found that application of IL-1β to primary astrocyte cultures resulted in increased ethidium bromide dye uptake ($p < 0.001$) (via Cx43 HCs) and this uptake was impaired using a CN auto-inhibtory peptide ($p < 0.01$) and ^{43}Gap52 ($p < 0.001$) (Fig 4.4).

While the results show that inhibition of CN/Cx43 interactions in astrocytes using ^{43}Gap52 can have an effect on HCs, it is still unclear what effect HC modulation has on synaptic function. Finding a way to study this *in vivo*, possibly through an AAV vector (see above), will be critical for understanding the consequences of CN/Cx43 inhibition on synaptic function. In addition to obtaining electrophysiological outcomes of synaptic function and plasticity (*i.e.* basal synaptic strength and LTP), outcome measurements

could also include protein levels of synapse-relevant proteins (*e.g.* PSD-95, synapsin 1, GluR1, and NR2A/NR2B) (Ansari et al., 2013; Scheff et al., 2013; Furman et al., 2016). Regardless, this study provides encouraging proof-of-concept results for inhibition of CN/Cx43 interactions and provides rationale for studying synaptic function *in vivo*.

Human Subjects						
Group Classification	***n***	**m/f**	**Age (years)**	**PMI (hours)**	**Braak Stage**	**MMSE**
Control (ND)	12	2/10	87.8 ± 0.7	2.9 ± 0.6	0.83 ± 1	29.1 ± 1.3
Mild Cognitive Impairment	9	4/5	89.8 ± 5.7	3.9 ± 2.4	3.4 ± 1.2	23.8 ± 3.9
Alzheimer's disease	15	6/9	79.1 ± 7.1	3.4 ± 0.87	5.7 ± 0.8	8.3 ± 7

Table 4.1 Description of human subject tissue from non-demented control, mild cognitive impairment, and Alzheimer's disease cases. Values expressed as Mean ± SD. PMI= postmortem autopsy interval. MMSE= mini mental state examination.

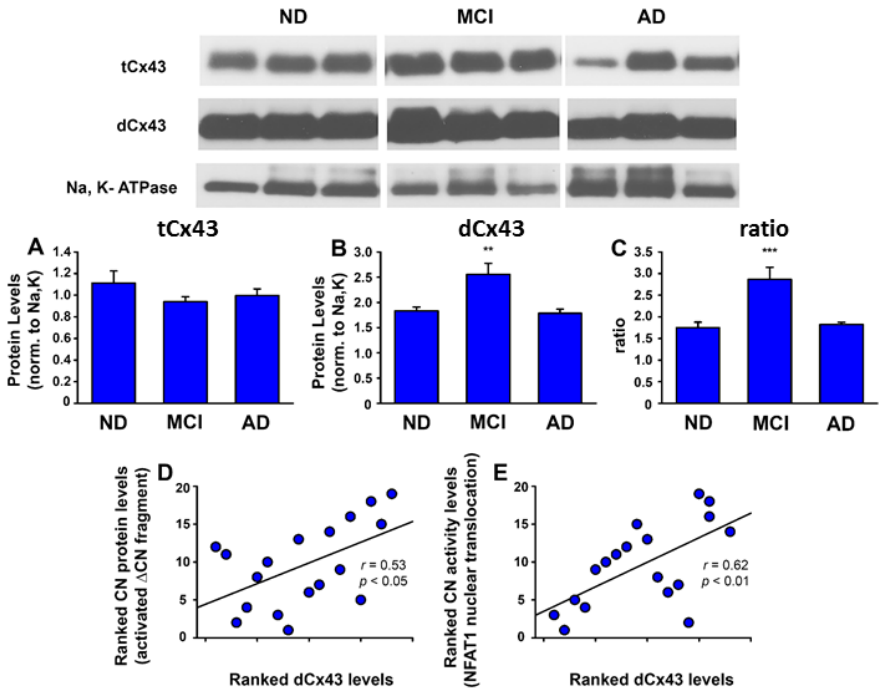

Figure 4.1 Levels of dephosphorylated connexin43 are elevated in MCI in tandem with increased CN activity. Representative bands and Mean ± SEM Cx43 (A) total Cx43, (B) Ser368 dephosphorylated Cx43 ($p < 0.01$), and (C) dephosphorylated:total Cx43 ($p < 0.001$) protein levels in human hippocampal tissue. Phosphorylation state changes markedly in MCI samples, but is not apparent in AD samples. Dephospho-Cx43 shows a significant positive correlation with the constitutively active form of CN (D) and to activated NFAT1 (E), a CN-dependent transcription factor.

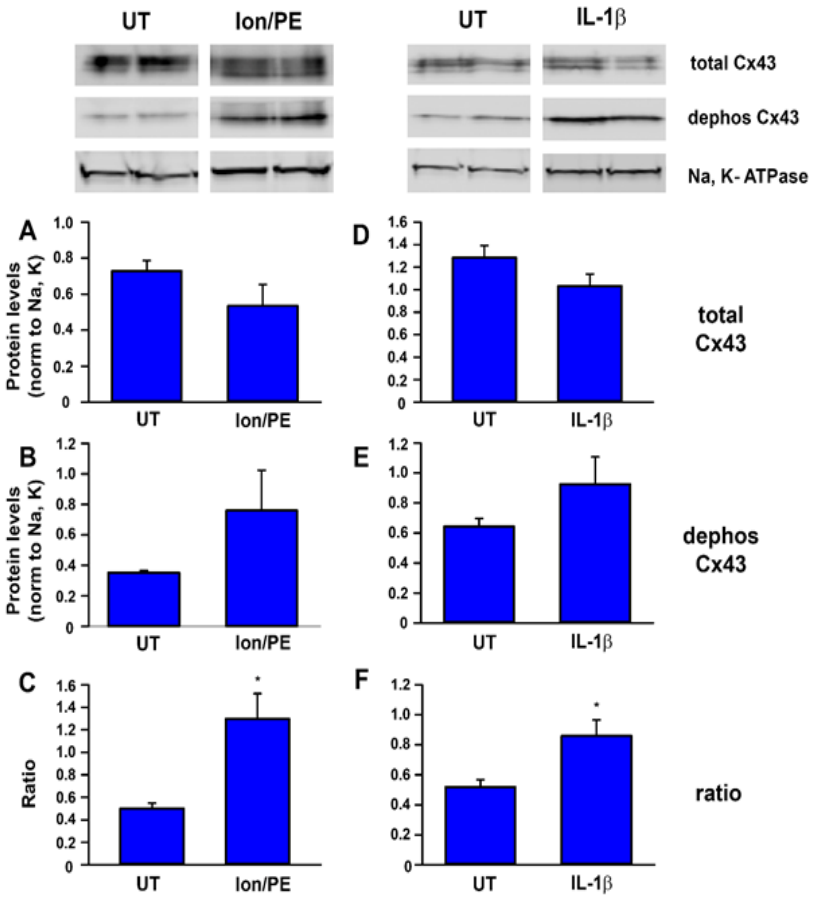

Figure 4.2 Levels of dephosphorylated connexin43 are elevated in rat primary astrocyte cultures treated with endogenous and exogenous stimulators of CN activity. Representative bands and mean ± SEM total Cx43 (A,D) and dephosphorylated Cx43 (B,E) protein levels normalized to Na^+/K^+ ATPase protein levels in primary astrocyte cultures treated for 1 hr with Ion/PE (Left panels) or IL-1β (Right panels). Stimulation of astrocytes with each treatment resulted in a significant increase in the ratio of dephosphorylated Cx43 to total Cx43 ($p < 0.05$) (C,F).

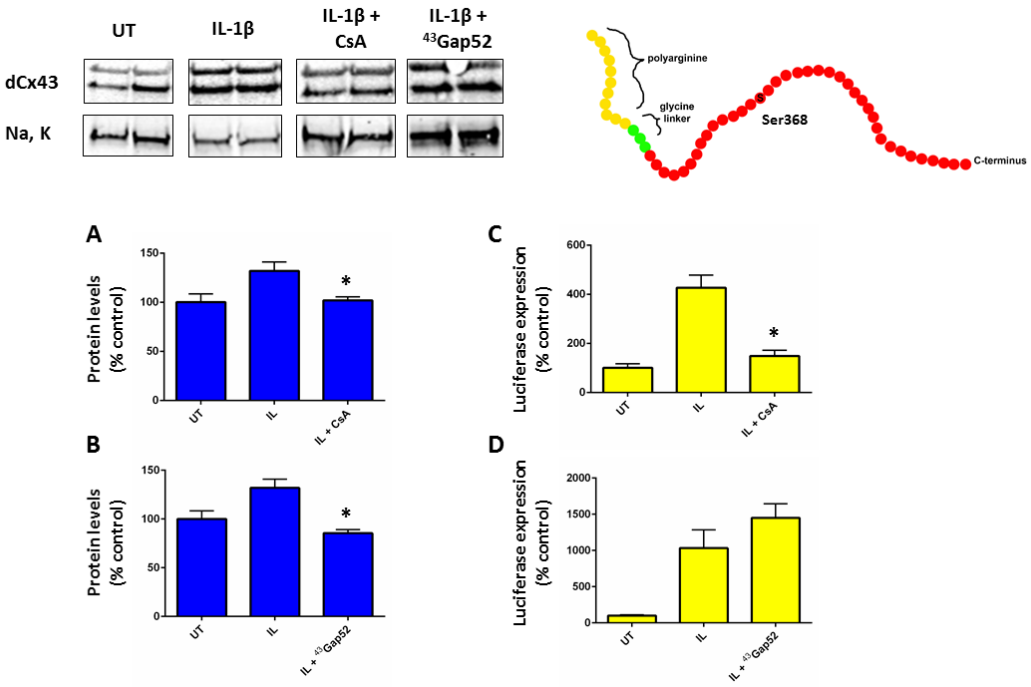

Figure 4.3 A decoy mimetic peptide, ^{43}Gap52, selectively inhibits CN/Cx43 interactions. Representative bands and Mean (% control) ± SEM dephosphorylated protein levels of primary astrocyte cultures treated with IL-1β in the presence or absence of CsA ($p < 0.05$) (A), or ^{43}Gap52 ($p < 0.05$) (B). Mean (% control) ± SEM NFAT-luciferase expression levels of primary astrocyte cultures treated with IL-1β in the presence or absence of CsA ($p < 0.05$) (C), or ^{43}Gap52 (D).

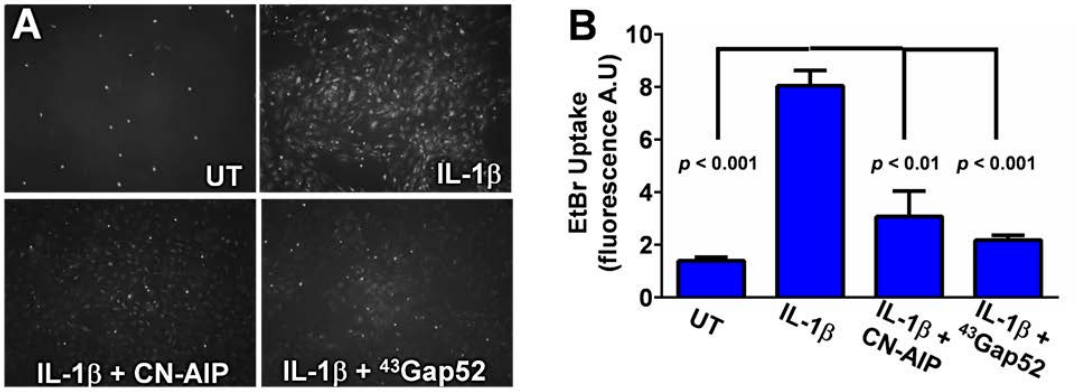

Figure 4.4 The mimetic peptide ^{43}Gap52 reduces ethidium bromide dye uptake into primary astrocyte cultures. 10x photomicrographs of EtBr uptake in UT p7 astrocytes (A, top left panel) and astrocytes treated for 3 h with 10 nM IL-1β (A, top right panel) with/without CN-AIP (A, bottom left panel), or ^{43}Gap52 (A, bottom right panel). (B) Mean±SEM EtBr uptake. Experiment was done in triplicate.

CHAPTER V: GENERAL CONCLUSIONS AND FUTURE DIRECTIONS

5.1 General Conclusions

Aging, injury, and neurodegenerative diseases have a unifying hallmark of neuroinflammation, characterized by neuroglial reactivity and a significant upregulation of cytokines, reactive oxygen species, and nitric oxide (Akiyama et al., 2000; Kitazawa et al., 2004; Skaper, 2007). Astrocytes, in tandem with microglia, help to coordinate the neuroinflammatory response which may be advantageous in an acute setting but detrimental under chronic conditions (Akiyama et al., 2000; Wyss-Coray and Mucke, 2002; Skaper, 2007; Meraz-Rios et al., 2013). Furthermore, under pathological conditions activated astrocytes not only undergo increased production of pro-inflammatory mediators but also lose or see a significant weakening in the regulation of critical, normal astrocyte functions (*e.g.* synaptic maintenance) (Fuller et al., 2009; Sofroniew and Vinters, 2010; Steele and Robinson, 2012). Several astrocyte signaling pathways have been implicated in neurodegeneration and one in particular, the protein phosphatase calcineurin, may help initiate and/or promote the activated astrocyte response (Norris et al., 2005; Fernandez et al., 2007; Canellada et al., 2008; Sama et al., 2008; Abdul et al., 2009; Furman et al., 2012; Pleiss et al., 2016). Moreover, aberrant Ca^{2+} dysregulation that is often seen in neurodegeneration may result in proteolysis of calcineurin that unregulated, constitutively active, and generally deleterious to cellular and synaptic function (Wu et al., 2004; Pleiss et al., 2016). Thus, astrocytic calcineurin signaling—both activation of and interactions with downstream targets is an ideal molecular target for modulating the harmful effects of activated astrocytes with neuroinflammation and neurodegeneration.

The all-encompassing goal of this dissertation was to explore calcineurin signaling in astrocytes in a variety of neurodegenerative conditions that share a neuroinflammatory hallmark. Using a novel antibody (ΔCN), we determined that highly active, proteolyzed calcineurin is abundant in astrocytes, especially those closely

associated with AD and vascular pathology (Chapter II) (Pleiss et al., 2016). A previous study using adeno-associated virus (AAV) to deliver an inhibitor of CN/NFAT signaling—VIVIT—specifically to astrocytes in APP/PS1 mice revealed reduced glial activity and amyloid deposition, as well as improved synaptic function and cognitive performance (Furman et al., 2012). Using the same strategy in a diet-induced mouse model of VCID, we determined that inhibition of CN/NFAT in astrocytes was synaptoprotective but had no significant effect on cognitive performance (Chapter III). To explore other possible downstream targets, we looked at interactions between CN and Cx43 in AD. Using a novel mimetic peptide 'decoy' (^{43}Gap52) to the C-terminus of Cx43, we determined that we could inhibit dephosphorylation of Cx43 without inhibiting CN's effects on other targets. Moreover, application of ^{43}Gap52 resulted in a functional normalization of Cx43 hemichannel function (Chapter IV) (Pleiss et al., *in preparation*). Taken together, these results suggest that both CN activation and its interactions with downstream targets in astrocytes can significantly contribute to neurodegenerative disease (*i.e.* AD and VCID) processes, and therefore provides a valuable molecular target for therapeutics.

5.2 The big picture: is astrocytic calcineurin a good therapeutic target for neurodegenerative diseases?

The section above provides the rationale for why I chose to study calcineurin signaling in astrocytes for this dissertation, but it is possible that this may not be the best target for neurodegenerative disease therapeutics. Here, I will explore three possibilities where targeting of astrocytic calcineurin signaling may not be effective or may even be harmful to cells in the brain.

5.2.1 Alternative cell types

While our previous work and the work in this dissertation presents strong evidence that inhibition of astrocytic CN is synaptoprotective (Furman et al., 2012; Furman et al., 2016; Sompol et al., *in preparation*), improves cognitive function (Furman et al., 2012; Sompol et al., *in preparation*), and reduces glial activation (Furman et al., 2012), it is possible that inhibition of CN signaling in other cell types (*e.g.* neurons or microglia) may be a more effective therapeutic. One study in AD transgenic mice revealed that acute, blanket inhibition of CN (which would include neurons and astrocytes) resulted in improved cognition (Dineley et al., 2007). Moreover, another study found that inhibition of CN in cortical cultures provided the neuroprotective effect of maintaining nitric oxide synthase catalytic activity (Dawson et al., 1993). Additionally, a recent study revealed that inhibition of NFAT—an almost exclusive substrate of CN-- in microglia, both *in vitro* and in a transgenic AD model, provides a robust anti-inflammatory effect (Rojanathammanee et al., 2013). A study that inhibited CN in oligodendrocytes saw a reduction in apoptosis (Sanchez-Gomez et al., 2003). Therefore, it is certainly plausible that astrocytes are not the only viable neural cell type where CN inhibition is protective.

Initial future studies in our lab could focus on putting VIVIT or ^{43}Gap52 into AAV vectors with neuronal-specific, microglial-specific, or oligodendrocyte-specific promoters to study the *in vivo* effect of CN inhibition in alternative neural cell types. Outcomes measures should include cognitive testing, synaptic transmission and plasticity, as well as protein/RNA measurements of glial activation and neuroinflammation. While multiple studies (including ours) have already established that inhibition of astrocytic CN provides cognitive and synaptic benefits, I think the next big obstacle to overcome in neuroscience research is dissecting the differences in phenotype between healthy and diseased tissue, and furthermore in response to different types of CNS injury and insult. In fact, a recent study in the Barres lab has started to explore this in healthy versus

diseased astrocytes in response to two different CNS insults (Zamanian et al., 2012), and I will elaborate on this more in section 5.2.2. This consideration is critical because many studies operate under the notion that all cells (*e.g.* all astrocytes) respond to disease insults uniformly when in fact the results in this dissertation (Fig 2.2 K, Fig 2.5) as well as other studies (*e.g.* Zamanian et al., 2012) suggest otherwise. Once these phenotypic differences are better understood, not only will we be able to target therapeutics to specific cell types, but we can hopefully target the specific cell phenotypes that exhibit detrimental properties (*i.*e. contribute to the disease processes) and at the same time maintain cells that are neuro-protective (*i.e.* function normally).

5.2.2 Is CN activity protective?

Our previous work and the work in this dissertation have established that exacerbated activation of CN is detrimental to synapses (Pleiss et al., 2016) and that inhibition of CN in astrocytes provides synaptic and cognitive benefits (Furman et al., 2012; Furman et al., 2016; Sompol et al., *in preparation*). However, it is possible that there are instances in which CN activation may be beneficial. First, time and duration of CN activity must be considered. In an acute setting, activation of CN and the glial response may be advantageous for isolating invading pathogens and/or sites of tissue damage. In fact, a study that examined the response of astrocytes to acute (ischemic) versus chronic (neuroinflammatory) insults found that astrocyte activation in acute injury is overwhelmingly protective and functions to repair the BBB, limits immune cell influx, and decreases neuronal cell death (Zamanian et al., 2012). Ignoring disease for a moment and focusing on healthy tissue, studies have shown that CN is abundant in neurons and plays a critical role in the maintenance of neuronal structure and function (*e.g.* dendritic spines and synaptic plasticity, respectively) (Halpain et al., 1998; Wu et al., 2010).

Moreover, outside of the CNS, calcineurin can play important roles in skeletal muscle differentiation (Friday et al., 2000) or Schwann cell differentiation (Kao et al., 2009).

On the contrary, while CN activation certainly has protective and beneficial functions in some cases, in chronic neurodegenerative conditions such as AD or VCID-- which are the focus of this dissertation-- I think that increased CN activity is tremendously harmful. For instance, acute inhibition of CN in Tg2576 mice restored cognitive deficits (Taglialatela et al., 2009) or inhibition of CN in an acute model of CNS injury was incredibly synaptoprotective (Furman et al., 2016). Moreover, chronic activation of CN/NFAT-dependent transcription of pro-inflammatory factors are associated with neurodegeneration (Van Wagoner et al., 1999; Fernandez et al., 2007; Sama et al., 2008). Additionally, a study that observed the response of astrocytes to a neuroinflammatory response found that activation of astrocytes in this instance was overwhelmingly detrimental through inhibition of axonal regeneration, secretion of pro-inflammatory factors, and activation of the complement cascade that ultimately contributes to synapse loss (Zamanian et al., 2012). Therefore, the focus on targeting CN-mediated astrocyte activation in these dissertation studies was on point; however, as mentioned in section 5.2.1, future studies should focus on better understanding astrocyte phenotypes in response to different CNS insults and diseases.

5.2.3 Non-calcineurin targets

While inhibition of CN in astrocytes has been shown to provide numerous cognitive and synaptic benefits (Furman et al., 2012; Furman et al., 2016; Sompol et al., *in preparation*), perhaps there are alternative, more effective therapeutic targets available. Many studies aimed at clearing or reducing Aβ levels in Alzheimer's disease have been performed, yet none have provided compelling evidence for cognitive improvement due to reduction of beta-amyloid levels (Rosenblum, 2014). A therapeutic aimed at general

neuroinflammation and/or specific componenets may be beneficial. For example, one study revealed a lessened inflammatory response and reduction in Aβ levels in APP/PS1 mice using intravenous immunoglobin, a general immune modulator (Sudduth et al., 2013 a). Many different studies have explored the use of non-steroidal anti-inflammatory drugs (NSAIDs) as a therapeutic for AD and other diseases with neuroinflammatory components, and while people that are on long-term NSAID regimens have a reduced risk of developing AD (Andersen et al., 1995; Rich et al., 1995; McGeer et al., 1996; Lee et al., 2010), controlled trials have not been able replicate these beneficial effects (Aisen et al., 2003; Reines et al., 2004). Furthermore, recent studies have revealed that upregulation of reactive oxygen species and reactive nitrogen species may contribute to neurodegenerative disease, and thus may provide a good therapeutic target (Nakamura et al., 2013). Alternatively, reduction of aberrant tau using an inhibitor to a specific heat shock protein revealed improved synaptic function *in vivo* (Abisambra et al., 2013). So while many non-CN targets exist and may be advantageous, the benefit of targeting CN is that Ca^{2+} dysregulation is a common denominator in many neurodegenerative diseases, and therefore therapeutics aimed at CN inhibition could be targeted to a broad spectrum of diseases. However, many complex and multi-factorial processes are occuring in neurodegeneration, and as such, I think that CN inhibition in tandem with other therapeutics (*e.g.* Aβ clearance) will provide the most beneficial results.

5.3 Concluding Remarks

The work in this dissertation has presented a broad picture of astrocytic calcineurin activation and its interactions with downstream targets in several neurodegenerative diseases. Using a novel antibody, I have shown that constitutively active, proteolyzed CN is found in astrocytes strongly associated with both AD and vascular pathology.

Additionally, using AAV-mediated astrocyte-specific inhibition of CN/NFAT in a mouse model of VCID revealed synaptoprotective effects. Furthermore, a novel “decoy” mimetic peptide to the C-terminus of Cx43 was able to selectively interact CN/Cx43 interactions and functionally normalize hemichannels in rat primary astrocyte cultures. Together, this suggests the astrocytic CN signaling pathways are not only a major player in neurodegenerative disease processes but should also be considered a viable target for AD and VCID therapeutics.

REFERENCES

Abdul, HM, Furman, JL, Sama, MA, Mathis, DM, Norris, CM (2010) NFATs and Alzheimer's Disease. Mol Cell Pharmacology 2:7-14.

Abdul, HM, Sama, MA, Furman, JL, Mathis, DM, Beckett, TL, Weidner, AM, Patel, ES, Baig, I. Murphy, MP, Levine, H, 3rd, Kraner, SD, Norris, CM (2009) Cognitive decline in Alzheimer's disease is associated with selective changes in calcineurin/NFAT signaling. J Neurosci 29:12957-12969.

Abisambra, J, Jinwal, UK, Miyata, Y, Rogers, J, Blair, L, Li, X, Seguin, SP, Wang, L, Jin, Y, Bacon, J, Brady, S, Cockman, M, Guidi, C, Zhang, J, Koren, J, Young, ZT, Atkins, CA, Zhang, B, Lawson, LY, Weeber, EJ, Brodsky, JL, Gestwicki, JE, Dickey, CA (2013) Allosteric heat shock protein 70 inhibitors rapidly rescue synaptic plasticity deficits by reducing aberrant tau. Biol Psychiatry 74:367-374.

Aisen, PS, Schafer, KA, Grundman, M, Pfeiffer, E, Sano, M, Davis, KL, Farlow, MR, Jin, S, Thomas, RG, Thal, LJ (2003) Effects of rofecoxib or naproxen vs placebo on Alzheimer disease progression: a randomized controlled trial. JAMA 289:2819-2826.

Akiyama, H, Barger, S, Barnum, S, Bradt, B, Bauer, J, Cole, GM, Cooper, NR, Eikelenboom, P, Emmerling, M, Fiebich, BL, Finch, CE, Frautschy, S, Griffin, WS, Hampel, H, Hull, M, Landreth, G, Lue, L, Mrak, R, Mackenzie, IR, McGeer, PL, O'Banion, MK, Pachter, J, Pasinetti, G, Plata-Salaman, C, Rogers, J, Rydel, R, Shen, Y, Streit, W, Strohmeyer, R, Tooyoma, I, Van Muiswinkel, FL, Veerhuis, R, Walker, D, Webster, S, Wegrzyniak, B, Wenk, G, Wyss-Coray, T (2000) Inflammation and Alzheimer's disease. Neurobiol Aging 21:383-421.

Alamed, J, Wilcock, DM, Diamond, DM, Gordon, MN, Morgan, D (2006) Two-day radial arm water maze learning and memory task; robust resolution of amyloid-related memory deficits in transgenic mice. Nat Protoc 1:1671-1679.

Aliabadi, AZ, Zuckermann, AO, Grimm, M (2007) Immunosuppressive therapy in older cardiac transplant patients. Drugs Aging 24:913-932.

Allen, NJ (2014) Astrocyte regulation of synaptic behavior. Annu Rev Cell Dev Biol 30:439-463.

Andersen, K, Launer, LJ, Ott, A, Hoes, AW, Breteler, MM, Hofman, A (1995) Do nonsteroidal anti-inflammatory drugs decrease the risk for Alzheimer's disease? The Rotterdam Study. Neurology 45:1441-1445.

Anoop, A, Singh, PK, Jacob, RS, Maji, SK (2010) CSF Biomarkers for Alzheimer's Disease Diagnosis. Int J Alzheimers Dis 2010.

Ansari, MA, Roberts, KN, Scheff, SW (2013) Dose- and time-dependent neuroprotective effects of Pycnogenol following traumatic brain injury. J Neurotrauma 30:1542-1549.

Aramburu, J, Yaffe, MB, Lopez-Rodriguez, C, Cantley, LC, Hogan, PG, Rao, A (1999) Affinity-driven peptide selection of an NFAT inhibitor more selective than cyclosporin A. Science 285:2129-2133.

Ashe, KH (2001) Learning and memory in transgenic mice modeling Alzheimer's disease. Learn Mem 8:301-308.

Avila, J, Lucas, JJ, Perez, M, Hernandez, F (2004) Role of tau protein in bot physiological and pathological conditions. Physiol Rev 84:361-384.

Avni, O, Lee, D, Macian, F, Szabo, SJ, Glimcher, LH, Rao, A (2002) T(H) cell differentiation is accompanied by dynamic changes in histone acetylation of cytokine genes. Nat Immunol 3:643-651.

Bachstetter, AD, Norris, CM, Sompol, P, Wilcock, DM, Goulding, D, Neltner, JH, St Clair, D, Watterson, DM, Van Eldik, LJ (2012) Early stage drug treatment that normalizes proinflammatory cytokine production attenuates synaptic dysfunction in a mouse model that exhibits age-dependent progression of Alzheimer's disease-related pathology. J Neurosci 32:10201-10210.

Bangen, KJ, Nation, DA, Clark, LR, Harmell, AR, Wierenga, CE, Dev, SI, Delano-Wood, L, Zlater, ZZ, Salmon, DP, Liu, TT, Bondi, MW (2014) Interactive effects of vascular risk burden and advanced age on cerebral blood flow. Front Aging Neurosci 6.

Baumbach, GL, Sigmund, CD, Bottiglieri, T, Lentz, SR (2002) Structure of cerebral arterioles in cystathionine-beta-synthase-deficient mice. Circ Res 91:931-937.

Ben Abdallah, NM, Fuss, J, Trusel, M, Galsworthy, MJ, Bobsin, K, Colacicco, G, Deacon, RM, Riva, MA, Kellendonk, C, Sprengel, R, Lipp, HP, Gass, P (2011) The puzzle box as a simple and efficient behavioral test for exploring impairments of general cognition and executive functions in mouse models of schizophrenia. Exp Neurol 227:42-52.

Billingsley, ML, Ellis, C, Kincaid, RL, Martin, J, Schmidt, ML, Lee, VM, Trojanowski, JQ (1994) Calcineurin immunoreactivity in Alzheimer's disease. Exp Neurol 126:178-184.

Bink, DI, Ritz, K, Aronica, E, van der Weerd, L, Daemen, MJ (2013) Mouse models to study the effect of cardiovascular risk factors on brain structure and cognition. J Cereb Blood Flow Metab 33:1666-1684.

Birrell, JM, Brown, VJ (2000) Medial frontal cortex mediates perceptual attentional set shifting in the rat. J Neurosci 20:4320-4324.

Braak, H, Braak, E (1991) Neuropathological stageing of Alzheimer-related changes. Acta Neuropathol 82:239-259.

Brattstrom, LE, Hardebo, JE, Hultberg, BL (1984) Moderate homocysteinemia—a possible risk factor for arteriosclerotic cerebrovascular disease. Stroke 15:1012-1016.

Bryan, KJ, Lee, H, Perry, G, Smith, MA, Casadesus, G (2009) Transgenic Mouse Models of Alzheimer's Disease: Behavioral Testing and Considerations. Methods of Behavior Analysis in Neuroscience.

Candelario-Jalil, E, Thompson, J, Taheri, S, Grossetete, M, Adair, JC, Edmonds, E, Prestopnik, J, Wills, J, Rosenberg, GA (2011) Matrix metalloproteinases are associated with increased blood-brain barrier opening in vascular cognitive impairment. Stroke 42:1345-1350.

Canellada, A, Ramirez, BG, Minami, T, Redondo, JM, Cano, E (2008) Calcium/calcineurin signaling in primary cortical astrocyte cultures: Rcan1-4 and cyclooxygenase-2 as target NFAT genes.

Celsi, F, Svedberg, M, Unger, C, Cotman, CW, Carri, MT, Ottersen, OP, Nordberg, A, Torp, R (2007) Beta-amyloid causes downregulation of calcineurin in neurons through induction of oxidative stress. Neurobiol Dis 26:342-352.

Chang, L, Munsaka, SM, Kraft-Terry, S, Ernst, T (2013) Magnetic resonance spectroscopy to assess neuroinflammation and neuropathic pain. J Neuroimmune Pharmacol 8:576-593.

Chen, WW, Zhang, X, Huang, WJ (2016) Role of neuroinflammation in neurodegenerative diseases (review). Mol Med Rep 13:3391-3396.

Chen, Y, Swanson, RA (2003) Astrocytes and brain injury. J Cereb Blood Flow Metab 23:137-149.

Cipolla, MJ (2009) The Cerebral Circulation.

Cognat, E, Cleophax, S, Domenga-Denier, V, Joutel, A (2014) Early white matter changes in CADASIL: evidence of segmental intramyelinic oedema in a pre -clinical mouse model. Acta Neuropathol Commun 2.
Colombo, E, Farina, C (2016) Astrocytes: Key Regulators of Neuroinflammation. Trends Immunol 37:608-620.
Corriveau, RA, Bosetti, F, Emr, M, Gladman, JT, Koenig, JI, Moy, CS, Pahigiannis, K, Waddy, SP, Koroshetz, W (2016) The Science of Vascular Contributions to Cognitive Impairment and Dementia (VCID): A Framework for Advancing Research Priorities in the Cerebrovascular Biology of Cognitive Decline. Cell Mol Neurobiol 36:281-288.
Counts, SE, Ikonomovic, MD, Mercado, N, Vega, IE, Mufson, EJ (2016) Biomarkers for the Early Detection and Progression of Alzheimer's Disease. Neurotherapeutics.
Crabtree, GR (2001) Calcium, calcineurin, and the control of transcription. J Biol Chem 276:2313-2316.
Crabtree, GR, Olson, EN (2002) NFAT signaling: choreographing the social lives of scells. Cell 109 Suppl:S67-S79.
Cui, W, Mizukami, H, Yanagisawa, M, Aida, T, Nomura, M, Isomura, Y, Takayanagi, R, Ozawa, K, Tanaka, K, Aizawa, H (2014) Glial dysfunction in the mouse habenula causes depressive-like behaviors and sleep disturbance. J Neurosci 34:16273-16285.
Cummings, BJ, Su, JH, Cotman, CW, White, R, Russell, MJ (1993) Beta-amyloid accumulation in aged canine brain: a model of early plaque formation in Alzheimer's disease. Neurobiol Aging 14:547-560.
Dai, W, Lopez, OL, Carmichael, OT, Becker, JT, Kuller, LH, Gach, HM (2009) Mild cognitive impairment and Alzheimer disease: patterns of altered cerebral blood flow at MR imaging. Radiology 250:856-866.
Davis, J, Xu, F, Deane, R, Romanov, G, Previti, ML, Zeigler, K, Zlokovic, BV, Van Nostrand, WE (2004) Early-onset robust cerebral microvascular accumulation of amyloid beta-protein in transgenic mice expressing low levels of a vasculotropic Dutch/Iowa mutant form of amyloid beta-protein precursor. J Biol Chem 279:20296-20306.
Dawson, TM, Steiner, JP, Dawson, VL, Dinerman, JL, Uhl, GR, Snyder, SH (1993) Immunosuppressant FK506 enhances phosphorylation of nitric oxide synthase and protects against glutamate neurotoxicity. Proc Natl Acad Sci U S A 90:9808-9812.
Dbouk, HA, Mroue, RM, El-Sabban, ME, Talhouk, RS (2009) Connexins: a myriad of functions extending beyond assembly of gap junction channels. Cell Commun Signal 7.
De Windt, LJ, Lim, HW, Taigen, T, Wencker, D, Condorelli, G, Dorn, GW, 2nd, Kitsis, RN, Molkentin, JD (2000) Calcineurin-mediated hypertrophy protects cardiomyocytes from apoptosis in vitro and in vivo: An apoptosis-independent model of dilated heart failure. Circ Res 86:255-263.
Demuro, A, Mina, E, Kayed, R, Milton, SC, Parker, I, Glabe, CG (2005) Calcium dysregulation and membrane disruption as a ubiquitous neurotoxic mechanism of soluble amyloid oligomers. J Biol Chem 280:17294-17300.
Devlin, AM, Arning, E, Bottiglieri, T, Faraci, FM, Rozen, R, Lentz, SR (2004) Effect of Mthfr genotype on diet-induced hyperhomocysteinemia and vascular function in mice. Blood 103:2624-2629.
Dineley, KT, Hogan, D, Zhang, WR, Taglialatela, G (2007) Acute inhibition of calcineurin restores associative learning and memory in Tg2576 APP transgenic mice. Neurobiol Learn Mem 88:217-224.

Dubois, MF, Hebert, R (2001) The incidence of vascular dementia in Canada: a comparison with Europe and East Asia. Neuroepidemiology 20:179-187.
Ehret, F, Vogler, S, Pojar, S, Elliott, DA, Bradke, F, Steiner, B, Kempermann, G (2015) Mouse model of CADASIL reveals novel insights into Notch3 function in adult hippocampal neurogenesis. Neurobiol Dis 75:131-141.
Elder, GA, Gama Sosa, MA, De Gasperi, R (2010) Transgenic mouse models of Alzheimer's disease. Mt Sinai J Med 77:69-81.
Ernest, S, Hosack, A, O'Brien, WE, Rosenblatt, DS, Nadeau, JH (2005) Homocysteine levels in A/J and C57BL/6J mice: genetic, diet, gender, and parental effects. Physiol Genomics 21:404-410.
Eng, LF (1985) Glial fibrillary acidic protein (GFAP): the major protein of glial intermediate filaments in differentiated astrocytes. J Neuroimmunol 8:203-214.
Fernandez, AM, Fernandez, S, Carrero, P, Garcia-Garcia, M, Torres-Aleman, I (2007) Calcineurin in reactive astrocytes plays a key role in the interplay between proinflammatory and anti-inflammatory signals. J Neurosci 27:8745-8756.
Fernandez, AM, Hervas, R, Dominguez-Fraile, M, Garrido, VN, Gomez-Guitierrez, P, Vega, M, Vitorica, J, Perez, JJ, Torres Aleman, I (2016) Blockade of the Interaction of Calcineurin with FOXO in Astrocytes Protects Against Amyloid beta-Induced Neuronal Death. J Alzheimers Dis 52:1471-1478.
Fernandez, AM, Jimenez, S, Mecha, M, Davila, D, Guaza, C, Vitorica, J, Torres-Aleman, I (2012) Regulation of the phosphatase calcineurin by insulin-like growth factor I unveils a key role of astrocytes in Alzheimer's pathology. Mol Psychiatry 17:705-718.
Filosa, JA, Nelson, MT, Gonzalez Bosc, LV (2007) Activity-dependent NFATc3 nuclear accumulation in pericytes from cortical parenchymal microvessels. Am J Physiol Cell Physiol 293:C1797-C1805.
Flood, DG, Reaume, AG, Dorfman, KS, Lin, YG, Lang, DM, Trusko, SP, Savage, MJ, Annaert, WG, De Strooper, B, Siman, R, Scott, RW (2002) FAD mutant PS-1 gene-targeted mice: increased A beta 42 and A beta deposition without APP overproduction. Neurobiol Aging 23: 335-348.
Foster, TC, Sharrow, KM, Masse, JR, Norris, CM, Kumar, A (2001) Calcineurin links Ca2+ dysregulation with brain aging. J Neurosci 21:4066-4073.
Friday, BB, Horsley, V, Pavlath, GK (2000) Calcineurin activity is required for the initiation of skeletal muscle differentiation. J Cell Biol 149:657-666.
Frugier, T, Conquest, A, McLean, C, Currie, P, Moses, D, Goldshmit, Y (2012) Expression and activation of EphA4 in the human brain after traumatic injury. J Neuropathol Exp Neurol 71:242-250.
Fuller, S, Munch, G, Steele, M (2009) Activated astrocytes: a therapeutic target in Alzheimer's disease? Expert Rev Neurother 9:1585-1594.
Fuller, S, Steele, M, Munch, G (2010) Acitvated astroglia during chronic inflammation in Alzheimer's disease—do they neglect their neurosupportive roles? Mutat Res 690:40-49.
Furman, JL, Norris, CM (2014) Calcineurin and glial signaling: neuroinflammation and beyond. J Neuroinflammation 11:158.
Furman, JL, Sama, DM, Gant, JC, Beckett, TL, Murphy, MP, Bachstetter, AD, Van Eldik, LJ, Norris, CM (2012) Targeting astrocytes ameliorates neurologic changes in a mouse model of Alzheimer's disease. J Neurosci 32:16129-16140.
Furman, JL, Sompol, P, Kraner, SD, Pleiss, MM, Putman, EJ, Dunkerson, J, Abdul, HM, Roberts, KN, Scheff, SW, Norris, CM (2016) Blockade of Astrocytic Calcineurin/NFAT Signaling Helps to Normalize Hippocampal Synaptic Function and Plasticity in a Rat Model of Traumatic Brain Injury. J Neurosci 36:1502-1515.

Gooch, J, Wilcock, DM (2016) Animal Models of Vascular Cognitive Impairment and Dementia (VCID). Cell Mol Neurobiol 36:233-239.
Gorelick, PB, Counts, SE, Nyenhuis, D (2016) Vascular cognitive impairment and dementia. Biochim Biophys Acta 1862:860-868.
Gorelick, PB, Scuteri, A, Black, SE, Decarli, C, Greenberg, SM, Iadecola, C, Launer, LJ, Laurent, S, Lopez, OL, Nyenhuis, D, Petersen, RC, Schneider, JA, Tzourio, C, Arnett, DK, Bennett, DA, Chui, HC, Higashida, RT, Lindquist, R, Nilsson, PM, Roman, GC, Sellke, FW, Sheshadri, S (2011) Vascular contributions to cognitive impairment and dementia: a statement for healthcare professionals from the American heart association/American stroke association. Stroke 42:2672-2713.
Goto, S, Matsukado, Y, Mihara, Y, Inoue, E, Miyamoto, E (1986) The distribution of calcineurin in rat brain by light and electron microscopic immunohistochemistry and enzyme-immunoassay. Brain Res 397:161-172.
Gotz, J, Chen, F, Barmettler, R, Nitsch, RM (2001a) Tau filament formation in transgenic mice expressing P301L tau. J Biol Chem 276:529-534.
Gotz, J, Chen, F, van Dorpe, J, Nitsch, RM (2001b) Formation of neurofibrillary tangles in P301l tau transgenic mice induced by Abeta42 fibrils. Science 293:1491-1495.
Graff-Radford, J, Kantarci, K (2013) Magnetic resonance spectroscopy in Alzheimer's disease. Neuropsychiatr Dis Treat 9:687-696.
Graham, IM, Daly, LE, Refsum, HM, Robinson, K, Brattstrom, LE, Ueland, PM, Palma Reis, RJ, Boers, GH, Sheahan, RG, Israelsson, B, Uiterwaal, CS, Meleady, R, McMaster, D, Verhoef, P, Witteman, J, Rubba, P, Bellet, H, Wautrecht, JC, de Valk, HW, Sales Luis, AC, Parrot-Rouland, FM, Tan, KS, Higgins, I, Garcon, D, Andria, G, et al. (1997) Plasma homocysteine as a risk factor for vascular disease. The European Concerted Action Project. JAMA 277:1775-1781.
Griffin, WS (2006) Inflammation and neurodegenerative diseases. Am J Clin Nutr 83:470S-474S.
Griffin, WS, Mrak, RE (2002) Interleukin-1in the genesis and progression of and risk for development of neuronal degeneration in Alzheimer's disease. J Leukoc Biol 72:233-238.
Griffin, WS, Sheng, JG, Royston, MC, Gentleman, SM, McKenzie, JE, Graham, DI, Roberts, GW, Mrak, RE (1998) Glial-neuronal interactions in Alzheimer's disease: the potential role of a 'cytokine cycle' in disease progression. Brain Pathol 8:65-72.
Grolla, AA, Fakhfouri, G, Balzaretti, G, Marcello, E, Gardoni, F, Canonico, PL, DiLuca, M, Genazzani, AA, Lim, D (2013) Abeta leads to Ca(2)(+) signaling alterations and transcriptional changes in glial cells. Neurobiol Aging 34:511-522.
Haass, C, Selkoe, DJ (1993) Cellular processing of beta-amyloid precursor protein and the genesis of amyloid beta-peptide. Cell 75:1039-1042.
Hainsworth, AH, Markus, HS (2008) Do in vivo experimental models reflect human cerebral small vessel disease? A systematic review. J Cereb Blood Flow Metab 28:1877-1891.
Halpain, S, Hipolito, A, Saffer, L (1998) Regulation of F-actin stability in dendritic spines by glutamate receptors and calcineurin.
Hamby, ME, Sofroniew, MV (2010) Reactive astrocytes as therapeutic targets for CNS disorders. Neurotherapeutics 7:494-506.
Hardy, JA, Higgins, GA (1992) Alzheimer's disease: the amyloid cascade hypothesis. Science 256:184-185.

Hashimoto, T, Kawamata, T, Saito, N, Sasaki, M, Nakai, M, Niu, S, Taniguchi, T, Terashima, A, Yasuda, M, Maeda, K, Tanaka, C (1998) Isoform-specific redistribution of calcineurin A alpha and A beta in the hippocampal CA1 region of gerbils after transient ischemia. J Neurochem 70:1289-1298.

Hashimoto, Y, Perrino, BA, Soderling, TR (1990) Identification of an autoinhibitory domain in calcineurin. J Biol Chem 265:1924-1927.

Hattori, Y, Enmi, J, Kitamura, A, Yamamoto, Y, Saito, S, Takahashi, Y, Iguchi, S, Tsuji, M, Yamahara, K, Nagatsuka, K, Iida, H, Ihara, M (2015) A novel mouse model of subcortical infarcts with dementia. J Neurosci 35:3915-3928.

Head, E (2013) A canine model of human aging and Alzheimer's disease. Biochim Biophys Acta 1832:1384-1389.

Heneka, MT, Carson, MJ, El Khoury, J, Landreth, GE, Brosseron, F, Feinstein, DL, Jacobs, AH, Wyss-Coray, T, Vitorica, J, Ransohoff, RM, Herrup, K, Frautschy, SA, Finsen, B, Brown, GC, Verkhratsky, A, Yamanaka, K, Koistinaho, J, Latz, E, Halle, A, Petzold, GC, Town, T, Morgan, D, Shinohara, ML, Perry, VH, Holmes, C, Bazan, NG, Brooks, DJ, Hunot, S, Joseph, B, Deigendesch, N, Garaschuk, O, Boddeke, E, Dinarello, CA, Breitner, JC, Cole, GM, Golenbock, DT, Kummer, MP (2015) Neuroinflammation in Alzheimer's disease. Lancet Neurol 14:388-405.

Herminghaus, S, Frolich, L, Gorriz, C, Pilatus, U, Dierks, T, Wittsack, HJ, Lanfermann, H, Maurer, K, Zanella, FE (2003) Brain metabolism in Alzheimer disease and vascular dementia assessed by in vivo proton magnetic resonance spectroscopy. Psychiatry Res 123:183-190.

Hernandez-Guillamon, M, Martinez-Saez, E, Delgado, P, Domingues-Montanari, S, Boada, C, Penalba, A, Boada, M, Pagola, J, Maisterra, O, Rodriguez-Luna, D, Molina, CA, Rovira, A, Alvarez-Sabin, J, Ortega-Aznar, A, Montaner, J (2012) MMP-2/MMP-9 plasma level and brain expression in cerebral amyloid angiopathy-associated hemorrhagic stroke. Brain Pathol 22:133-141.

Herzig, MC, Winkler, DT, Burgermeister, P, Pfeifer, M, Kohler, E, Schmidt, SD, Danner, S, Abramowski, D, Sturchler-Pierrat, C, Burki, K, van Duinen, SG, Maat Schieman, ML, Staufenbiel, M, Mathews, PM, Jucker, M (2004) Abeta is targeted to the vasculature in a mouse model of hereditary cerebral hemorrhage with amyloidosis. Nat Neurosci 9:954-960.

Hofmann, MA, Lalla, E, Lu, Y, Gleason, MR, Wolf, BM, Tanji, N, Ferran, LJ, Jr, Kohl, B Rao, V, Kisiel, W, Stern, DM, Schmidt, AM (2001) Hyperhomocysteinemia enhances vascular inflammation and accelerates atherosclerosis in a murine model. J Clin Invest 107:675-683.

Hong, HS, Hwang, JY, Son, SM, Kim, YH, Moon, M, Inhee, MJ (2010) FK506 reduces amyloid plaque burden and induces MMP-9 in AbetaPP/PS1 double transgenic mice. J Alzheimers Dis 22:97-105.

Hsiao, K, Chapman, P, Nilsen, S, Eckman, C, Harigaya, Y, Younkin, S, Yang, F, Cole, G (1996) Correlative memory deficits, Abeta elevation, and amyloid plaques in transgenic mice. Science 274:99-102.

Huang, W, Fileta, JB, Dobberfuhl, A, Filippopolous, T, Guo, Y, Kwon, G, Grosskreutz, CL (2005) Calcineurin cleavage is triggered by elevated intraocular pressure, and calcineurin inhibition blocks retinal ganglion cell death in experimental glaucoma. Proc Natl Acad Sci U S A 102:12242-12247.

Hudry, E, Wu, HY, Arbel-Ornath, M, Hashimoto, T, Matsouaka, R, Fan, Z, Spires-Jones, TL, Betensky, RA, Bacskai, BJ, Hyman, BT (2012) Inhibition of the NFAT pathway alleviates amyloid beta neurotoxicity in a mouse model of Alzheimer's disease. J Neurosci 32:3176-3192.

Hyman, BT, Phelps, CH, Beach, TG, Bigio, EH, Cairns, NJ, Carillo, MC, Dickson, DW, Duyckaerts, C, Frosch, MP, Masliah, E, Mirra, SS, Nelson, PT, Schneider, JA, Thal, DR, Thies, B, Trojanowski, JQ, Vinters, HV, Montine, TJ (2012) National Institute on Aging-Alzheimer's Association guidelines for the neuropathologic assessment of Alzheimer's disease. Alzheimers Dement 8:1-13.

Ighodaro, ET, Abner, EL, Fardo, DW, Lin, AL, Katsumata, Y, Schmitt, FA, Kryscio, RJ, Jicha, GA, Neltner, JH, Monsell, SE, Kukull, WA, Moser, DK, Appiah, F, Bachstetter, AD, Van Eldik, LJ, ADNI, Nelson, PT (2016) Risk factors and global cognitive status related to brain arteriolosclerosis in elderly individuals. J Cereb Blood Flow Metab.

Ingram, G, Loveless, S, Howell, OW, Hakobyan, S, Dancey, B, Harris, CL, Robertson, NP, Neal, JW, Morgan, BP (2014) Complement activation in multiple sclerosis plaques: an immunohistochemical analysis. Acta Neuropathol Commun 2.

Irvine, GB, El-Agnaf, OM, Shankar, GM, Walsh, DM (2008) Protein aggregation in the brain: the molecular basis for Alzheimer's and Parkinson's diseases. Mol Med 14:451-464.

Jankowsky, JL, Slunt, HH, Gonzales, V, Jenkins, NA, Copeland, NG, Borchelt, DR (2004) APP processing and amyloid deposition in mice haplo-insufficient for presenilin 1. Neurobiol Aging 25:885-892.

Jin, SM, Cho, HJ, Kim, YM, Hwang, JY, Mook-Jung, I (2012) Abeta-induced Ca(2+) influx regulates astrocytic BACE1 expression via calcineurin/NFAT4 signals. Biochim Biophys Res Commun 425:649-655.

Jiwa, NS, Garrard, P, Hainsworth, AH (2010) Experimental models of vascular dementia and vascular cognitive impairment: a systematic review. J Neurochem 115:814-828.

Jones, EV, Bernardinelli, Y, Tse, YC, Chierzi, S, Wong, TP, Murai, KK (2011) Astrocytes control glutamate receptor levels at developing synapses through SPARC-beta integrin interactions. J Neurosci 31:4154-4165.

Joutel, A, Monet-Lepretre, M, Gosele, C, Baron-Menguy, C, Hammes, A, Schmidt, S, Lemaire-Carrette, B, Domenga, V, Schedl, A, Lacombe, P, Hubner, N (2010) Cerebrovascular dysfunction and microcirculation rarefaction precede white matter lesions in a mouse genetic model of cerebral ischemic small vessel disease. J Clin Invest 120:433-445.

Kalaria, RN, Akinyemi, R, Ihara, M (2012) Does vascular pathology contribute to Alzheimer changes? J Neurol Sci 322:141-147.

Kammoun, S, Gold, G, Bouras, C, Giannakopoulos, P, McGee, W, Hernmann, F, Michel, JP (2000) Immediate causes of death of demented and non-demented elderly. Acta Neurol Scand Suppl 176:96-99.

Kao, SC, Wu, H, Xie, J, Chang, CP, Ranish, JA, Graef, IA, Crabtree, GR (2009) Calcineurin/NFAT signaling is required for neuregulin-regulated Schwann cell differentiation. J Neurosci 323:651-654.

Kapasi, A, Schneider, JA (2016) Vascular contributions to cognitive impairment, clinical Alzheimer's disease, and dementia in older persons. Biochim Biophys Acta 1862:878-886.

Karch, CM, Jeng, AT, Goate, AM (2013) Calcium phosphatase calcineurin influences tau metabolism. Neurobiol Aging 34:374-386.

Kim, B, Jeong, HK, Kim, JH, Lee, SY, Jou, I, Joe, EH (2011) Uridine 5'-diphosphate induces chemokine expression in microglia and astrocytes through activation of the P2Y6 receptor. J Immunol 186:3701-3709.

Kincaid, RL, Giri, PR, Higuchi, S, Tamura, J, Dixon, SC, Marietta, CA, Amorese, DA, Martin, BM (1990) Cloning and characterization of molecular isoforms of the catalytic subunit of calcineurin using nonisotopic methods. J Biol Chem 265:11312-11319.

Kitazawa, M, Cheng, D, Tsukamoto, MR, Koike, MA, Wes, PD, Vasilevko, V, Cribbs, DH, LaFerla, FM (2011) Blocking IL-1 signaling rescues cognition, attenuates tau pathology, and restores neuronal beta-catenin pathway function in an Alzheimer's disease model. J Immunol 187:6539-6549.

Kitazawa, M, Yamasaki, TR, LaFerla, FM (2004) Microglia as a potential bridge between the amyloid-beta peptide and tau. Ann N Y Acad Sci 1035:85-103.

Klee, CB (1991) Concerted regulation of protein phosphorylation and dephosphorylation by calmodulin. Neurochem Res 16:1059-1065.

Klein, T, Bischoff, R (2011) Physiology and pathophysiology of matrix metalloproteases. Amino Acids 41:271-290.

Korczyn, AD, Vakhapova, V, Grinberg, LT (2012) Vascular dementia. J Neurol Sci 322:2-10.

Koulakoff, A, Mei, X, Orellana, JA, Saez, JC, Giaume, C (2012) Glial connexin expression and function in the context of Alzheimer's disease. Biochim Biophys Acta 1818:2048-2057.

Kromer Vogt, LJ, Hyman, BT, Van Hoesen, GW, Damasio, AR (1990) Pathological alterations in the amygdala in Alzheimer's disease. Neuroscience 37:377-385.

Kuchibhotla, KV, Goldman, ST, Lattarulo, CR, Wu, HY, Hyman, BT, Bacskai, BJ (2008) Abeta plaques lead to aberrant regulation of calcium homeostasis in vivo resulting in structural and functional disruption of neuronal networks. Neuron 59:214-225.

Kulic, L, McAfoose, J, Welt, T, Tackenberg, C, Spani, C, Wirth, F, Finder, V, Konietzko, U, Giese, M, Eckert, A, Noriaki, K, Shimizu, T, Murakami, K, Irie, K, Rasool, S, Glabe, C, Hock, C, Nitsch, RM (2012) Early accumulation of intracellular fibrillar oligomers and late congophilic amyloid angiopathy in mice expressing the Osaka intra-Abeta APP mutation. Transl Psychiatry 2.

Kumar-Singh, S (2009) Hereditary and sporadic forms of abeta-cerebrovascular amyloidosis and relevant transgenic mouse models. Int J Mol Sci 10:1872-1895.

Kuno, T, Mukai, H, Ito, A, Chang, CD, Kishima, K, Saito, N, Tanaka, C (1992) Distinct cellular expression of calcineurin A alpha and A beta in rat brain. J Neurochem 58:1643-1651.

Ladner, CJ, Czech, J, Maurice, J, Lorrens, SA, Lee, JM (1996) Reduction of calcineurin enzymatic activity in Alzheimer's disease: correlation with neuropathologic changes. J Neuropathol Exp Neurol 55:924-931.

Lampe, PD, Lau, AF (2000) Regulation of gap junctions by phosphorylation of connexins. Arch Biochem Biophys 384:205-215.

Lampe, PD, Lau, AF (2004) The effects of connexin phosphorylation on gap junctional communication. Int J Biochem Cell Biol 36:1171-1186.

Lee, Y, Messing, A, Su, M, Brenner, M (2008) GFAP promoter elements required for region-specific and astrocyte-specific expression. Glia 56:481-493.

Lee, YJ, Han, SB, Nam, SY, Oh, KW, Hong, JT (2010) Inflammation and Alzheimer's disease. Arch Pharm Res 33:1539-1556.

Li, WE, Nagy, JI (2000) Activation of fibers in rat sciatic nerve alters phosphorylation state of connexin-43 at astrocytic gap junctions in spinal cord: evidence for junction regulation by neuronal-glial interactions. Neuroscience 97:113-123.

Lian, Q, Ladner, CJ, Magnuson, D, Lee, JM (2001) Selective changes of calcineurin (protein phosphatase 2B) activity in Alzheimer's disease cerebral cortex. Exp Neurol 167:158-165.
Lin, AL, Jahrling, JB, Zhang, W, DeRosa, N, Bakshi, V, Romero, P, Galvan, V, Richardson, A (2015) Rapamycin rescues vascular, metabolic, and learning deficits in apolipoprotein E4 transgenic mice with pre-symptomatic Alzheimer's disease. J Cereb Blood Flow Metab.
Lin, AL, Powell, D, Caban-Holt, A, Jicha, G, Robertson, W, Gold, BT, Davis, R, Abner, E, Wilcock, DM, Schmitt, FA, Head, E (2016) (1)H-MRS metabolites in adults with Down syndrome: Effects of dementia. Neuroimage Clin 11:728-735.
Lin, AL, Rothman, DL (2014) What have novel imaging techniques revealed about metabolism in the aging brain? Future Neurol 9:341-354.
Liu, F, Grundke-Iqbal, I, Iqbal, K, Oda, Y, Tomizawa, K, Gong, CX (2005) Truncation and activation of calcineurin A by calpain I in Alzheimer disease brain. J Biol Chem 280:37755-37762.
Lovestone, S (2000) Fleshing out the amyloid cascade hypothesis: the molecular biology of Alzheimer's disease. Dialogues Clin Neurosci 2:101-110.
Maccioni, RB, Munoz, JP, Barbeito, L (2001) The molecular bases of Alzheimer's disease and other neurodegenerative disorders. Arch Med Reserve 32:367-381.
Manfredsson, FP, Rising, AC, Mandel, RJ (2009) AAV9: a potential blood-brain barrier buster. Mol Ther 17:403-405.
Marks, AR (1996) Cellular functions on immunophilins. Physiol Rev 76:631-649.
Mathis, DM, Furman, JL, Norris, CM (2011) Preparation of acute hippocampal slices from rats and transgenic mice for the study of synaptic alterations during aging and amyloid pathology. J Vis Exp.
Mattson, MP (2004) Pathways towards and away from Alzheimer's disease. Nature 430:631-639.
McAlonan, K, Brown, VJ (2003) Orbital prefrontal cortex mediates reversal learning and not attentional set shifting in the rat. Brain Behav Res 146:97-103.
McCaffrey, PG, Goldfeld, AE, Rao, A (1994) The role of NFATp in cyclosporin A sensitive tumor necrosis factor-alpha gene transcription. J Biol Chem 269:30445-30450.
McCoy, MK, Tansey, MG (2008) TNF signaling inhibition in the CNS: implications for normal brain function and neurodegenerative disease. J Neuroinflammation 5.
McGeer, PL, Schulzer, M, McGeer, EG (1996) Arthritis and anti-inflammatory agents as possible protective factors for Alzheimer's disease: a review of 17 epidemiological studies. Neurology 47:425-432.
Meier, S, Bell, M, Lyons, DN, Rodriguez-Rivera, J, Ingram, A, Fontaine, SN, Mechas, E, Chen, J, Wolozin, B, Levine, H, 3rd, Zhu, H, Abisambra, JF (2016) Pathological Tau Promotes Neuronal Damage by Impairing Ribosomal Function and Decreasing Protein Synthesis. J Neurosci 36:1001-1007.
Miao, J, Xu, F, Davis, J, Otte-Holler, I, Verbeek, MM, Van Nostrand, WE (2005) Cerebral microvascular amyloid beta protein deposition induces vascular degeneration and neuroinflammation in transgenic mice expressing human vasculotropic mutant amyloid beta precursor protein. Am J Pathol 167:505-515.
Mirra, SS, Heyman, A, McKeel, D, Sumi, SM, Crain, BJ, Brownlee, LM, Vogel, FS, Hughes, JP, van Belle, G, Berg, L (1991) The Consortium to Establish a Registry for Alzheimer's Disease (CERAD). Part II. Standardization of the neuropathologic assessment of Alzheimer's disease. Neurology 41:479-486.

Mohmmad Abdul, H, Baig, I, Levine, H, 3rd, Guttmann, RP, Norris, CM (2011) Proteolysis of calcineurin is increased in human hippocampus during mild cognitive impairment and is stimulated by oligomeric Abeta in primary cell culture. Aging Cell 10:103-113.

Montine, TJ, Phelps, CH, Beach, TG, Bigio, EH, Cairns, NJ, Dickson, DW, Duyckaerts, C, Frosch, MP, Masliah, E, Mirra, SS, Nelson, PT, Schneider, JA, Thal, DR, Trojanowski, JQ, Vinters, HV, Hyman, BT, National Institute on Aging, Alzheimer's Association (2012) National Institute on Aging-Alzheimer's Association guildelines for the neuropathologic assessment of Alzheimer's disease: a practical approach. Acta Neuropathol 123:1-11.

Moore, KB, O'Brien, J (2015) Connexins in neurons and glia: targets for intervention in disease and injury. Neural Regen Res 10:1013-1017.

Mrak, RE, Griffin, SW (2001a) Interleukin-1, neuroinflammation, and Alzheimer's disease. Neurobiol Aging 22:903-908.

Mrak, RE, Griffin, SW (2005a) Glia and their cytokines in the progression of neurodegeneration. Neurobiol Aging 26:349-354.

Mrak, RE, Griffin, SW (2005b) Potential inflammatory biomarkers in Alzheimer's disease. J Alzheimers Dis 8:369-375.

Mrak, RE, Griffin, SW (2001b) The role of activated astrocytes and of the neurotrophic cytokine S100B in the pathogenesis of Alzheimer's disease. Neurobiol Aging 22:915-922.

Muller, M, van der Graaf, Y, Vissersen, FL, Mali, WP, Geerlings, MI, Smart Study Group (2012) Hyptertension and longitudinal changes in cerebral blood flow: the SMART-MR study. Ann Neurol 71:825-833.

Munoz, L, Ammit, AJ (2010) Targeting p38 MAPK pathway for the treatment of Alzheimer's disease. Neuropharmacology 58:561-568.

Munoz, L, Ralay Ranaivo, H, Roy, SM, Hu, W, Craft, JM, McNamara, LK, Chico, LW, Van Eldik, LJ, Watterson, DM (2007) A novel p38 alpha MAPK inhibitor suppresses brain proinflammatory cytokine up-regulation and attenuates synaptic dysfunction and behavioral deficits in an Alzheimer's disease mouse model. J Neuroinflammation 4.

Murai, KK, Pasquale, EB (2011) Eph receptors and ephrins in neuron-astrocyte communication at synapses. Glia 59:1567-1578.

Murphy, GM, Jr., Ellis, WG, Lee, YL, Stultz, KE, Shrivastava, R, Tinklenberg, JR, Eng, LF (1992) Astrocytic gliosis in the amygdala in Down's syndrome and Alzheimer's disease. Prog Brain Res 94:475-483.

Nagamoto-Combs, K, Combs, CK (2010) Microglial phenotype is regulated by activity of the transcription factor, NFAT (nuclear factor of activated T cells). J Neurosci 30:9641-9646.

Nakaji, K, Ihara, M, Takahashi, C, Itohara, S, Noda, M, Takahashi, R, Tomimoto, H (2006) Matrix metalloproteinase-2 plays a critical role in the pathogenesis of white matter lesions after chronic cerebral hypoperfusion in rodents. Stroke 37:2816-2823.

Nakamura, T, Tu, S, Akhtar, MW, Sunico, CR, Okamoto, S, Lipton, SA (2013) Aberrant protein s-nitrosylation in neurodegenerative diseases. Neuron 78:596-614.

Nelson, AR, Sweeney, MD, Sagare, AP, Zlokovic, BV (2016) Neurovascular dysfunction and neurodegeneration in dementia and Alzheimer's disease. Biochim Biophys Acta 1862:887-900.

Nelson, PT, Alafuzoff, I, Bigio, EH, Bouras, C, Braak, H, Cairns, NJ, Castellani, RJ, Crain, BJ, Davies, P, Del Tredici, K, Duyckaerts, C, Frosch, MP, Haroutunian, V, Hof, PR, Hulette, CM, Hyman, BT, Iwatsubo, T, Jellinger, KA, Jicha, GA, Kovari, E, Kukull, WA, Leverenz, JB, Love, S, Mackenzie, IR, Mann, DM, Masliah, E, McKee, AC, Montine, TJ, Morris, JC, Schneider, JA, Sonnen, JA, Thal, DR, Trojanowski, JQ, Troncoso, JC, Wisniewski, T, Woltjer, RL, Beach, TG (2012) Correlation of Alzheimer disease neuropathologic changes with cognitive status: a review of the literature. J Neuropathol Exp Neurol 71:362-381.

Nelson, PT, Jicha, GA, Schmitt, FA, Liu, H, Davis, DG, Mendiondo, MS, Abner, EL, Markesbery, WR (2007) Clinicopathologic correlations in a large Alzheimer disease center autopsy cohort: neuritic plaques and neurofibrillary tangles “do count” when staging disease severity.

Neria, F, del Carmen Serrano-Perez, M, Velasco, P, Urso, K, Tranque, P, Cano, E (2013) NFATc3 promotes Ca(2+) –dependent MMP3 expression in astroglial cells. Glia 61:1052-1066.

Neto, CJ, Paganelli, RA, Benetoli, A, Lima, KC, Milani, H (2005) Permanent, 3-stage, 4 vessel occlusion as a model of chronic and progressive brain hypoperfusion in rats: a neurohistological and behavioral analysis. Behav Brain Res 160:312-322.

Niedowicz, DM, Reeves, VL, Platt, TL, Kohler, K, Beckett, TL, Powell, DK, Lee, TL, Sexton, TR, Song, ES, Brewer, LD, Latimer, CS, Kraner, SD, Larson, KL, Ozcan, S, Norris, CM, Hersh, LB, Porter, NM, Wilcock, DM, Murphy, MP (2014) Obesity and diabetes cause cognitive dysfunction in the absence of accelerated beta amyloid deposition in a novel murine model of mixed or vascular dementia. Acta Neuropathol Commun 2.

Norris, CM, Blalock, EM, Chen, KC, Porter, NM, Thibault, O, Kraner, SD, Landfield, PW (2010) Hippocampal ‘zipper’ slice studies reveal a necessary role for calcineurin in the increased activity of L-type Ca(2+) channels with aging. Neurobiol Aging 31:328-338.

Norris, CM, Blalock, EM, Thibault, O, Brewer, LD, Clodfelter, GV, Porter, NM, Landfield, PW (2006) Electrophysiological mechanisms of delayed excitotoxicity: positive feedback loop between NMDA receptor current and depolarization-mediated glutamate release. J Neurophysiol 96:2488-2500.

Norris, CM, Kadish, I, Blalock, EM, Chen, KC, Thibault, V, Porter, NM, Landfield, PW, Kraner, SD (2005) Calcineurin triggers reactive/inflammatory processes in astrocytes and is upregulated in aging and Alzheimer’s models. J Neurosci 25:4649-4658.

Norris, CM, Sompol, P, Roberts, KN, Ansari, M, Scheff, SW (2016) Pycnogenol protects CA3-CA1 synaptic function in a rat model of traumatic brain injury. Exp Neurol 276:5-12.

Nunan, J, Small, DH (2000) Regulation of APP cleavage by alpha-, beta-, and gamma-secretases. FEBS Lett 483:6-10.

Oakley, H, Cole, SL, Logan, S, Maus, E, Shao, P, Craft, J, Guillozet-Bongaarts, A, Ohno, M, Disterhoft, J, Van Eldik, L, Berry, R, Vassar, R (2006) Intraneuronal beta-amyloid aggregates, neurodegeneration, and neuron loss in transgenic mice with five familial Alzheimer’s disease mutations: potential factors in amyloid plaque formation. J Neurosci 26:10129-10140.

Oddo, S, Caccamo, A, Shepherd, JD, Murphy, MP, Golde, TE, Kayed, R, Metherate, R, Mattson, MP, Akbari, Y, LaFerla, FM (2003) Triple-transgenic model of Alzheimer’s disease with plaques and tangles: intracellular Abeta and synaptic dysfunction. Neuron 39:409-421.

Olsen, ML, Khakh, BS, Skatchkov, SN, Zhou, M, Lee, CJ, Rouach, N (2015) New Insights on Astrocyte Ion Channels: Critical for Homeostasis and Neuron-Glia Signaling. J Neurosci 35:13827-13835.
Orellana, JA, Froger, N, Ezan, P, Jiang, JX, Bennett, MV, Naus, CC, Giaume, C, Saez, JC (2011) ATP and glutamate released via astroglial connexin 43 hemichannels mediate neuronal death through activation of pannexin 1 hemichannels. J Neurochem 118:826-840.
Orellana, JA, Saez, PJ, Shoji, KF, Schalper, KA, Palacios-Prado, N, Velarde, V, Giaume, C, Bennett, MV, Saez, JC (2009) Modulation of brain hemichannels and gap junction channels by pro-inflammatory agents and their possible role in neurodegeneration. Antioxid Redox Signal 11:369-399.
Orellana, JA, Sanchez, HA, Schalper, KA, Figueroa, V, Saez, JC (2012) Regulation of intercellular calcium signaling through calcium interactions with connexin-based channels. Adv Exp Med Biol 740:777-794.
Orellana, JA, Shoji, KF, Abudara, V, Ezan, P, Amigou, E, Saez, PJ, Jiang, JX, Naus, CC, Saez, JC, Giaume, C (2011) Amyloid beta-induced death in neurons involves glial and neuronal hemichannels. J Neurosci 31:4962-4977.
Ortinski, PI, Dong, J, Mungenast, A, Yue, C, Takano, H, Watson, DJ, Haydon, PG, Coulter, DA (2010) Selective induction of astrocytic gliosis generates deficits in neuronal inhibition. Nat Neurosci 13:584-591.
Palanki, MS (2002) Inhibitors of AP-1 and NF-kappa B mediated transcriptional activation: therapeutic potential in autoimmune diseases and structural diversity. Curr Med Chem 9:219-227.
Pantoni, L (2010) Cerebral small vessel disease: from pathogenesis and clinical characteristics to therapeutic challenges. Lancet Neurol 9:689-701.
Parnetti, L, Tarducci, R, Presciutti, O, Lowenthal, DT, Pippi, M, Palumbo, B, Gobbi, G, Pellicciioli, GP, Senin, U (1997) Proton magnetic resonance spectroscopy can differentiate Alzheimer's disease from normal aging. Mech Ageing Dev 97:9-14.
Peca, S, McCreary, CR, Donaldson, E, Kumarpillai, G, Shobha, N, Sanchez, K, Charlton, A, Steinback, CD, Beaudin, AE, Fluck, D, Pillay, A, Fick, GH, Poulin, MJ, Frayne, R, Goodyear, BG, Smith, EE (2013) Neurovascular decoupling is associated with severity of cerebral amyloid angiopathy. Neurology 81:1659-1665.
Pekny, M, Nilsson, M (2005) Astrocyte activation and reactive gliosis. Glia 50:427-432.
Penny, M, Pekna, M (2014) Astrocyte reactivity and reactive astrogliosis: costs and benefits. Physiol Rev 94:1077-1098.
Pekny, M, Pekna, M (2016) Reactive gliosis in the pathogenesis of CNS diseases. Biochim Biophys Acta 1862:483-491.
Pekny, M, Pekna, M, Messing, A, Steinhauser, C, Lee, JM, Parpura, V, Hol, EM, Sofroniew, MV, Verkhratsky, A (2016) Astrocytes: a central element in neurological diseases. Acta Neuropathol 131:323-345.
Pereira, FM, Ferreira, D, de Oliveira, RM, Milani, H (2012) Time-course of neurodegeneration and memory impairment following the 4-vessel occlusion/internal carotid artery model of chronic cerebral hypoperfusion in middle-aged rats. Brain Behav Res 229:340-348.
Perrino, BA, Ng, LY, Soderling, TR (1995) Calcium regulation of calcineurin phosphatase activity by its B subunit and calmodulin. Role of the autoinhibitory domain. J Biol Chem 270:340-346.
Pickering, M, O'Connor, JJ (2007) Pro-inflammatory cytokines and their effects in the dentate gyrus. Prog Brain Res 163:339-354.

Pleiss, MM, Abdul, HM, Furman, JL, Norris, CM (in preparation) Calcineurin-mediated dephosphorylation of connexin43 in astrocytes: implications for hemichannel function in the progression of Alzheimer's disease.
Pleiss, MM, Sompol, P, Kraner, SD, Abdul, HM, Furman, JL, Guttmann, RP, Wilcock, DM, Nelson, PT, Norris, CM (2016) Calcineurin proteolysis in astrocytes: Implications for impaired synaptic function. Biochim Biophys Acta 1862: 1521-1532.
Porter, NM, Thibault, O, Thibault, V, Chen, KC, Landfield, PW (1997) Calcium channel density and hippocampal cell death with age in long-term culture. J Neurosci 17:5629-5639.
Provencher, SW (1993) Estimation of metabolite concentrations from localized in vivo proton NMR spectra. Magn Reson Med 30:672-679.
Quintanilla, RA, Orellana, JA, von Bernhardi, R (2012) Understanding risk factors for Alzheimer's disease: interplay of neuroinflammation, connexin-based communication and oxidative stress. Arch Med Res 43:632-644.
Reese, LC, Taglialatela, G (2011) A role for calcineurin in Alzheimer's disease. Curr Neuropharmacol 9:685-692.
Reese, LC, Zhang, W, Dineley, KT, Kayed, R, Taglialatela, G (2008) Selective induction of calcineurin activity and signaling by oligomeric amyloid beta. Aging Cell 7:824-835.
Reines, SA, Block, GA, Morris, JC, Liu, G, Nessly, ML, Lines, CR, Norman, BA, Baranak, CC (2004) Rofecoxib: no effect on Alzheimer's disease in a 1-year, randomized, blinded controlled study. Neurology 62:66-71.
Rich, JB, Rasmusson, DX, Folstein, MF, Carson, KA, Kawas, C, Brandt, J (1995) Nonsteroidal anti-inflammatory drugs in Alzheimer's disease. Neurology 45:51-55.
Ridet, JL, Malhotra, SK, Privat, A, Gage, FH (1997) Reactive astrocytes: cellular and molecular cues to biological function. Trends Neurosci 20:570-577.
Rojanathammanee, L, Floden, AM, Manocha, GD, Combs, CK (2015) Attenuation of microglial activation in a mouse model of Alzheimer's disease via NFAT inhibition. J Neuroinflammation 12.
Rojanathammanee, L, Puig, KL, Combs, CK (2013) Pomegranate polyphenols and extract inhibit nuclear factor of activated T-cell activity and microglial activation in vitro and in a transgenic mouse model of Alzheimer's disease. J Nutr 143:597-605.
Roof, RL, Shielke, GP, Ren, X, Hall, ED (2001) A comparison of long-term functional outcome after 2 middle cerebral artery occlusion models in rats. Stroke 32:2648-2657.
Rosenblum, WI (2014) Why Alzheimer trials fail: removing soluble oligomeric beta amyloid is essential, inconsistent, and difficult. Neurobiol Aging 35:969-974.
Rosenkraz, K, May, C, Meier, C, Marcus, K (2012) Proteomic analysis of alterations induced by perinatal hypoxic-ischemic brain injury. J Proteome Res 11:5794-5803.
Rossi, D (2015) Astrocyte pathophysiology: At the crossroads of intercellular networking, inflammation, and cell death. Prog Neurobiol 130:86-120.
Rossi, D, Volterra, A (2009) Astrocytic dysfunction: insights on the role in neurodegeneration. Brain Res Bull 80:224-232.
Rozkalne, A, Hyman, BT, Spires-Jones, TL (2011) Calcineurin inhibition with FK506 ameliorates dendritic spine density deficits in plaque-bearing Alzheimer mice model. Neurobiol Dis 41:650-654.

Saganova, K, Galik, J, Blasko, J, Korimova, A, Racekova, E, Vanicky, I (2012) Immunosuppressant FK506: focusing on neuroprotective effects following brain and spinal cord injury. Life Sci 91:77-82.
Sakai, N, Yanai, K, Ryu, JH, Nagasawa, H, Hasegawa, T, Sasaki, T, Kogure, K, Watanabe, T (1996) Behavioral studies on rats with transient cerebral ischemia induced by occlusion of the middle cerebral artery. Behav Brain Res 77:181-188.
Sama, DM, Norris, CM (2013) Calcium dysregulation and neuroinflammation: discrete and integrated mechanisms for age-related synaptic dysfunction. Ageing Res Rev 12:982-995.
Sama, MA, Mathis, DM, Furman, JL, Abdul, HM, Artiushin, IA, Kraner, SD, Norris, CM (2008) Interleukin-1beta-dependent signaling between astrocytes and neurons depends critically on astrocytic calcineurin/NFAT activity. J Biol Chem 283:21953-21964.
Sanchez-Gomez, MV, Alberdi, E, Ibarettxe, G, Torre, I, Matute, C (2003) Caspase dependent and caspase-independent oligodendrocyte death mediated by AMPA and kainate receptors. J Neurosci 23:9519-9528.
Scearce-Levie, K (2011) Monitoring spatial learning and memory in Alzheimer's disease mouse models using the Morris Water Maze. Methods Mol Biol 670:191-205.
Scheff, SW, Ansari, MA, Mufson, EJ (2016) Oxidative stress and hippocampal synaptic protein levels in elderly cognitively intact individuals with Alzheimer's disease pathology. Neurobiol Aging 42:1-12.
Scheff, SW, Price, DA, Ansari, MA, Roberts, KN, Schmitt, FA, Ikonomovic, MD, Mufson, EJ (2015) Synaptic change in the posterior cingulate gyrus in the progression of Alzheimer's disease. J Alzheimers Dis 43:1073-1090.
Scheff, SW, Price, DA, Schmitt, FA, Roberts, KN, Ikonomovic, MD, Mufson, EJ (2013) Synapse stability in the precuneus early in the progression of Alzheimer's disease. J Alzheimers Dis 35:599-609.
Schneider, JA, Bennett, DA (2010) Where vascular meets neurodegenerative disease. Stroke 41:S144-S146.
Seifert, G, Carmignoto, G, Steinhauser, C (2010) Astrocyte dysfunction in epilepsy. Brain Res Rev 63:212-221.
Seifert, G, Schilling, K, Steinhauser, C (2006) Astrocyte dysfunction in neurological disorders: a molecular perspective. Nat Rev Neurosci 7:194-206.
Selkoe, DJ (2001) Azheimer's disease: genes, proteins, and therapy. Physiol Rev 81:741-766.
Seo, MS, Park, JS, Yang, SR, Park, KS, Hong, IS, Jo, EH, Kang, KS, Lee, YS (2006) Expression of MAP kinases and connexins in the differentiation of rat mammary and epithelial cells. J Vet Med Sci 68:567-571.
Serrano-Perez, MC, Martin, ED, Vaquero, CF, Azcoitia, I, Calvo, S, Cano, E, Tranque, P (2011) Response of transcription factor NFATc3 to excitotoxic and traumatic brain insults: identification of a subpopulation of reactive astrocytes. Glia 59:94-107.
Seshadri, S, Beiser, A, Selhub, J, Jacques, PF, Rosenberg, IH, D'Agostino, RB, Wilson, PW, Wolf, PA (2002) Plasma homocysteine as a risk factor for dementia and Alzheimer's disease. N Engl J Med 346:476-483.
Shaftel, SS, Griffin, WS, O'Banion, MK (2008) The role of interleukin-1 in neuroinflammation and Alzheimer disease: an evolving perspective. J Neuroinflammation 7.

Shankar, GM, Bloodgood, BL, Townsend, M, Walsh, DM, Selkoe, DJ, Sabatini, BL (2007) Natural oligomers of the Alzheimer amyloid-beta protein induce reversible synapse loss by modulating an NMDA-type glutamate receptor-dependent signaling pathway. J Neurosci 27:2866-2875.

Shankar, GM, Li, S, Mehta, TH, Garcia-Munoz, A, Shepardson, NE, Smith, I, Brett, FM, Farrell, MA, Rowan, MJ, Lemere, CA, Regan, CM, Walsh, DM, Sabatini, BL, Selkoe, DJ (2008) Amyloid-beta protein dimers isolated directly from Alzheimer's brains impair synaptic plasticity and memory. Nat Med 14:837-842.

Shibata, M, Yamasaki, N, Miyakawa, T, Kalaria, RN, Fujita, Y, Ohtani, R, Ihara, M, Takahashi, R, Tomimoto, H (2007) Selective impairment of working memory in a mouse model of chronic cerebral hypoperfusion. Stroke 38:2826-2832.

Shih, AY, Blinder, P, Tsai, PS, Friedman, B, Stanley, G, Lyden, PD, Kleinfeld, D (2013) The smallest stroke: occlusion of one penetrating vessel leads to infarction and a cognitive deficit. Nat Neurosci 16:55-63.

Shioda, N, Han, F, Moriguchi, S, Fukunaga, K (2007) Constitutively active calcineurin mediates delayed neuronal death through Fas-ligand expression via activation of NFAT and FKHR transcriptional activities in mouse brain ischemia. J Neurochem 102:1506-1507.

Shioda, N, Moriguchi, S, Shirasaki, Y, Fukunaga, K (2006) Generation of constitutively active calcineurin by calpain contributes to delayed neuronal death following mouse brain ischemia. J Neurochem 98:310-320.

Shiratori, M, Tozaki-Saitoh, H, Yoshitake, M, Tsuda, M, Inoue, K (2010) P2X7 receptor activation induces CXCL2 production in microglia through NFAT and PKC/MAPK pathways. J Neurochem 114:810-819.

Shukitt-Hale, B, McEwen, JJ, Szprengiel, A, Joseph, JA (2004) Effect of age on the radial arm water maze- a test of spatial learning and memory. Neurobiol Aging 25:223-229.

Sinclair, LI, Tayler, HM, Love, S (2015) Synaptic protein levels altered in vascular dementia. Neuropathol Appl Neurobiol 41:533-543.

Skaper, SD (2007) The brain as a target for inflammatory processes and neuroprotective strategies. Ann N Y Acad Sci 1122:23-34.

Smith, EE, Schneider, JA, Wardlaw, JM, Greenberg, SM (2012) Cerebral microinfarcts: the invisible lesions. Lancet Neurol 11:272-282.

Snyder, HM, Corriveau, RA, Craft, S, Faber, JE, Greenberg, SM, Knopman, D, Lamb, BT, Montine, TJ, Nedergaard, M, Schaffer, CB, Schneider, JA, Wellington, C, Wilcock, DM, Zipfel, GJ, Zlokovic, B, Bain, LJ, Bosetti, F, Galis, ZS, Koroshetz, W, Carrillo, MC (2015) Vascular contributions to cognitive impairment and dementia including Alzheimer's disease. Alzheimers Dement 11:710-717.

Sofroniew, MV (2009) Molecular dissection of reactive astrogliosis and glial scar formation. Trends Neurosci 32:638-647.

Sofroniew, MV, Vinters, HV (2010) Astrocytes: biology and pathology. Acta Neuropathol 119:7-35.

Solan, JL, Lampe, PD (2009) Connexin43 phosphorylation: structural changes and biological effects. Biochem J 419:261-272.

Solan, JL, Lampe, PD (2014) Specific Cx43 phosphorylation events regulate gap junction turnover in vivo. FEBS Lett 588:1423-1429.

Sompol, P, Pleiss, MM, Kraner, SD, Artiushin, I, Simmerman, L, Batten, SR, Quintero, G, Gerhardt, GA, Norris, CM (*in preparation*) Inhibition of the astrocytic calcineurin/NFAT4 pathway quells glutamatergic hyperactivity in a mouse model of Alzheimer's disease.

Springer, JE, Azbill, RD, Nottingham, SA, Kennedy, SE (2000) Calcineurin-mediated BAD dephosphorylation activates the caspase-3 apoptotic cascade in traumatic spinal cord injury. J Neurosci 20: 7246-7251.
Stankunas, K, Graef, IA, Neilson, JR, Park, SH, Crabtree, GR (1999) Signaling through calcium, calcineurin, and NF-AT in lymphocyte activation and development. Cold Spring Harb Symp Quant Biol 64:505-516.
Steinhauser, C, Seifert, G, Bedner, P (2012) Astrocyte dysfunction in temporal lobe epilepsy: K+ channels and gap junction coupling. Glia 60:1192-1202.
Stevens, B, Allen, NJ, Vazquez, LE, Howell, GR, Christopherson, KS, Nouri, N, Micheva, KD, Mehalow, AK, Huberman, AD, Stafford, B, Sher, A, Litke, AM, Lambris, JD, Smith, SJ, John, SW, Barres, BA (2007). The classical complement cascade mediates CNS synapse elimination. Cell 131:1164-1178.
Stipanuk, MH, Ueki, I (2011) Dealing with methionine/homocysteine sulfur: cysteine metabolism to taurine and inorganic sulfur. J Inherit Metab Dis 34:17-32.
Sudduth, TL, Greenstein, A, Wilcock, DM (2013a) Intracranial injection of Gammagard, a human IVIg, modulates the inflammatory response of the brain and lowers Abeta in APP/PS1 mice along a different time course than anti-Abeta antibodies. J Neurosci 33:9684-9692.
Sudduth, TL, Powell, DK, Smith, CD, Greenstein, A, Wilcock, DM (2013b) Induction of hyperhomocysteinemia models vascular dementia by induction of cerebral microhemorrhages and neuroinflammation. J Cereb Blood Flow Metab 33:708-715.
Sudduth, TL, Weekman, EM, Brothers, HM, Braun, K, Wilcock, DM (2014) beta-amyloid deposition is shifted to the vasculature and memory impairment is exacerbated when hyperhomocysteinemia is induced in APP/PS1 transgenic mice. Alzheimers Res Ther 6.
Sun, Y, Cao, W, Ding, W, Wang, Y, Han, X, Zhou, Y, Xu, Q, Zhang, Y, Xu, J (2016) Cerebral Blood Flow Alterations as Assessed by 3D ASL in Cognitive Impairment in Patients with Subcortical Vascular Cognitive Impairment: A Marker for Disease Severity. Front Aging Neurosci 8.
Tackenberg, C, Brandt, R (2009) Divergent pathways mediate spine alterations and cell death induced amyloid-beta, wild-type tau and R406W tau. J Neurosci 29:14439-14450.
Taglialatela, G, Hogan, D, Zhang, WR, Dineley, KT (2009) Intermediate- and long-term recognition memory deficits in Tg2576 mice are reversed with acute calcineurin inhibition. Behav Brain Res 200:95-99.
Taglialatela, G, Rastellini, C, Cicalese, L (2015) Reduced Incidence of Dementia in Solid Organ Transplant Patients Treated with Calcineurin Inhibitors. J Alzheimers Dis 47:329-333.
Takeda, S, Sato, N, Uchio-Yamada, K, Sawada, K, Kunieda, T, Takeuchi, D, Kurinami, H, Shinohara, M, Rakugi, H, Morishita, R (2010) Diabetes-accelerated memory dysfunction via cerebrovascular inflammation and Abeta deposition in an Alzheimer mouse model with diabetes. Proc Natl Acad Sci U S A 107:7036-7041.
Takeuchi, H, Suzumura, A (2014) Gap junctions and hemichannels composed of connexins: potential therapeutic targets for neurodegenerative diseases. Front Cell Neurosci 8.
Tence, M, Ezan, P, Amigou, E, Giaume, C (2012) Increased interaction of connexin43 with zonula occludens-1 during inhibition of gap junctions by G protein-coupled receptor agonists. Cell Signal 24:86-98.

Troen, AM, Chao, WH, Crivello, NA, D'Anci, KE, Shukitt-Hale, B, Smith, DE, Selhub, J, Rosenberg, IH (2008) Cognitive impairment in folate-deficient rats corresponds to depleted brain phosphatidylcholine and is prevented by dietary methionine without lowering plasma homocysteine. J Nutr 138:2502-2509.
Van Eldik, LJ, Griffin, WS (1994) S100 beta expression in Alzheimer's disease: relation to neuropathology in brain regions. Biochim Biophys Acta 1223:398-403.
Van Eldik, LJ, Thompson, WL, Ralay Ranaivo, H, Behanna, HA, Watterson, MD (2007) Glia proinflammatory cytokine upregulation as a therapeutic target for neurodegenerative diseases: function-based and target-based discovery approaches. Int Rev Neurobiol 82:277-296.
van Norden, AG, van Dijk, EJ, de Laat, KF, Scheltens, P, Olderikkert, MG, de Leeuw, FE (2012) Dementia: Alzheimer pathology and vascular factors: from mutually exclusive to interaction. Biochim Biophys Acta 1822:340-349.
van Veluw, SJ, Zwanenburg, JJ, Rozemuller, AJ, Luijten, PR, Spliet, WG, Biessels, GJ (2015) The spectrum of MR detectable cortical microinfarcts: a classification study with 7-tesla postmortem MRI and histopathology. J Cereb Blood Flow Metab 35:676-683.
Van Wagoner, NJ, Benveniste, EN (1999) Interleukin-6 expression and regulation in astrocytes. J Neuroimmunol 100:124-139.
Vemuri, P, Knopman, DS (2016) The role of cerebrovascular disease when there is concomitant Alzheimer disease. Biochim Biophys Acta 1862:952-965.
Verkhratsky, A, Nedergaard, M, Hertz, L (2015) Why are astrocytes important? Neurochem Res 40:389-401.
Verkhratsky, A, Rodriguez, JJ, Parpura, V (2012) Calcium signalling in astroglia. Mol Cell Endocrinol 353:45-56.
Wallays, G, Nuyens, D, Silasi-Mansat, R, Souffreau, J, Callaerts-Vegh, Z, Van Nuffelen, A, Moons, L, D'Hooge, R, Lupu, F, Carmeliet, P, Collen, D, Dewerchin, M (2011) Notch3 Arg170Cys knock-in mice display pathologic and clinical features of the neurovascular disorder cerebral autosomal dominant arteriopathy with subcortical infarcts and leukoencephalopathy. Arterioscler Thromb Vasc Biol 31:2881-2888.
Wang, HG, Pathan, N, Ethell, IM, Krajewski, S, Yamaguchi, Y, Shibasaki, F, McKeon, F, Bobo, T, Franke, TF, Reed, JC (1999) Ca2+-induced apoptosis through calcineurin dephosphorylation of BAD. Science 284:339-343.
Wang, M, Iliff, JJ, Liao, Y, Chen, MJ, Shinseki, MS, Venkataraman, A, Cheung, J, Wang, W, Nedergaard, M (2012) Cognitive deficits and delayed neuronal loss in a mouse model of multiple microinfarcts. J Neurosci 32:17948-17960.
Webster, SJ, Bachstetter, AD, Nelson, PT, Schmitt, FA, Van Eldik, LJ (2014) Using mice to model Alzheimer's dementia: an overview of the clinical disease and the preclinical behavioral changes in 10 mouse models. Front Genet 5.
Weekman, EM, Sudduth, TL, Caverly CN, Kopper, TJ, Phillips, OW, Powell, DK, Wilcock, DM (2016) Reduced Efficacy of Anti-Abeta Immunotherapy in a Mouse Model of Amyloid Deposition and Vascular Cognitive Impairment Comorbidity. J Neurosci 36:9896-9907.
White, JA, Manelli, AM, Holmberg, KH, Van Eldik, LJ, Ladu, MJ (2005) Differential effects of oligomeric and fibrillar amyloid-beta 1-42 on astrocyte-mediated inflammation. Neurobiol Dis 18:459-465.
Wilcock, DM, Schmitt, FA, Head, E (2016) Cerebrovascular contributions to aging and Alzheimer's disease in Down Syndrome. Biochim Biophys Acta 1862:909-914.
Wisniewski, HM, Wegiel, J (1991) Spatial relationships between astrocytes and classical plaque components. Neurobiol Aging 12:593-600.

Wu, HY, Hudry, E, Hashimoto, T, Kuchibhotla, K, Rozkalne, A, Fan, Z, Spires-Jones, T, Xie, H, Arbel-Ornath, M, Grosskreutz, CL, Bacskai, BJ, Hyman, BT (2010) Amyloid beta induces the morphological neurodegenerative triad of spine loss, dendritic simplification, and neuritic dystrophies through calcineruin activation. J Neurosci 30:2636-2649.

Wu, HY, Tomizawa, K, Oda, Y, Wei, FY, Lu, YF, Matsushita, M, Li, ST, Moriwaki, A, Matsui, H (2004) Critical role of calpain-mediated cleavage of calcineurin in excitotoxic neurodegeneration. J Biol Chem 279:4929-4940.

Yan, HQ, Shin, SS, Ma, X, Li, Y, Dixon, CE (2014) Differential effect of traumatic brain injury on the nuclear factor of activated T Cells C3 and C4 isoforms in the rat hippocampus. Brain Res 1548:63-72.

Yin, JX, Turner, GH, Lin, HJ, Coons, SW, Shi, J (2011) Deficits in spatial learning and memory is associated with hippocampal volume loss in aged apolipoprotein E4 mice. J Alzheimers Dis 27:89-98.

Yoshizaki, K, Adachi, K, Kataoka, S, Watanabe, A, Tabira, T, Takahashi, K, Wakita, H (2008) Chronic cerebral hypoperfusion induced by right unilateral common carotid artery occlusion causes delayed white matter lesions and cognitive impairment in adult mice. Exp Neurol 210:585-591.

Yun, HS, Park, MS, Ji, ES, Kim, TW, Ko, IG, Kim, HB, Kim, H (2014) Treadmill exercise ameliorates symptoms of attention deficit/hyperactivity disorder through reducing Purkinje cell loss and astrocytic reaction in spontaneous hypertensive rats. J Exer Rehabil 10:22-30.

Zaiss, AK, Muruve, DA (2005) Immune responses to adeno-associated virus vectors. Curr Gene Ther 5:323-331.

Zamanian, JL, Xu, L, Foo, LC, Nouri, N, Zhou, L, Giffard, RG, Barres, BA (2012) Genomic analysis of reactive astrogliosis. J Neurosci 32:6391-6410.

Zhu, X, Schuff, N, Kornak, J, Soher, B, Yaffe, K, Kramer, JH, Ezekiel, F, Miller, BL, Jagust, WJ, Weiner, MW (2006) Effects of Alzheimer disease on fronto-parietal brain N-acetyl aspartate and myo-inositol using magnetic resonance spectroscopic imaging. Alzheimer Dis Assoc Discord 20:77-85.

VITA

Melanie Marie Pleiss

Education:

2011-present **University of Kentucky**, Lexington, KY
Ph.D. Candidate, passed Qualifying Exams 08/05/2013
Dept. of Molecular and Biomedical Pharmacology
Cumulative GPA: 3.64/4.0

2007-2011 **Marshall University**, Huntington, WV
Bachelor of Science in Biomedical Sciences
Minors: Chemistry, Classical Studies
Cumulative GPA: 3.89/4.0, Summa cum Laude

2003-2007 **Mercy High School**, Baltimore, MD
HS Graduate, Advanced Placement and Honors Curriculum
Cumulative GPA: 4.3/4.0

Research Interests:

Alzheimer's disease, neurodegeneration, neuroinflammation, astrocytes, calcineurin

Research Training:

MRI imaging and analysis, electrophysiology: field and single cell recordings, rodent behavior testing: radial arm water maze and active avoidance paradigm, rodent stereotaxic surgery, confocal microscopy, immunohistochemistry/immunofluorescence, protein biochemistry, RNA purification, qPCR, primary neural cell culture

Research Experience:

2012-present University of Kentucky, Sanders-Brown Center on Aging
Dept. of Molecular and Biomedical Pharmacology
Alzheimer's disease and neuroinflammation
Advisor: Dr. Christopher M. Norris

Fall 2011-Spring 2012 University of Kentucky
Integrated Biomedical Science
Neuroscience
Lab Rotation Advisors: Drs. Elizabeth Head, Brian Gold, and Christopher Norris

Funding:

2015-2018 NIH F31 Pre Doctoral Fellowship, 3-year award
Project: *Astrocytic Calcineurin and Connexin43 Gap Junctions in Alzheimer's Disease*
Award dates: 02/01/15- 01/31/18
Total award amount: $29,736

2014-2015 PhRMA Foundation Pre Doctoral Fellowship in Pharmacology/Toxicology, 2-year award
Project: *Astrocytic Calcineurin and Connexin43 Gap Junctions in Alzheimer's Disease*
Award dates: 03/01/14- 01/31/15
Total award amount: $20,000

Honors and Awards:

2016 University of Kentucky Graduate School Travel Award to attend 2016 Society for Neuroscience conference in San Diego, CA
2016 University of Kentucky Graduate School Travel Award to attend 2016 American Society for Neurochemistry conference in Denver, CO
2015 University of Kentucky Graduate School Travel Award to attend 2015 American Society for Neurochemistry conference in Atlanta, GA
2014 Graduate Chapter Travel Award to attend 2014 Society for Neuroscience conference in Washington, D.C.
2014 University of Kentucky College of Pharmacy Symposium on Drug Discovery & Development, Outstanding Poster Presentation, Second Place
2014 Alzheimer's Association Travel Fellowship to attend 2014 Alzheimer's Association International conference in Copenhagen, Denmark
2013 University of Kentucky Graduate Student Travel Award to attend 2013 Society for Neuroscience conference in San Diego, CA
2012 2nd Annual Markesbery Symposium on Aging and Dementia Outstanding Poster Award
2012 University of Kentucky Graduate Student Travel Award to attend 2012 Society for Neuroscience conference in New Orleans, LA
2011 Who's Who All-College Student
2010 Marshall University Hoy Latin Scholarship
2007-2011 Dean's List, Marshall University
2007 John Marshall Scholarship
2003-2007 The Mercy Scholarship
2003 Girl Scout Silver Award

Professional Development:

2015	Certificate in Business Administration Series 2, University of Kentucky, The Gatton College of Business and Economics *completed May 21*
2014	Certificate in Business Administration Series 1, University of Kentucky, The Gatton College of Business and Economics *completed November 13*
2014	Alzheimer's Fast Track Workshop sponsored by the BrightFocus Foundation *November 12-14*

Professional Memberships:

2014-present	American Society for Neurochemistry, Student Member
2013-present	ISTAART, Student Member
2012-present	International Society for Neurochemistry, Student Member
2012-present	Bluegrass Chapter of the Society for Neuroscience (BGSfN), Student Member
2012-present	Society for Neuroscience, Student Member
2011	Phi Kappa Phi Honor Society, Member
2009-2011	Eta Sigma Phi Classics Fraternity, Member
2008-2011	Alpha Chi Sigma Chemistry Fraternity, President, VP, Master of Ceremonies

Professional Service and Community Outreach:

2016	Science Fair Judge, Morton Middle School, Lexington, KY
2015	Kentucky American Water Science Fair Outreach with BGSfN, Tates Creek High School, Lexington, KY
2014	Alzheimer's Association Memory Walk, Team Captain, Lexington, KY
2014	Ronald McDonald Dinner Preparation with Student Association, Lexington, KY
2014	American Heart Association Walk, Participant, Lexington, KY
2014	Career Day Outreach with BGSfN, Northern Elementary, Lexington, KY
2014	Kentucky American Water Science Fair Outreach with BGSfN, Bryan Station High School, Lexington, KY
2013	Science Fair Judge, Veterans Park Elementary School, Lexington, KY
2012	Jingle Bell Jog 5K, Alzheimer's Fundraiser, Participant
2011-2013	Alzheimer's Association Memory Walk, Team Captain, Dayton, OH

Service and Mentoring:

2014	NIH "Bridges to the Doctorate" (R25) Student Mentor for Elizabeth Horn
2014-2015	Secretary, Nutritional Sciences and Pharmacology Students (NSPS) Association
2008-2010	Teaching Assistant and Grader for General and Organic Chemistry labs
2009	Teaching Assistant and Laboratory Prep for Microbiology labs
Spring 2008	Tutor for General Chemistry I

Peer-Reviewed Publications (in chronological order):

Head, E., Murphey, H.L., Dowling, A.L.S., McCarty, K.L., Bethel, S.R., Nitz, J.A., **Pleiss, M.,** Vanrooyen, J., Grossheim, M., Smiley, J.R., Murphy, M.P., Beckett, T.L., Pagani, D., Bresch, F., Hendrix, C. (2012) A Combination Cocktail Improves Spatial Attention in a Canine Model of Human Aging and Alzheimer's disease. *Journal of Alzheimer's Disease*, 32(4): 1029-1042.

Furman, J.L., Kraner, S.D., Sompol, P., **Pleiss, M.M.,** Putman, E.J., Dunkerson, J, Abdul, H.M., Roberts, K.N., Scheff, S., Norris, C.M. (2016) Blockade of astrocytic calcineurin/NFAT signaling helps to normalize hippocampal synaptic function and plasticity in a rat model of traumatic brain injury. *Journal of Neuroscience*, 36(5): 1502-15.

Pleiss, M.M., Sompol, P., Mohmmad Abdul, H., Furman, J.L., Guttmann, R.P., Nelson, P.T., Wilcock, D.M., Norris, C.M. (2016) Calcineurin proteolysis in astrocytes associated with Alzheimer's disease and small vessel pathology, *Biochimica et Biophysica Acta,* 1862(9):1521-32.

Published Abstracts (in chronological order):

Furman J.L., **Pleiss M.M.**, Mohmmad Abdul H, Norris C.M. (2012) Alterations in connexin 43
phosphorylation during the progression of Alzheimer's disease: Possible role of
astrocytic calcineurin. *Alzheimer's Association International Conference*. P2-109.

Pleiss, M.M., Furman, J.L., Abdul, Hafiz Mohmmad, Norris, C.M. (2012) Dephosphorylation of the astrocytic gap junction protein, connexin 43, is increased in human hippocampus during Mild Cognitive Impairment. *Society for Neuroscience Abstracts*. **42**:49.26.

Pleiss, M.M., Furman, J.L., Abdul, Hafiz Mohmmad, Norris, C.M. (2012) Dephosphorylation of the astrocytic gap junction protein, connexin 43, is increased in human hippocampus during Mild Cognitive Impairment. *2nd Annual Markesbery Symposium on Aging and Dementia*. 5.

Pleiss, M.M., Furman, J.L., Abdul, Hafiz Mohmmad, Norris C.M. (2013) Astrocytic Calcineurin and Connexin 43 Gap Junctions in Neuroinflammation and Alzheimer's Disease. *Bluegrass Society for Neuroscience Spring Neuroscience Research Day.* 101.

Pleiss, M.M., Furman, J.L., Abdul, Hafiz Mohmmad, Norris, C.M. (2013) The astrocytic gap junction protein connexin43 exhibits calcineurin-related changes in phosphorylation status during the progression of Alzheimer's disease. *Society for Neuroscience Abstracts.* 116.13 [**nanosymposium—oral presentation**]

Pleiss, M.M., Furman, J.L., Abdul, Hafiz Mohmmad, Norris, C.M. (2013) The astrocytic gap junction protein connexin43 exhibits calcineurin-related changes in phosphorylation status during the progression of Alzheimer's disease. *3rd Annual Markesbery Symposium on Aging and Dementia*. 21.

Pleiss, M.M., Furman, J.L. Abdul, Hafiz Mohmmad, Norris, C.M. (2014) A novel reagent modulates CN/Cx43 interactions during the progression of Alzheimer's disease. *Bluegrass Society for Neuroscience Spring Neuroscience Research Day.* 128.

Pleiss, M.M., Furman, J.L. Abdul, Hafiz Mohmmad, Norris, C.M. (2014) A novel reagent modulates CN/Cx43 interactions during the progression of Alzheimer's disease. *5th Annual ApoE, ApoE Receptors & Neurodegeneration Symposium.* 21.

Pleiss, M.M., Furman, J.L., Abdul, Hafiz Mohmmad, Norris, C.M. (2014) A novel reagent modulates CN/Cx43 interactions during the progression of Alzheimer's disease. *Alzheimer's Association International Conference*.

Pleiss, M.M., Abdul, Hafiz Mohmmad, Furman, J.L., Guttmann, R.P., Patel, E., Wilcock, D.M., Nelson, P.T., Norris, C.M. (2014) Calcineurin proteolysis is associated with astrocyte and small vessel pathology. *Society for Neuroscience Abstracts*. 43.

Pleiss, M.M., Abdul, Hafiz Mohmmad, Furman, J.L., Guttmann, R.P., Patel, E., Wilcock, D.M., Nelson, P.T., Norris, C.M. (2014) Calcineurin proteolysis is associated with astrocyte and small vessel pathology. *4th Annual Markesbery Symposium on Aging and Dementia*. 9.

Pleiss, M.M., Abdul, Hafiz Mohmmad, Furman, J.L., Guttmann, R.P., Patel, E., Wilcock, D.M., Nelson, P.T., Norris, C.M. (2015) A custom antibody detects calcineurin proteolysis in astrocytes and small vessels in human AD brain specimens. *46th Annual American Society for Neurochemistry Meeting*. PTW01-10.

Pleiss, M.M., Abdul, Hafiz Mohmmad, Furman, J.L., Guttmann, R.P., Patel, E., Wilcock, D.M., Nelson, P.T., Norris, C.M. (2015) A custom antibody detects calcineurin proteolysis in astrocytes and small vessels in human AD brain specimens. *Bluegrass Society for Neuroscience Spring Neuroscience Research Day*. 118.

Pleiss, M.M., Sompol, P., Artiushin, I., Kraner, S.D., Powell, D., Bakshi, V., Lin, A., Nelson, P.T., Wilcock, D.M., Norris, C.M. (2016) Inhibition of astrocytic calcineurin/NFAT signaling in a mouse model of vascular cognitive impairment and dementia. *47th Annual American Society for Neurochemistry Meeting.* PTW08-02.

Pleiss, M.M., Sompol, P., Artiushin, I., Kraner, S.D., Powell, D., Bakshi, V., Lin, A-L., Nelson, P.T., Wilcock, D.M., Norris, C.M. (2016) Inhibition of astrocytic calcineurin/NFAT signaling in a mouse model of vascular cognitive impairment and dementia. *Society for Neuroscience abstracts.* 482.09 [**nanosymposium-- oral presentation]**